








# Multimodality imaging for patient selection, procedural guidance, and follow-up of transcatheter interventions for structural heart disease: a consensus document of the EACVI Task Force on Interventional Cardiovascular Imaging: part 1: access routes, transcatheter aortic valve implantation, and transcatheter mitral valve interventions

Eustachio Agricola <sup>1,2\*</sup>, Francesco Ancona <sup>1</sup>, Thomas Bartel<sup>3</sup>, Eric Brochet<sup>4</sup>, Marc Dweck<sup>5</sup>, Francesco Faletra<sup>6,7</sup>, Patrizio Lancellotti <sup>8,9</sup>, Hani Mahmoud-Elsayed<sup>10</sup>, Nina Ajmone Marsan<sup>11</sup>, Pal Maurovich-Hovart<sup>12</sup>, Mark Monaghan<sup>13</sup>, Gianluca Pontone <sup>14</sup>, Leyla Elif Sade <sup>15,16</sup>, Martin Swaans<sup>17</sup>, Ralph Stephan Von Bardeleben <sup>18</sup>, Nina Wunderlich<sup>19</sup>, Jose-Luis Zamorano<sup>20</sup>, Bogdan A. Popescu<sup>21</sup>, Bernard Cosyns<sup>22</sup>, and Erwan Donal <sup>23</sup>

<sup>1</sup>Cardiovascular Imaging Unit, Cardio-Thoracic-Vascular Department, IRCCS San Raffaele Scientific Institute, via Olgettina 60, Milan 20132, Italy; <sup>2</sup>Vita-Salute San Raffaele University, via Olgettina 58, Milan 20132, Italy; <sup>3</sup>Heart & Vascular Institute, Cleveland Clinic Abu Dhabi, 26th Street, Dubai, United Arab Emirates; <sup>4</sup>Cardiology Department, Hôpital Bichat, 46 rue Huchard, Paris 75018, France; <sup>5</sup>Centre for Cardiovascular Science, University of Edinburgh, Edinburgh EH16 4SB, UK; <sup>6</sup>Senior SHD Consultant Istituto Cardiocentro Via Tesserete 48, CH-6900 Lugano, Switzerland; <sup>7</sup>Senior Imaging Consultant ISMETT UPCM Hospital, Discesa dei Giudici, 4, 90133 Palermo, Italy; <sup>8</sup>Department of Cardiology, University of Liège Hospital, Domaine Universitaire du Sart Tilman, Liège B4000, Belgium; <sup>9</sup>Gruppo Villa Maria Care and Research, Maria Cecilia Hospital, Cotignola, and Anthea Hospital, Bari, Italy; <sup>10</sup>Aswan Heart Centre, Magdi Yacoub Foundation, Aswan, Egypt; <sup>11</sup>Department of Cardiology, Leiden University Medical Center, Leiden, The Netherlands; <sup>12</sup>Medical Imaging Centre, Semmelweis University, Budapest, Hungary; <sup>13</sup>King's College Hospital, London, UK; <sup>14</sup>Department of Perioperative Cardiology and Cardiovascular Imaging, Centro Cardiologico Monzino IRCCS, Milan, Italy; <sup>15</sup>University of Pittsburgh—Heart & Vascular Institute UPMC, 200 Lothrop St Ste E354.2, Pittsburgh, PA 15213, USA; <sup>16</sup>Cardiology Department, Baskent University, Ankara, Turkey; <sup>17</sup>Department of Cardiology, St. Antonius Hospital, Nieuwegein, The Netherlands; <sup>18</sup>Department of Cardiology, Heart and Vascular Center, Uniklinik Mainz, Germany; <sup>19</sup>Asklepios Klinik Langen Röntgenstrasse 20, Langen 63225, Germany; <sup>20</sup>University Hospital Ramon y Cajal, Madrid, Spain; <sup>21</sup>Department of Cardiology, University of Medicine and Pharmacy 'Carol Davila' -Euroecolab, Emergency Institute for Cardiovascular Diseases 'Prof. Dr. C. C. Iliescu', Bucharest, Romania; <sup>22</sup>Cardiology Department, Centrum voor Hart en Vaatziekten (CHVZ), Universitair ziekenhuis Brussel, Brussels, Belgium; and <sup>23</sup>Cardiologie, CHU de RENNES, LTSI UMR1099, INSERM, Université de Rennes-1, Rennes, France

Received 4 April 2023; accepted 5 April 2023; online publish-ahead-of-print 7 June 2023

Transcatheter therapies for the treatment of structural heart diseases (SHD) have expanded dramatically over the last years, thanks to the developments and improvements of devices and imaging techniques, along with the increasing expertise of operators. Imaging, in particular echocardiography, is pivotal during patient selection, procedural monitoring, and follow-up. The imaging assessment of patients undergoing transcatheter interventions places demands on imagers that differ from those of the routine evaluation of patients with SHD, and there is a need for specific expertise for those working in the cath lab. In the context of the current rapid developments and growing use of SHD therapies, this document intends to update the previous consensus document and address new advancements in interventional imaging for access routes and treatment of patients with aortic stenosis and regurgitation, and mitral stenosis and regurgitation.

\* Corresponding author. E-mail: [agricola.eustachio@hsr.it](mailto:agricola.eustachio@hsr.it)

© The Author(s) 2023. Published by Oxford University Press on behalf of the European Society of Cardiology. All rights reserved. For permissions, please e-mail: [journals.permissions@oup.com](mailto:journals.permissions@oup.com)

**Keywords**

interventional imaging • interventional echocardiography • structural heart disease • transcatheter aortic valve implantation—transcatheter mitral valve therapy

**Introduction**

Transcatheter therapy of structural heart diseases (SHD) has seen great advances in the last decades, thanks to development of new devices, improvement of their performance, advances in imaging techniques, and the increase in the skill of operators. Imaging plays a pivotal role at each step along the therapeutic path: patient selection, pre-procedural planning, procedural monitoring, and follow-up. The imaging assessment of patients undergoing transcatheter interventions requires specific training, competences, and skills that differ from those involved in the routine evaluation of patients with SHD.<sup>1</sup> Transcatheter therapies for aortic valve (AV) stenosis, mitral stenosis (MS), and mitral regurgitation (MR) are well established and included in guidelines.<sup>2</sup> In the context of the current rapid developments and growing use of transcatheter therapies, the present consensus document summarizes the current role of imaging: what to assess and which imaging technique to use prior, during, and after transcatheter interventions for access routes and treatment of patients with aortic stenosis (AS) and regurgitation, and MS and regurgitation.

**Access routes****Transseptal puncture****Anatomy of interatrial septum**

Left-side percutaneous SHD and complex electrophysiological procedures require a direct route to the left atrium (LA). The easiest way is through the interatrial septum (IAS). An in-depth understanding of the anatomy of IAS is therefore of paramount relevance for an effective and safe transseptal puncture (TSP). In the normal adult heart, the IAS is formed by the fusion of two components: the septum primum (SP) and the septum secundum (SS). While the SP is a membrane-like structure made up by fibrous and elastic tissue and corresponds to the floor of the fossa ovalis (FO), the SS is an extensive muscular area, surrounding the FO, made up by an enfolding of the left and right atrial walls. This enfolding, known as Waterston's groove or simply as the interatrial groove,<sup>3</sup> is filled externally by epicardial adipose tissue (EAT). Thus, the actual structure of SS includes three layers: the left and right atrial walls and EAT in-between (Figure 1A). Though the SS functions as a partition between the two atria, a puncture through it causes an exit from the cavities of the heart into epicardial fat and extracardiac space<sup>4,5</sup> (Figure 1B). With sufficient pressure applied to the catheter, the needle may pass throughout the three layers, into the LA. However, this erroneous manoeuvre first reduces manoeuvrability of the catheter after entering the LA and second, and more important, may potentially lead to haemopericardium after the transseptal sheath's removal. However, the FO ranges from few millimetres to 2–3 cm in length,<sup>6</sup> and while the site-specific TSP is possible with large or medium-sized FO, searching for a specific site may be extremely challenging in hearts with small FO (Figure 1C and D). Finally, a few millimetres separate the anterior superior margin of the FO from the right atrial wall, overlying the non-coronary aortic sinus. Indeed, the most feared complication of TSP is puncturing the aortic root (Figure 2).

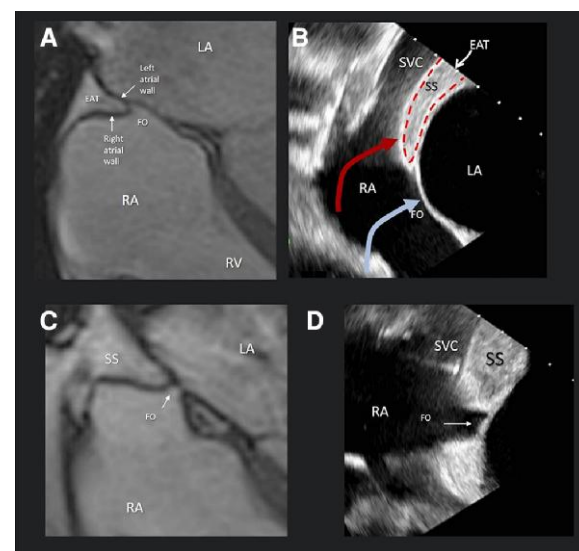
**Procedural guidance**

The TSP kit includes the needle, dilator, and a long pre-shaped plastic sheath. The Brockenbrough needle and Mullins or a Swartz SL transseptal sheath are the most commonly used.<sup>7</sup> Electrocautery to the

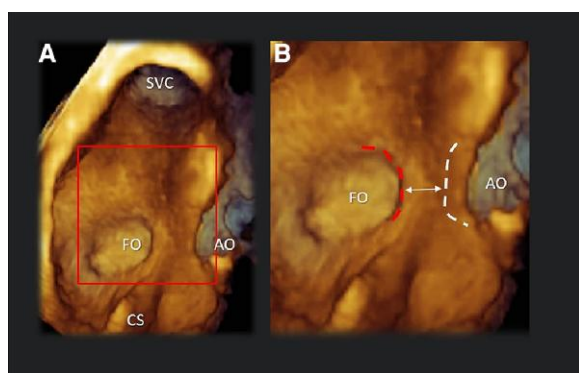
standard needle tip can be used to perform safe and successful TSP without the need for significant mechanical forces.<sup>8</sup> Another technical advancement is the steerable transeptal needle which provides real-time adjustable deflection without the need to remove and reshape the needle.<sup>9</sup> Because anatomical landmarks are not visible under fluoroscopy, the use of 2D/3D transoesophageal echocardiography (TOE) has become mandatory to increase safety and allow the precise identification of optimum site for crossing the FO with respect to the planned procedure. The wide variety of percutaneous procedures requiring transeptal puncture have called attention to the importance of 'site-specific' TSP within the FO. Table 1 summarizes the most common left-side transcatheter procedures and their recommended site-specific TSP. Table 2 describes the sequential steps of the procedure.

**Fluoroscopy**

Knowledge of the fluoroscopic anatomy of the FO and its anatomical relationships with the aorta (AO) is of paramount relevance for a correct understanding in the use of fluoroscopic projections and safer puncture. In patients lying in the supine position, the most useful fluoroscopic projections for TSP are the anteroposterior (AP) projection, the 30° right anterior oblique (RAO), and the 30° left anterior oblique (LAO). In the AP projection, the right atrial cavity is right and anterior,



**Figure 1** (A) CMR in cross-sectional four-chamber view showing as the SS is actually an enfolding of left and right atrial walls. This fold, called Waterston groove, is externally filled by EAT assuming a 'three-layered' appearance. (B) 2D TOE in cross-sectional bi-caval view in attitudinal correct orientation, showing the three-layered appearance of SS. The fold is marked by a dotted red line. The curved red arrow points at the wrong TSP through SS (see text), while a curved light blue arrow points at the right TSP through the FO. (C) CMR in cross-sectional four-chamber view and (D) 2D TOE in bi-caval view (TOE), in correct attitudinal orientation. The small FO makes the site-specific TSP very challenging.



**Figure 2** (A) 3D TOE image of the right side of the IAS showing the FO, the superior vena cava (SVC), and the orifice of CS. (B) Magnified image of structures inside the red square of (A). The red dotted line marks the superior/anterior border of the FO, while the white dotted line marks the aortic sinus abutting on the RA. The double head arrow points at the minimal distance between the two borders. An anterior and superior puncture outside the FO may injure the aortic sinus. AO, aorta.

whereas the LA cavity is left and posterior. As a result, the FO is oriented left to right with an angle of about  $65^\circ$  with respect to the sagittal plane of the body. In AP projection, the FO is partially covered by the aortic root (AO), which lies anterior and left to the FO. In RAO projection, the FO is projected 'en face' and the AO lies on the left with no overlapping. Finally, in LAO projection, FO is projected 'tangentially' dividing the left from the right atrium (RA) cavity, with an almost complete overlap with the AO (Figure 3).

## 2D/3D TOE

Currently, TSP is usually performed under the TOE guidance. X-plane cross-section, with the bi-caval and perpendicular views, allows recognition of the FO and the specific site of the puncture (tenting). Indeed, the bi-caval view helps determine the superior–inferior position, while the cross-section determines the anterior–posterior position (Figure 4). 3D TOE may follow all steps of the TSP procedure (Figure 5).

## Fusion imaging

In the dual imaging–based approach (i.e. fluoroscopy and TOE), catheters and devices are best visualized through fluoroscopy on one screen, while IAS is best visualized with 2D/3D TOE on a second screen. A novel imaging technique (Echo-Navigator, Philips Medical System, Best, The Netherlands) is able to overlap patient-specific imaging data from both fluoroscopic projections and 2D/3D TOE, providing a kind of hybrid image in which soft tissues of IAS are displayed within the standard fluoroscopic silhouettes in a single screen. Indeed, adding fiducial markers on standard fluoroscopic images, fusion imaging may facilitate the site-specific positioning of the needle (Figure 6).

## Intracardiac echocardiography

There is a growing interest in intracardiac echocardiography (ICE) as an alternative to TOE.<sup>10</sup> In contrast to TOE, in fact, ICE can be performed

by the same interventionalists who perform the procedure; under conscious sedation without endotracheal intubation, ICE may potentially reduce fluoroscopy exposure, shorten procedure length, and allow early recognition of complications. ICE may facilitate TSP: positioning the ICE catheter in RA, the FO is seen in 2D with two orthogonal plans and in 3D in 'en face' view (Figure 7).

## TSP: key points

- (i) Acquire an in-depth understanding of the anatomy of the IAS and the standard fluoroscopic projections.
- (ii) Understand why any single SHD procedure has its own site-specific TSP.
- (iii) Use 2D TOE X-plane cross-section bi-caval and short-axis (SAX) view.
- (iv) 3D TOE image may help show the FO in an 'en face' view.
- (v) Make sure that the 'tenting' is always within the margins of FO.
- (vi) Make sure that the wire is in the LA before advancing the sheath.

## Transapical puncture

### Procedure

Transapical (TA) access provides a direct route to cardiac structures difficult to reach with TSP. Some cases of paravalvular leak (PVL) closure, mitral valve (MV) repair with neo-chordae, and transcatheter mitral valve replacement (TMVR) are approached by TA access.

Computed tomography (CT) is fundamental for pre-procedural planning, particularly for selecting the optimal entry point through the chest wall and in defining the puncture site in the apex of the left ventricle (LV), which are essential in terms of safety and collinearity to the target point. The pre-procedural planning is the result of the CT analysis based on the localization of the LV apex and its relationships with the coronary arteries, the position of the papillary muscles, the hypothetical trajectories towards the target, and the extension of the lung tissue over the LV cavity. In addition, CT allows the optimal fluoroscopic working plane to be derived together with the angle of entry.

### Procedural guidance

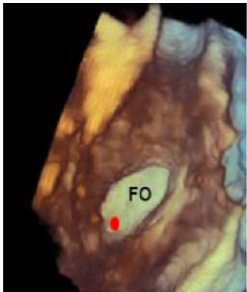
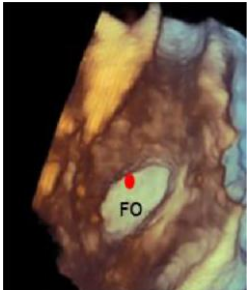
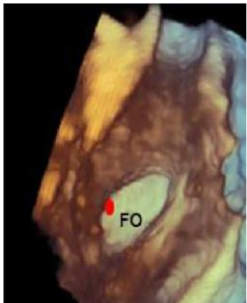
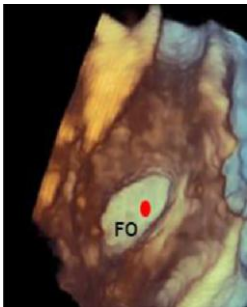
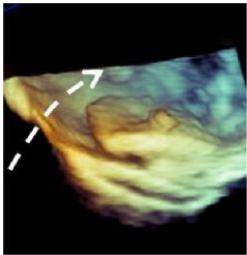
The chosen puncture site is marked on the patient's skin over the pre-specified intercostal space according to CT data.

The access site is checked by transthoracic echocardiography (TTE) confirming the location of the true apex. It is important to note that the pre-specified apical access point usually is not exactly located at the true LV apical point, in order to ensure proper perpendicularity to the MV.

Once the cardiac apex has been exposed by the surgeon, 2D TOE is essential in guiding the identification of the exact entry site by visualization of the imprinted point by the interventionalist's finger. On simultaneous biplane, using the commissural view as the main view and long-axis (LAX) view as the derived one allows appreciation of the optimum position along the medio-lateral and anterior–posterior planes, as well as the spatial relationship with both papillary muscles.

Once the access site is defined (Figure 8A), TA puncture is accomplished via a 21-gauge micropuncture needle. During the puncture, visualization of entrance into the LV cavity is facilitated by contrast dye

**Table 1** The different site-specific accesses

Procedure	Site-specific	Reason	Image
LAA closure	Posterior and inferior TSP is recommended to align the sheath with long axis of LAA.	Allows positioning of the delivery sheath deep into the LAA facilitating coaxial device deployment	
Edge-to-edge procedure	Usually superior and posterior TSP.	Allows adequate free movement of the CDS within the LA	
PVL repair	A superior TSP crossing site is recommended for lateral leaks. For medial leaks, the TSP is difficult due to the acute angle of guide catheter. A retrograde or TA approach is recommended.	Posterior and superior site allows appropriate working height within the LA and easy access to lateral defects.	
Pulmonary vein isolation	An anterior/central TSP is recommended.	Adequate room for deflectable sheaths and catheters	
Prior septal device	The available space of FO outside the device. Usually inferior–posterior border.		

Abbreviations as in the text.

### Table 2 TSP procedural steps

Step	Name	Procedure
Step 1	Femoral puncture	Access via the right femoral vein is preferred because of the almost linear trajectory to the RA. Echo guidance with a linear probe allows guidance of the puncture needle into the vein while avoiding the femoral artery. An alternative option is to palpate the femoral pulse and puncture 4 cm below the inguinal ligament, medial to the femoral pulse, and with a 45° inclination starting medial and shifting lateral.
Step 2	Sheath introduction and Brockenbrough needle insertion	A 00.32 inch J tip guidewire is advanced under fluoroscopy guidance to the SVC. TOE is recommended to confirm that the guidewire has reached the SVC position. Maintaining fluoroscopic and TOE projections, the transseptal sheath and dilator are advanced over the guidewire to the SVC. Once the sheath has reached the SVC, the wire is removed.
Step 3	Pullback	The needle and the sheath are gently pulled back from the SVC. A first jump is perceived as the sheath is pulled back from the SVC to the RA. A second jump is perceived when the sheath falls in the FO. Both tactile feedback (i.e. the perception of elasticity of the tissue and the atrial pulsation which bounces back to the sheaths) and TOE confirm FO engagement.
Step 4	Tenting	Once the FO has been engaged, a slight pressure on the needle allows identification of the puncture site as the apex of the 'tenting' appearance.
Step 5	TSP	Finally, the needle is advanced against the FO while keeping the sheath in place. Gentle movements prevent the system from slipping anteriorly towards the AO or posteriorly towards the SS. The puncture is usually followed by the release of tenting. 2D/3D TOE should confirm the wire is in LA before advancing the sheath.

Abbreviations as in the text

injection through the needle that produces transient bubbles inside the LV. Afterwards, the appropriate delivery sheath is introduced according to procedural needs: this step is usually monitored by simultaneous biplane imaging (*Figure 8B*).

## TA puncture: key points

- (i) TA access site is heavily dependent on pre-procedural CT imaging.
- (ii) TTE and in particular TOE biplane imaging are essential for procedural guidance.

## Transcatheter aortic valve implantation

Since the first report of Cribier et al. in 2002, transcatheter aortic valve implantation (TAVI) has become the standard therapy for many patients with severe AS. In addition, commercially available<sup>11</sup> and investigational<sup>12</sup> devices have been used to treat native aortic regurgitation (AR).

Imaging plays a central role to assess (Table 3) patient selection; AS severity; AV anatomy; pre-procedural planning: (i) annular size and shape, (ii) extent and distribution of valve and vascular calcification, (iii) risk of coronary ostial obstruction, (iv) aortic root dimensions, (v) optimal fluoroscopic projections for valve deployment, (vi) feasibility of vascular access (femoral, subclavian, axillary, carotid, transcaval, or TA), and (vii) prosthetic type and size; procedural guidance; and follow-up.

## TAVI devices

Current-generation commercially available valves include balloon-expandable (BE) [e.g. SAPIEN 3, SAPIEN 3 Ultra (Edwards Lifesciences),

and Myval (Meril)] and self-expanding (SE) valves [e.g. Evolut PRO+ (Medtronic), ACURATE neo2 (Boston Scientific), Allegra (NVT), and Portico (Abbott Vascular)]<sup>13</sup> (Table 4).

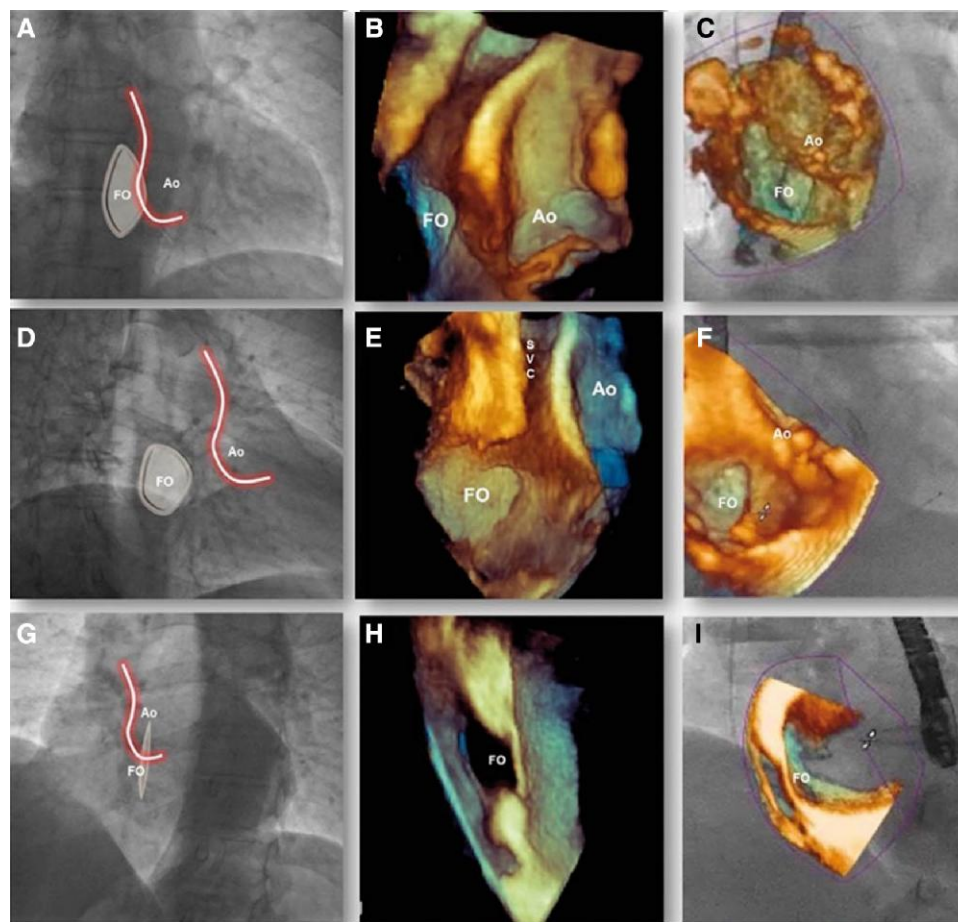
Newer-generation devices have been developed in an attempt to reduce the risk of stroke, vascular complications, PVLs, and conduction disturbances.<sup>14</sup>

The latest-generation Edwards SAPIEN 3 valve consists of bovine pericardial leaflets mounted within a BE cobalt–chromium stent with an outer seal cuff. The latest SAPIEN 3 Ultra has an increased outer skirt height to further reduce PVL.<sup>15</sup> The SAPIEN valves are intra-annular devices, possibly resulting in higher residual gradients compared with supra-annular designs, particularly in patients with smaller annuli. They are not repositionable although a distal flex mechanism and fine positioning control are incorporated for accurate placement.<sup>16</sup> The lower stent frame profile makes coronary re-access after TAVI easier and causes less protrusion into the left ventricular outflow tract (LVOT), thereby reducing the risk of conduction disturbances and requirement for pacemaker implantation.

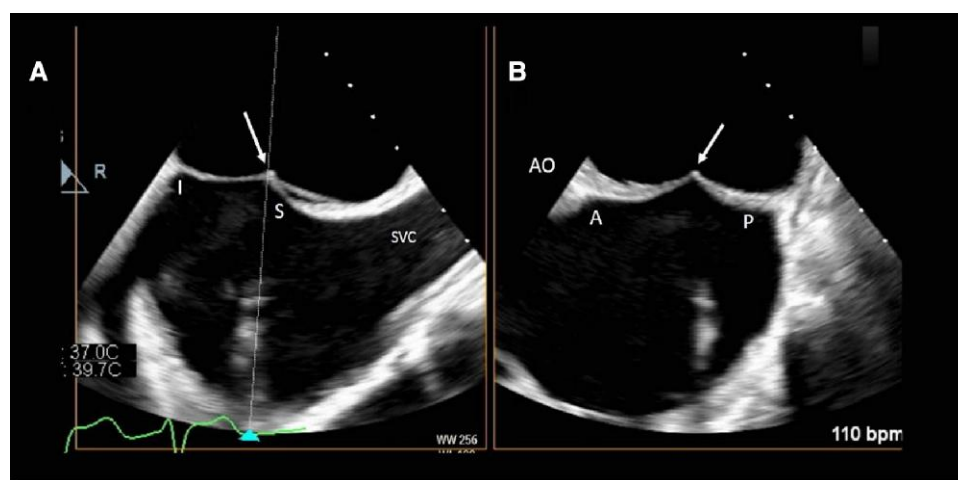
The latest-generation CoreValve device, the Evolut PRO, has a SE nitinol frame with mounted leaflets of porcine pericardium and a skirt designed to reduce the risk of PVL.<sup>16</sup> These are supra-annular valves with increased effective orifice areas (EOA) and lower gradients than intra-annular devices. Moreover, as opposed to former generations, the current systems are repositionable and retrievable. Compared with BE systems, the Evolut delivery system is not steerable and has an increased frame height (lower in the latest-generation devices) with a diamond frame lattice that may make coronary re-access more challenging.<sup>17</sup>

The MyVal valve is a next-generation BE valve made up of a nickel-cobalt frame and bovine pericardium leaflets, with open cells on the upper half to ensure un-jailing of the coronary ostia, closed cells on the lower half for high radial strength, and a sealing cuff to minimize PVL. The valve received CE mark in 2019 after the results of the 1-year MyVal-1 study.<sup>18</sup>

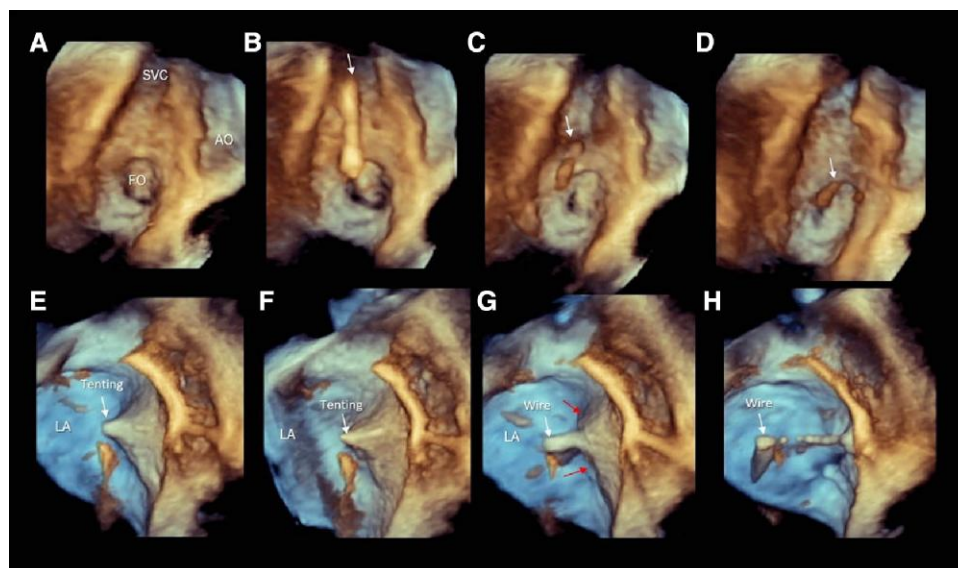




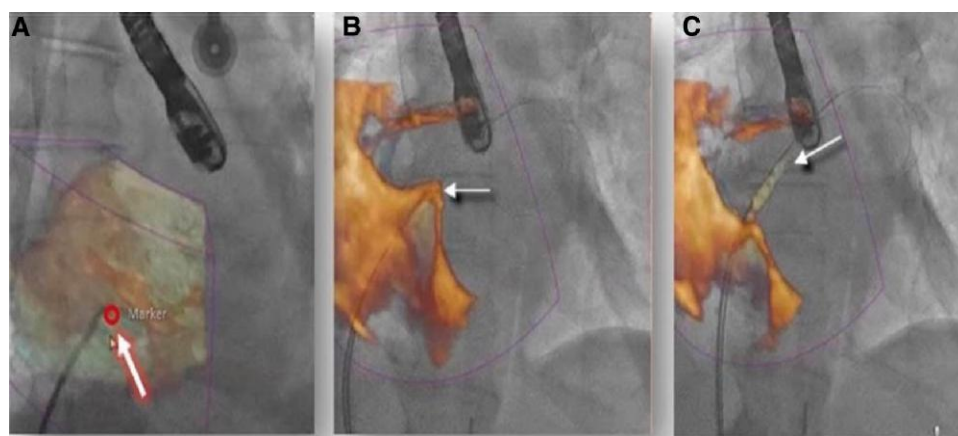
**Figure 3** Fluoroscopic, 3D TOE, and fusion image showing the anatomic relationship between FO and AO. (A–C) AP projection: the white/red line marks the right profile of the AO, partially overlapping the FO. (D–F) RAO 30° projection: the FO is displayed 'en face' and the AO does not overlap the FO. (G–I) LAO 30° projection: the AO nearly completely overlaps the FO; thus, both in 3D TOE and in fusion imaging, the AO must be removed for visualizing the FO in cross-section. SVC, superior vena cava (with the permission of Faletra et al.<sup>180</sup>).



**Figure 4** (A, B) 2D TOE X-plane showing a correct tenting (arrows). The bi-caval view (A) allows to determine the superior (S) and inferior (I) positions, while the SAX view of the AO (B) allows to determine the anterior (A) and posterior (P) positions.



**Figure 5** (A–D) 3D TOE, showing the right side of IAS in en face view. The sequence of still frames shows as the tip of the needle slides down from the SVC to the FO (arrow) (E–H) 3D TOE showing the IAS in ‘tangential view’. The sequence of still frames shows the tenting (arrow) (E, F) and the wire entering in LA (G, H).



**Figure 6** Fusion imaging. Site-specific TSP. (A) The site of the puncture is best localized in RAO 30° where the FO is seen ‘en face’. The fiducial marker (circle and arrow) facilitates the manoeuvre. (B) The ‘tenting’ is seen in LAO 30°. (C) The guidewire is seen crossing the FO (arrow) (with the permission of Faletra et al.<sup>180</sup>).

The Portico valve is made by bovine pericardial leaflets mounted proximal to the ventricular end of a nitinol SE stent, aiming to reduce subannular protrusion and thus conduction disturbances. It is an intra-annular SE valve with a next-generation low-profile delivery system.<sup>19</sup>

The Symetis Acurate Neo SE supra-annular valve consists of an aortic stentless porcine valve mounted on a SE nitinol stent, with low placement of the leaflets. It is provided with an anchoring system to facilitate optimal positioning, it is repositionable, and it has an additional cuff to reduce the risk of PVL.<sup>16</sup>

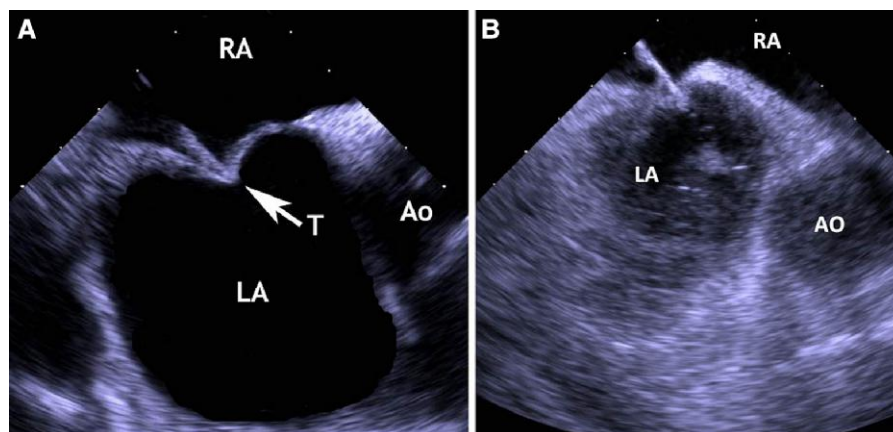
The JenaValve is a porcine root valve mounted within a nitinol SE stent with an anchoring system of three feelers designed to embrace

the native cusps during implantation, thus targeting also native pure aortic regurgitation (NPAR).<sup>20</sup>

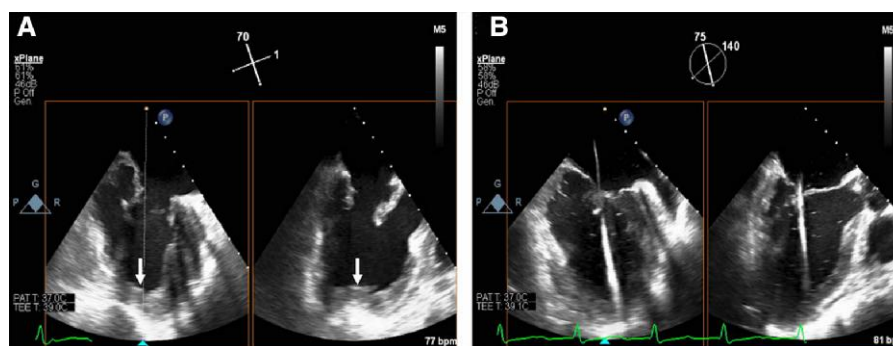
The specific choice of a BE valve or SE valve depends on patient anatomy, clinical, and technical considerations.<sup>21</sup>

### Patient selection

Intervention is recommended in symptomatic patients with severe AS, regardless of left ventricular ejection fraction (LVEF), in asymptomatic patients with severe AS and impaired LV function of no other cause, and in those who are asymptomatic during normal activities but develop symptoms during exercise testing.<sup>2</sup>



**Figure 7** (A) Transatrial ICE view for safe TSP (left panel) and (B) after puncturing the fossa with the appearance of microbubbles in LA.



**Figure 8** Simultaneous bi-plane imaging starting from commissural view showing apex fingered (arrow) by the surgeon (A). (B) The introduction of the sheath, wire, and delivery system is monitored by simultaneous bi-plane imaging, in order to properly evaluate medio-lateral and anterior-posterior location and to exclude aortic engagement or papillary muscle entrapment.

The choice of the most appropriate mode of intervention should be carefully considered by the Heart Team in all patients, accounting for age, estimated life expectancy, comorbidities (including frailty and overall quality of life), anatomical and procedural characteristics, the relative risks of surgical aortic valve replacement (SAVR) and TAVI and their long-term outcomes, prosthetic heart valve durability, feasibility of transfemoral TAVI, and local experience and outcome data.<sup>2</sup>

Prosthetic heart valve durability is a key consideration in younger patients (<75 years) at low surgical risk, and SAVR (if feasible) is therefore the preferred treatment option. Conversely, durability is a lower priority in older patients (≥75 years), or those who are inoperable or high risk for surgery, and TAVI is preferred in these groups [particularly if feasible via transfemoral approach (TFA)].<sup>2</sup>

In summary, SAVR is recommended in younger patients who are low risk for surgery (<75 years and STSPROM/EuroSCORE II <4%) or in patients who are operable and unsuitable for transfemoral TAVI (Class I, Level B).<sup>2</sup> TAVI is recommended in older patients (≥75 years) or in those who are high risk (STSPROM/EuroSCORE II >8%) or unsuitable for surgery (Class I, Level B).<sup>2</sup> For the remaining patients, the Heart Team should make tailored recommendations (SAVR or TAVI)

based upon their individual clinical, anatomical, and procedural characteristics (Class I, Level B).<sup>2</sup>

### Patient selection: key point

- (i) The interventional imager should clearly underline in the report all the important imaging aspects to be considered by the Heart Team for the decision between SAVR and TAVI.

### Severity of AS

#### Transthoracic echocardiography

TTE is the key imaging modality for evaluation of AS. It allows the quantification of AS severity, visualization of the number and position of cusps, qualitative assessment of calcium deposition, and the presence of concomitant abnormalities.



**Table 3** Imaging in TAVI

Essential assessments	Imaging modalities
Severity of AS	2D TTE, CT, 2D TOE, 3D TOE, and Stress Echo
Valve morphology	2D TTE–TOE and CT
LV morphology	2D/3D TTE, 2D/3D TOE, CT, and CMR
LV function	2D/3D TTE and MRI
LVOT evaluation	2D/3D TTE–TOE and CT
RV morphology and function	2D/3D TTE and CMR
Concomitant valvulopathies	2D/3D TTE–TOE
Annulus measurement	CT and 3D TOE
Aortic root measurement	CT and 2D/3D TOE
Vascular accesses	CT
Procedural monitoring	Fluoroscopy, 2D TTE, 2D TOE, and fusion imaging
Follow-up	2D/3D TTE, 3D/3D TOE, CT, and CMR

Abbreviations as in the text.

Current international recommendations for the echocardiographic evaluation of AS depend upon measurement of mean pressure gradient, peak transvalvular velocity ( $V_{max}$ ), and valve area.<sup>22</sup> Although valve area is the theoretically relatively flow independent, its evaluation is technically demanding incorporating several sources of error which make measurement precision relatively poor. Echocardiographic measures of AS severity is discordant in between a fifth and a third of patients, most commonly where the peak velocity and mean gradient (MG) suggest moderate stenosis but the aortic valve area (AVA) is in the severe range.

Additional parameters must be taken into account in discordant cases and to accurately categorize patients with AS: stroke volume (SV), degree of valve calcification, LV function, and the presence or absence of LV hypertrophy. Low flow is arbitrarily defined by a stroke volume index ( $SV_i$ )  $\leq 35$  mL/m<sup>2</sup>.








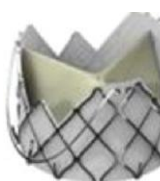

In addition, TTE is essential to identify additional findings such as concomitant valvular diseases, intracardiac masses, haemodynamically significant LVOT dynamic obstruction or LV anatomy at risk of LVOT obstruction (LVOTO) after valve replacement, severe pulmonary hypertension, and right ventricular (RV) dysfunction.<sup>23</sup> Among concomitant valvular disease, MR is frequent: large TAVI series have highlighted these patients to have worse baseline clinical profile with worse LV remodelling, lower LVEF, larger volumes, smaller AVA, higher systolic pulmonary pressure, and higher overall morbidity and mortality.<sup>24</sup>

#### Transoesophageal echocardiography

Although pre-procedural TOE to evaluate the AV and aortic root complex is not mandatory, it may be appropriate, particularly when CT is contraindicated or unavailable or when TTE is not diagnostic or anatomical features seen by TTE raise concern for TAVI feasibility or suggest a high risk for complications.<sup>25</sup>

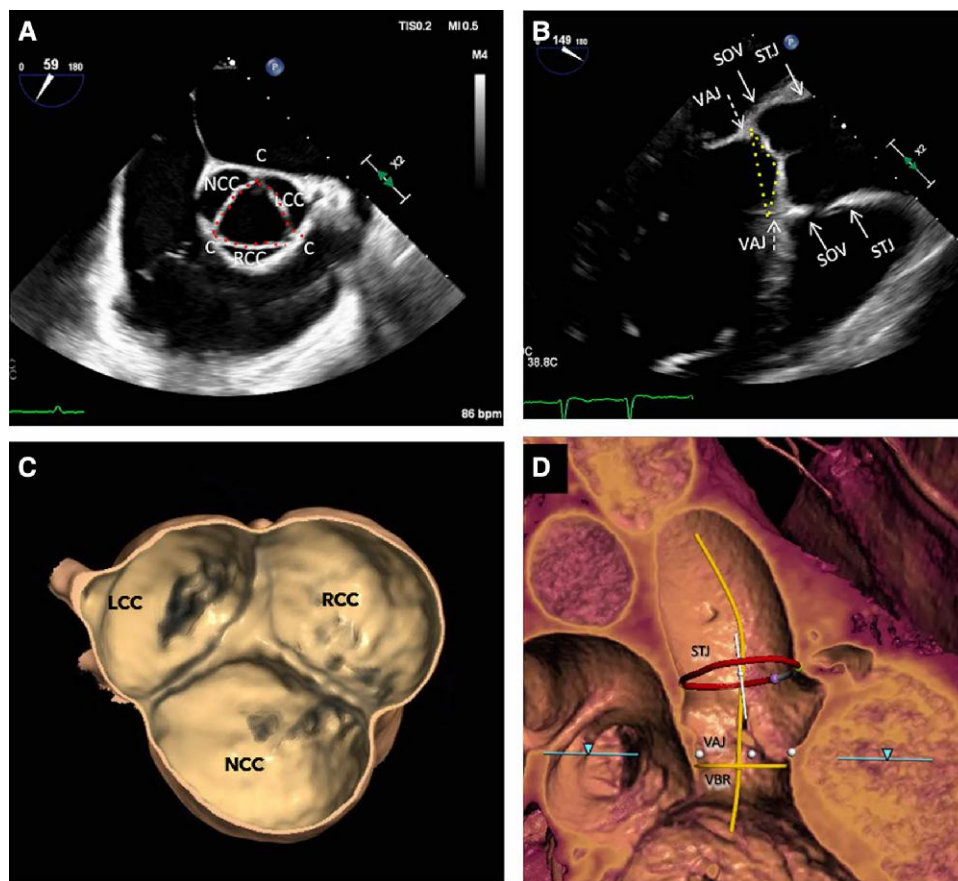
TOE can give essential and additional information regarding the morphology of the AV, the aortic root, the basal LV septum, and sub-aortic pathology, better quantification of AR, delineation of associated aortopathy and evaluation of thoracic aortic plaques, and concomitant

**Table 4** CE-marked available devices for TAVI

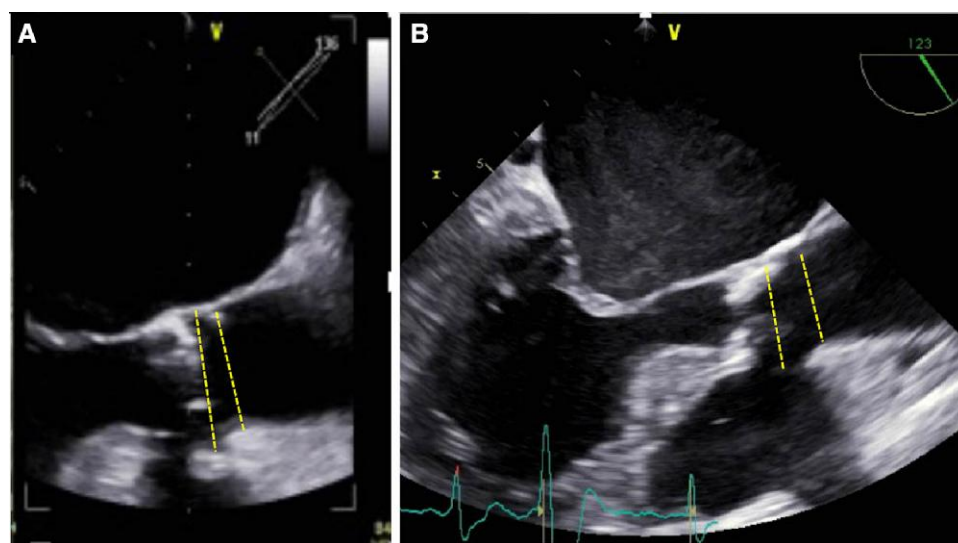
BE devices		
		
SAPIEN 3 (Edwards Lifesciences, Irvine, CA)		
		
Myval (Meril Life Sciences Pvt Ltd, India)		
SE devices		
Supra-annular	Intra-annular	
		
Evolut R/PRO (Medtronic, Minneapolis, MN)	Portico (Abbott, Abbott Park, IL)	Navitor (Abbott, Abbott Park, IL)
		
ACURATE neo 2 (Boston Scientific, Marlborough, MA)	J-Valve (JC Medical Inc, Burlingame, CA, USA)	
Devices for AR		
		
J-Valve (JC Medical Inc, Burlingame, CA, USA)	JenaValve (JenaValve Technology, Munich, Germany)	

valvulopathies (i.e. MR) to clarify its severity and mechanism and to exclude or confirm intracardiac masses. When TTE is not diagnostic to define the severity of AS, TOE can be used to assess the morphology of the AV, the 2D and 3D AVA,<sup>26,27</sup> and for comprehensive Doppler interrogation using transgastric and deep transgastric views. Finally, TOE can be an alternative imaging modality for aortic annulus sizing.



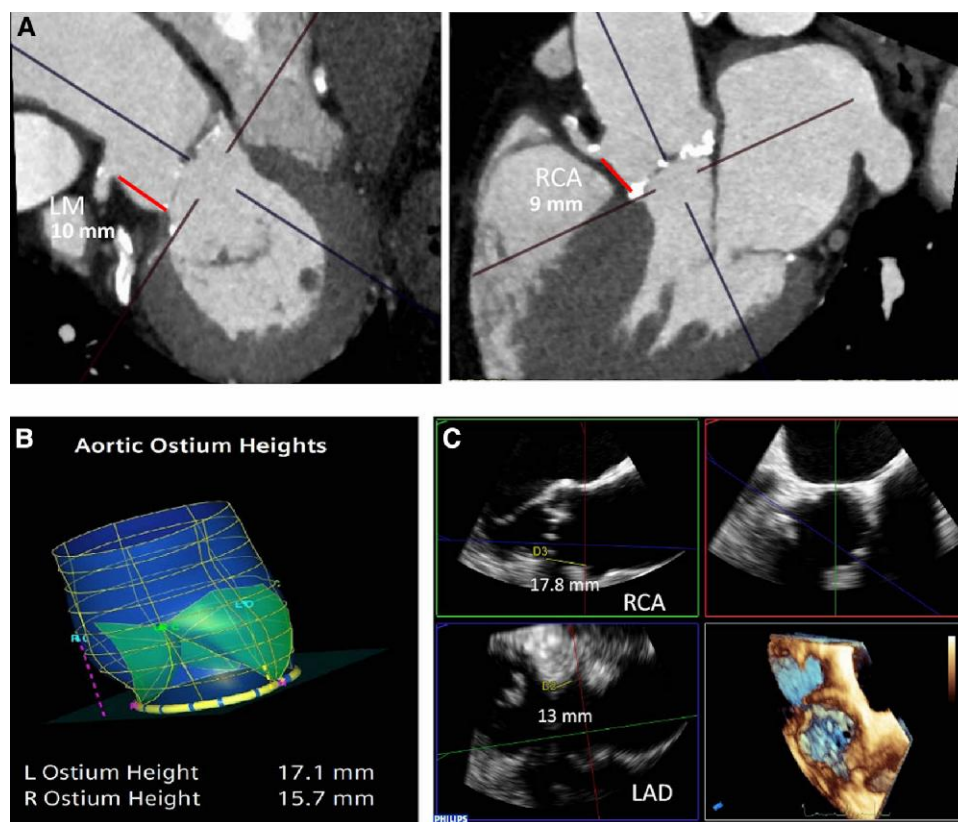


**Figure 9** The anatomy of the aortic root. (A, B) 3D TOE reconstruction (dashed lines: lunule; yellow triangle: interleaflet triangle). (C, D) CT reconstruction. NCC, non-coronary cusp; LCC, left posterior sinus; RCC, right posterior; C, commissures; STJ, sino-tubular junction; VAJ, ventricular-arterial junction; SOV, sinuses of Valsalva; VBR, virtual basal ring.



**Figure 10** Different morphologies of SOV and STJ. 2D ME LAX views showing comparison between normal (A) and small aortic root diameter (27 mm at SOV) and the presence of shallow/obliteration of SOV-STJ (B).





**Figure 11** Localization of the coronary orifices and measurement of coronary ostial annular distance. (A) CT MPR: evaluation of coronary ostia height from annular plane. (B) 3D TOE reconstruction of the coronary ostia height by semi-automatic software. (C) MPR post-processing of a 3D data set of the aortic root. The height of coronary ostia from annular plane can be obtained by adjusting on the transverse plane the sagittal and coronal planes in order to intercept the right and the left coronary ostia, respectively.

image reconstruction thickness  $\leq 1$  mm in order to obtain accurate 2D/3D multiplanar reconstructions (MPR); therefore, it is mandatory to have at least a 64-multidetector CT scanner.

Images reconstructed in the systolic phase should be preferred for the measurement of annulus sizes because in this phase, the annulus is slightly but significantly larger than in diastole.<sup>36</sup>

The evaluation of the aortic annulus must be performed using specific oblique 3D reformatted planes (Figure 13). 2D/3D MPR tools provide the specific aortic planes (long axis and orthogonal planes). These aortic planes can be automatically generated by dedicated software with a specific TAVI module. The LAX and SAX diameters, the cross-sectional area, the perimeter, and the three corresponding derived mean diameters should all be reported. The report should also include the diastolic intraluminal (inner edge-to-inner edge) maximum diameters of the SOV, as well as the STJ and ascending and descending AO.

Recent advances have illustrated the potential of patient-specific 3D-printed models to aid in pre-procedural planning, device sizing, and estimation of the possible risk of PVL.<sup>37</sup> Future 3D-printed models may incorporate information from multimodal imaging to capitalize upon the advantages of each imaging modality. This may be especially helpful in patients with complex anatomy.

#### Echocardiography

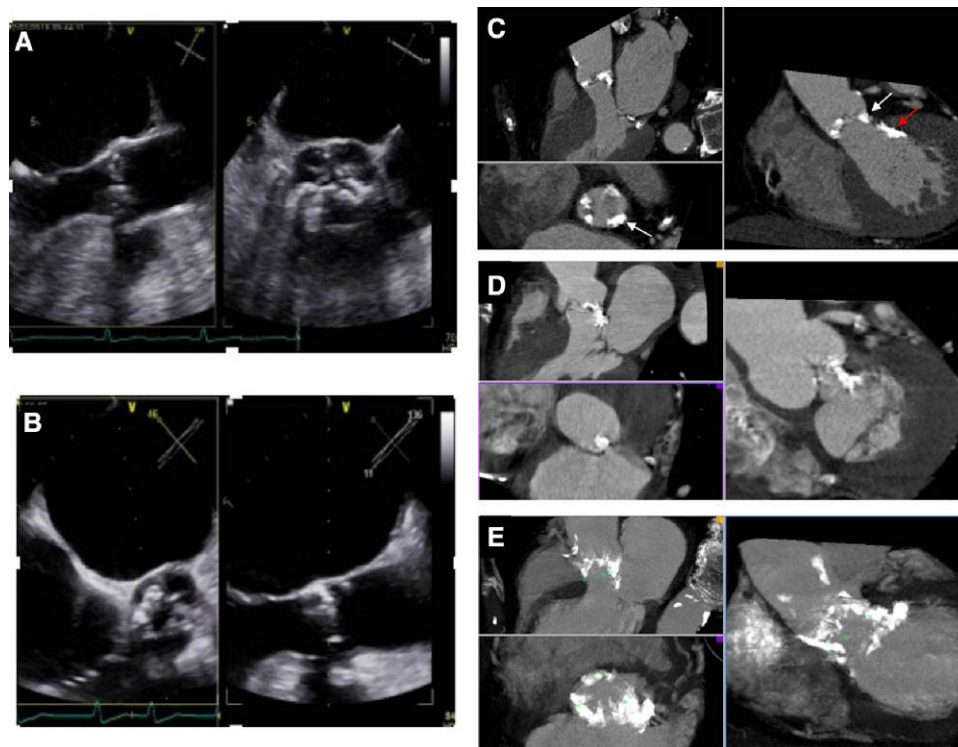
When contrast CT cannot be performed (i.e. chronic renal failure and urgent TAVI), 3D TOE offers an alternative imaging approach to

evaluate the aortic root.<sup>38,39</sup> 3D zoom acquisition should be performed being careful to include the entire annulus in the data set giving priority to frame rate and imaging resolution. Once a 3D volume data set has been obtained, the annulus can be measured by two methods: (i) MPR which allows direct manual measurements (Figure 13) and (ii) semi-automated software which performs quantitative analysis of the aortic root (Figure 13). The semi-automated software provides a static or dynamic model and geometric measurements of the aortic root.

The published data show a good correlation between 3D TOE and CT measurements both manual and semi-automated analyses even though 3D TOE underestimates the major diameter, area, and perimeter compared with respective CT measurements by 3.5–7.4%, but they do not change significantly the choice of the transcatheter heart valve (THV) size in general.<sup>39</sup> Hence, if 3D TOE data are the sole source of annulus measurements, then the local expertise and reliability should influence the confidence on these measurements for selection of THV size.

2D and 3D echocardiography can provide additional data on valve anatomy and surrounding structures, calcifications in LVOT, basal septal hypertrophy, distribution of valvular calcification, and localization of the coronary orifices. The determination of the right coronary ostial-annular distance from the annular plane is possible with 2D TOE in mid-oesophageal (ME) LAX view, but the left coronary annular-ostial distance can only be measured from the coronal plane that cannot be acquired by standard 2D imaging and thus requiring 3D TOE MPR imaging (Figure 11B and C).





**Figure 12** Assessment of the burden and distribution of AV calcification. (A, B) Biplane view of severely calcified AV stenosis. SAX view allows for the qualitative evaluation of calcium burden in terms of location, extension, and distribution. (A) A case of symmetric distribution. (B) A case of asymmetric distribution. (C–E) CT MPR. (C) A case of symmetric distribution of calcium with an extent to the annulus (white arrow) and LVOT (red arrow). (D) A case of asymmetric location of calcium, with the extent to mitral–aortic curtain. (E) Severe and circumferential calcification of LVOT.

### Other imaging techniques

CMR offers an alternative to contrast CT although this is not commonly used.<sup>40</sup> Despite excellent spatial resolution and the accuracy of the CMR measurements, the protocols are time consuming. Additionally, calcification cannot be assessed or quantified by CMR, and while this may aid assessments of the peripheral vasculature (avoiding problems with calcium blooming), it limits assessment of the calcium burden in the valve and LVOT.

## Annular sizing: key points

- (i) CT is the reference imaging modality for aortic annular sizing.
- (ii) The aortic annulus evaluation must be performed using specific oblique 3D reformatted planes carefully re-orientated into the valve.
- (iii) It is mandatory to detail the anatomy of AV, LVOT, basal septal hypertrophy, SOV diameters and heights, STJ and ascending and descending aortic diameters, coronary ostia, distance of coronary ostia from the annular plane, and amount and distribution of aortic calcification.
- (iv) 3D TOE is a valuable alternative imaging modality to evaluate the aortic root when contrast CT cannot be performed.

### Procedural access assessment

## Femoral: CT

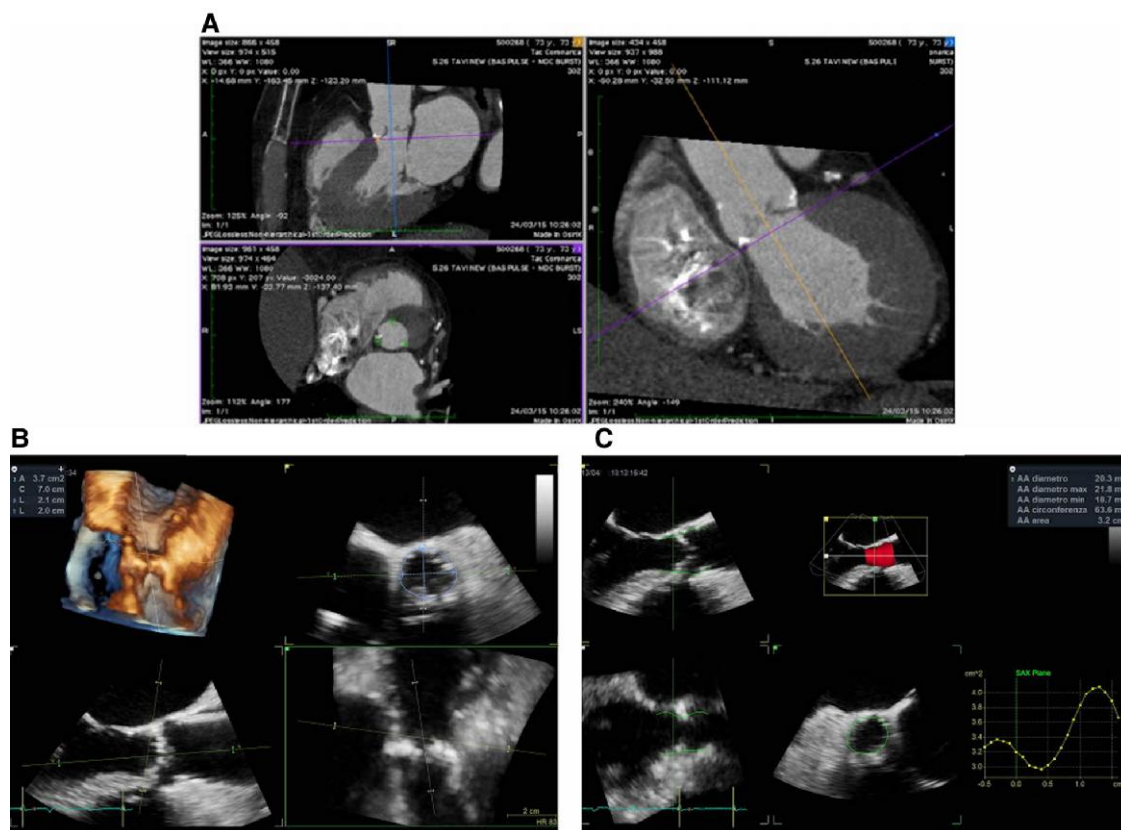
Nowadays, the retrograde TFA is still the most used in clinical practice thanks to the minimal invasiveness.<sup>41</sup> Despite the wide use of TFA, several multicentre trials showed that this technique is not free of complications.<sup>42</sup> Indeed, complications related to procedure range from 10 to 20% including vessel rupture, dissection of superficial circumflex iliac artery, common iliac artery, AO, vessel occlusion, bleeding, haematoma, or development of false aneurysm.<sup>43</sup> Therefore, the selection of patients needs to be evaluated carefully. Commonly, the approach in TFA is percutaneous; however, in selected cases, open surgical access may be appropriate.<sup>44</sup>

CT angiography can provide information regarding the morphology and the presence and nature of atherosclerotic disease affecting all the vessels involved in TAVI performed with TFA. Acquisition protocols for the evaluation of the peripheral vessels should include the administration of contrast agents and high spatial resolution acquisition.

Suggested diameters of the peripheral vessels should be at least 6 mm with little tortuosity, no severe stenosis, or calcifications. This is to accommodate the TAVI deliver catheters which have a calibre ranging from 14 to 20 French (F).<sup>45</sup>

In patients that have previously undergone stent implantation in the AO, iliac, or femoral arteries, the indication for TAVI and optimal access route should be carefully evaluated.<sup>41</sup>

Some clinical cases of femoral access evaluation are listed in *Figure 14*.



**Figure 13** Measurement of aortic annular dimension. (A) CT MPR method shows coronal, sagittal, and transverse planes adjusted to get the true cross-sectional plane of aortic annulus (marked by the coplanarity of the three green markers placed on the cusps nadir). (B) 3D TOE aortic annulus measurement by MPR method. In clockwise order, 3D volume cropped along the coronal plane, transverse plane (short axis), coronal plane (major diameter), and sagittal plane (minor diameter). (C) Annulus measurement by semi-automatic software.

#### Non-femoral access routes: what to assess at CT?

Forms of access that can be used as an alternative when femoral access is contraindicated include the subclavian (the second most commonly used), transaortic (TAo), and TA approaches. The latter two require a surgical approach and are therefore less commonly used.

#### Subclavian

The subclavian approach represents an optimal alternative in cases where there is contraindication to TFA and the TA approach.<sup>46</sup> The most common approach is surgical with a dissection or retraction of pectoralis followed by exposition of the subclavian artery.<sup>45</sup> Several anatomical evaluations are required to effectively plan TAVI procedures using the transsubclavian artery approach. Evaluation with CTA represents a fundamental tool for this purpose assessing the calibre, calcification, and tortuosity of the subclavian artery. In addition, TAVI procedures via the right subclavian artery may be challenging when the angulation between the plane of the valve and the horizontal plane is  $\geq 30^\circ$ .<sup>45</sup> Careful evaluation should be considered in patients who underwent previous coronary artery bypass graft (CABG) surgery,<sup>47,48</sup> where the subclavian artery may be calcified or small and there may also be abnormalities of vertebral arteries.<sup>49</sup>

#### Transaortic

Patients who do not have suitable peripheral vessels may benefit from a direct TAo approach. Two different kinds of TAo approaches have

been described in the literature that allow exposure of the ascending AO. If the ascending AO is positioned on the right side of the mediastinum in proximity to the rib cage, a right anterior thoracotomy is preferred. Conversely, if the AO is in the midline or deeper, a mini-sternotomy is suggested.<sup>50,51</sup>

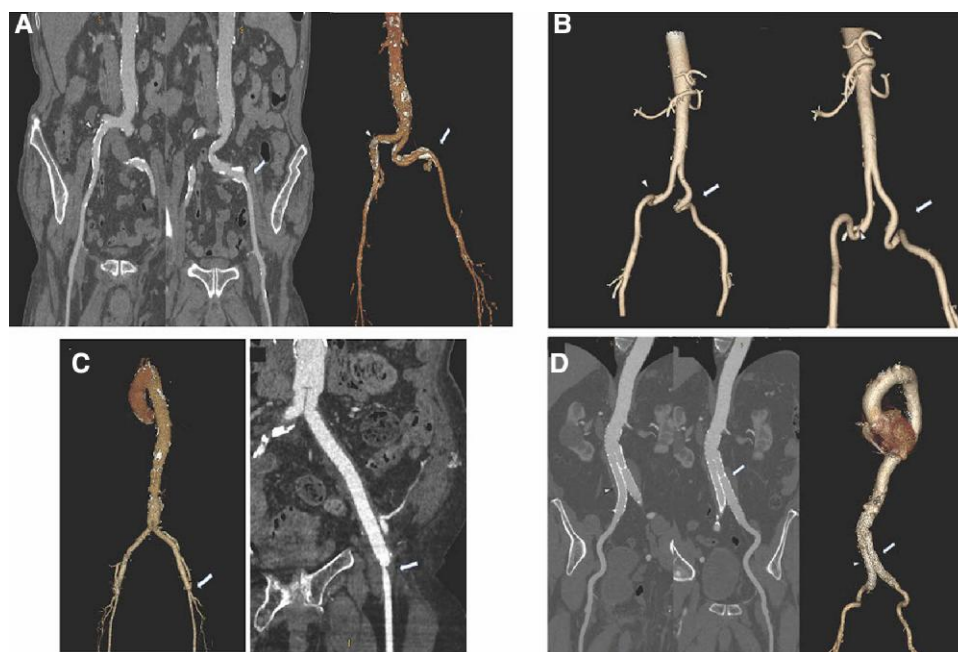
Evaluation with CTA in patients who will undergo a TAo approach is focused on evaluation of the ascending AO anatomy and selection of the most feasible approach as well as assessment of aortic calcifications. Indeed, in patients with a porcelain AO, the TAo approach is often not suitable.<sup>52</sup>

#### Transapical

The TA approach is an alternative to the aforementioned vascular approaches that can be performed in almost every patient.<sup>53</sup> In the TA technique, a left antero-lateral mini-thoracotomy is usually performed in the fifth or sixth intercostal space, followed by exposure of the pericardium and access to the left ventricular apex.

#### Others

Despite the relatively safe and wide clinical use of TFA, several other approaches have been described in literature. These include the caval-aortic approach where the descending abdominal AO is reached through the ilio-femoral veins and inferior vena cava. Again, CT is fundamental in the evaluation of the anatomy of both the arterial and venous system and the presence and severity of associated atherosclerosis.<sup>54</sup> The transcatheter



**Figure 14** Femoral access evaluation by CT for planning of TAVI with TFA. (A) Multiplanar and 3D volume rendering reconstructions show kinking and calcifications of both right (arrowhead, left and right panels) and left (arrow central and right panels) superficial iliac arteries. (B) 3D volume rendering shows the kinking of both right (arrowhead) and left (arrow) common and superficial circumflex iliac arteries. (C) Presence of severe stenosis on the left distal graft of aorto-bifemoral bypass showing diameters of  $3.8 \times 3$  mm (arrows). (D) CTA showed the presence of aortoiliac stent in order to exclude presence of abdominal aneurysm. Both common iliac arteries are patent and suitable for TF approach (arrows).

(TC) surgical technique has been described by Modine *et al.*<sup>55</sup> Firstly, the carotid artery is exposed; subsequently, TAVI delivery catheters are inserted inside the vessel lumen. The main advantage of the TC approach is the direct access it provides to the aortic root, although it is contraindicated in patients at risk of neurological implications due to temporary occlusion of the carotid artery.<sup>56</sup> CT is again useful in evaluating the anatomy of the carotid arteries, aortic arch, and intracranial arteries.<sup>57</sup>

### Vascular access: key points

- (i) CT is the main imaging modality to evaluate the optimal access point and route for TAVI.
- (ii) TFA is the preferred vascular access technique. Information on the presence and severity of atherosclerosis as well as vessel calibre, calcification, and tortuosity of all the vessels involved in the selected TAVI procedure must be reported.
- (iii) In case of absolute contraindications to CT scan, echographic evaluation of iliac and femoral arteries should be carried out.
- (iv) Other access routes should be considered with caution, as they carry a higher procedural complexity and risk of complications than TFA.

### Areas in development

#### Bicuspid aortic valve

Bicuspid aortic valve (BAV) is a congenital disease affecting up to 2% of the general population and up to 20% of octogenarians and nonagenarians referred for AV replacement.<sup>58</sup>

A TAVI-directed simplified BAV classification, according to (i) the number of commissures (two vs. three) and (ii) presence or absence of a raphe, has been proposed. Three morphologies are encountered: (i) tricommissural, often referred to as 'functional' or 'acquired' BAV (not part of the Sievers classification); (ii) bicommissural raphe-type (equivalent to Sievers Type 1), when there is a fibrous, calcified fusion raphe that does not reach the height of the commissure; and (iii) bicommissural non-raphe-type (equivalent to Sievers Type 0).<sup>59</sup> This classification was designed as a simplified representation relevant to TAVI to take into account the interface of prosthesis and the aortic–valvular complex, at both the basal leaflet plane (presence or absence of a raphe) and at the commissural level (presence of two or three commissures). A raphe, particularly if calcified, may influence TAVI expansion and apposition at the annular level. Moreover, the concept of a supra-annular commissural seal mitigating the PVL<sup>60</sup> and the presence or absence of a third commissure may also influence TAVI apposition, as well as there is some relevance in the intercommissural distance for the prediction in PVL in bicommissural but not tricommissural BAV.

BAV stenosis is often associated with aortopathy, a larger and more oval-shaped annulus, heavily calcified leaflets, asymmetric calcium distribution, and unusual orientation of the coronary ostia. Each of these constitutes a potential technical challenge for TAVI valve sizing, optimal device positioning, and expansion.

The technical approach for TAVI in a patient with BAV involves balloon valvuloplasty before prosthesis deployment, avoidance of aggressive oversizing in relation to the aortic annulus diameter or supra-annular sizing, and slow gradual deployment.<sup>61,62</sup>

A recent meta-analysis showed that BAV patients treated with TAVI had similar 30-day and 1-year mortality as well as stroke, vascular complications, and new pacemaker implantation rates compared with tricuspid valve subjects, but carried higher risk of moderate/severe PVL,

need for implantation of a second valve, annular rupture, conversion to surgery, and device failure.<sup>63</sup> Event rates significantly decreased with the use of new-generation devices, but TAVI still showed better procedural results in tricuspid valve compared with BAV.<sup>63</sup>

Open questions remain concerning the most favourable candidate anatomy, the role of aortic root morphology, the best sizing method, and the relationship between under-expansion and device durability.

In particular, there is a lack of consensus on the optimal sizing methods in BAV.<sup>64</sup> Different methods have been proposed: (i) based on the annulus plane, as for tricuspid valves, and (ii) the supra-annular one, where the so-called intercommissural distance is identified. Sizing methods take into consideration these two planes, separately or in combination.<sup>65</sup> In addition, two other methods have been proposed: (i) a balloon-sizing method relying on the intra-procedural evaluation during pre-dilation and (2) a method in which the sizing is performed at the level of the raphe where valve anchoring is assumed (Level of Implantation at the RAphe method).<sup>66</sup>

Aortic regurgitation

Surgical treatment is nowadays the gold standard for NPAR. TAVI appears an option for inoperable/high-risk patients<sup>11</sup>; however, it still remains an off-label indication until randomized control trials are performed and long-term results available. In this setting, TAVI shows higher rates of in-hospital mortality and complications, but lower stroke rate compared with results in AS populations.

The relatively low burden of valve calcification in NPAR patients is a challenge for the procedure and, in particular, for landmark identification at fluoroscopy and prosthesis anchoring. In fact, the available devices are not strictly designed to address NPAR. In addition, the annular or aortic dimensions are usually bigger and more spherical, and together with the increased SV secondary to severe regurgitation, device positioning and deployment is made very difficult with predisposition to embolization or malposition and subsequent higher risk of moderate-to-severe post-procedural AR (associated with worst clinical outcomes).<sup>67</sup>

Valve oversizing has been proposed to reduce the risk of valve migration: published data recommend a 15–20% oversize with the caution not to oversize beyond 20% due to the risk of annular rupture and conduction system abnormalities.<sup>68,69</sup> Given the absence of calcification and fluoroscopic landmarks, it has been suggested to use two pigtail catheters in different SOV or fusion-guided imaging to enhance anatomical landmarks for valve deployment. Balloon pre-dilatation should not be performed and rapid pacing is mandatory for BE valves and helpful also with SE valves to reduce the SV, stabilizing the aortic annulus and limiting device motion.

Procedural guidance

TTE vs. TOE

Procedural guidance based on TOE vs. TTE for TAVI procedures has its individual merits and demerits. In 2002, Prof. Alain Cribier performed the first in-man TAVI using general anaesthesia and TOE.<sup>70</sup> In 2012, American College of Cardiology (ACC) recommended that TOE is mandatory for all patients undergoing TAVI.<sup>71</sup> However, in 2017, ACC suggested that TTE can be used as an alternative tool for TAVI procedures.<sup>72</sup>

The rise of the minimalist approach can inhibit TOE for procedural imaging, but we need to consider the advantages/disadvantages compared with the TTE only and local anaesthesia approach (Table 5). TTE is used generally when TAVI is performed under monitored anaesthesia care, whereas TOE is performed in patients requiring a TA or TAo approach. The European trend in experienced centres (who has overcome the learning curve) is to use peri-procedural TTE alongside fluoroscopy for TAVI with TFA.<sup>73</sup>

Table 5 Intra-operative imaging with TTE and TOE

Advantages	Disadvantages
TTE	
Monitored anaesthesia care	Image quality may be compromised
Standard views for assessment of the heart	Needs of sterile field, leading to frequent delay in procedural performance and interruption
Easy availability	Lower resolution and frame rates compared with TOE
Early recovery, not needing general anaesthesia	Frequent exposure of interventional echocardiographer to higher radiation
TOE	
Requires general anaesthesia	Performing TOE in local anaesthesia can be challenging and uncomfortable
Early detection of peri-procedural complications	Trauma to oesophagus and surrounding anatomical structures is possible
Imaging is possible during the entire procedure	Image quality can be compromised due to heavy calcification causing acoustic shadowing
High resolution and high frame rates for 2D/3D TOE	Probe manipulation may be continuously required and can interfere with fluoroscopy
Post-operative assessment can be done in the operating room	Peri-procedural costs may be higher and additional set up is required

The form of anaesthesia largely dictates the mode of ultrasound as TOE guidance is quite uncomfortable for patients. In addition, transnasal TOE and ICE have been suggested as alternative imaging methods in procedures with monitored anaesthesia care.<sup>74</sup>

Nowadays, a minimalist approach based on TTE is preferred, with possible conversion to TOE guidance when haemodynamic deterioration or complications occurred.<sup>75</sup> Still, in newer programmes or in patients at increased risk of procedural complications, TOE guidance may be more appropriate.

In case of minimalistic approach, fluoroscopic guidance based on CT-derived working projections is used during all the steps of the procedure as fluoroscopy is often sufficient for metallic structure of devices and calcifications of the native AV imaging; aortic angiography is a complementary imaging modality.

What to assess? Critical procedural steps

Table 6 summarizes the procedural steps and imaging assessment (Figure 15).

Assessment of AV apparatus

If TOE guidance is used, the procedural re-assessment of the AV apparatus is a critical first step, as faulty measurements can lead to serious complications.



**Table 6** Procedural steps and imaging assessment

Procedural step	Imaging recommendations	2D/3D TEE views	2D TTE views
Pacing wire position <sup>a</sup>	<ul style="list-style-type: none"> <li>Confirm position in RV</li> <li>Exclude perforation and pericardial effusion</li> </ul>	<ul style="list-style-type: none"> <li>ME 4-Ch view (0–30°), TG LAX view (90–120°)</li> <li>ME views, TG SAX view (0–30°)</li> </ul>	<ul style="list-style-type: none"> <li>P-LAX, P-SAX, apical views</li> </ul>
Stiff wire position	<ul style="list-style-type: none"> <li>Exclude interferences with MV apparatus</li> <li>Exclude perforation and pericardial effusion</li> </ul>	<ul style="list-style-type: none"> <li>ME biplane view of MV (2-Ch 60–90°, LAX 120–140°)</li> <li>ME views, TG SAX view (0–30°)</li> </ul>	<ul style="list-style-type: none"> <li>P-LAX, P-SAX, apical views</li> <li>P-LAX, P-SAX, apical views</li> </ul>
BAV	<ul style="list-style-type: none"> <li>Image during and immediately following BAV for AR</li> <li>Exclude coronary obstruction by calcified leaflet</li> <li>Evaluate risk for annular rupture/exclude annular rupture</li> </ul>	<ul style="list-style-type: none"> <li>ME biplane view of AV (SAX 30–60°, LAX 120–140°)</li> <li>ME SAX view (30–60°), LAX, MPR</li> <li>ME biplane view of AV</li> </ul>	<ul style="list-style-type: none"> <li>P-LAX, P-SAX</li> <li>Apical views</li> <li>P-LAX, P-SAX</li> </ul>
Positioning of THV	<ul style="list-style-type: none"> <li>BE valve: outflow edge should cover the native leaflets while being below STJ.</li> <li>SE valve: higher edge of the stent should be 5 mm below the annulus.</li> </ul>	<ul style="list-style-type: none"> <li>ME LAX view (120–140°)</li> <li>ME LAX view (120–140°)</li> </ul>	<ul style="list-style-type: none"> <li>P-LAX</li> <li>P-LAX</li> </ul>
TA puncture	<ul style="list-style-type: none"> <li>Confirm location of the TA puncture site by imaging the apex. Optimal position will avoid the RV, and be angulated away from the interventricular septum.</li> </ul>	<ul style="list-style-type: none"> <li>ME biplane view of LV (2-Ch view, LAX view)</li> <li>Deep TG view (90–110°)</li> </ul>	
Post-deployment	<p>Assess stent positioning, shape, and leaflet motion; perform comprehensive haemodynamic measurements [MG, peak velocity, EOA, and Doppler velocity index (DVI)].</p> <p>PVL assessment</p> <p>Assess coronary artery patency and LV function</p> <p>MV function assessment</p> <p>Estimate pulmonary pressure</p> <p>Exclude perforation and pericardial effusion</p>	<ul style="list-style-type: none"> <li>ME biplane view of AV (SAX 30–60°, LAX 120–140°)</li> <li>Deep TG view (90–110°)</li> <li>ME biplane view of AV (SAX 30–60°, LAX 120–140°)</li> <li>ME SAX view of AV (30–60°); ME and TG SAX views</li> <li>ME biplane view, 3D en face view</li> <li>ME SAX view (0–30°), modified bi-caval view (90–110°)</li> <li>ME views, TG SAX view (0–30°)</li> </ul>	<ul style="list-style-type: none"> <li>P-LAX, P-SAX, apical 5-Ch and 3-Ch views</li> <li>P-LAX, P-SAX, apical 5-Ch and 3-Ch views</li> <li>Apical views for LV function</li> <li>P-LAX, parasternal SAX (PSAX), apical views</li> <li>P off-axis, apical 4-Ch view</li> <li>P-LAX, P-SAX, apical views</li> </ul>

Abbreviations as in the text.

<sup>a</sup>Direct pacing from the wire in the LV is an alternative option.

### Guidewire placement

Complications that can occur during guidewire placement include the following (*Figure 15A*):

- (i) Guidewire entrapment in the secondary chords of the MV.
- (ii) Guidewire is not able to align with the AV and reaches the LA or has a difficult alignment owing to a hypertrophied LV. Despite the fact that placement of the guidewire is more straightforward using the TFA, TOE may still be helpful during this approach.

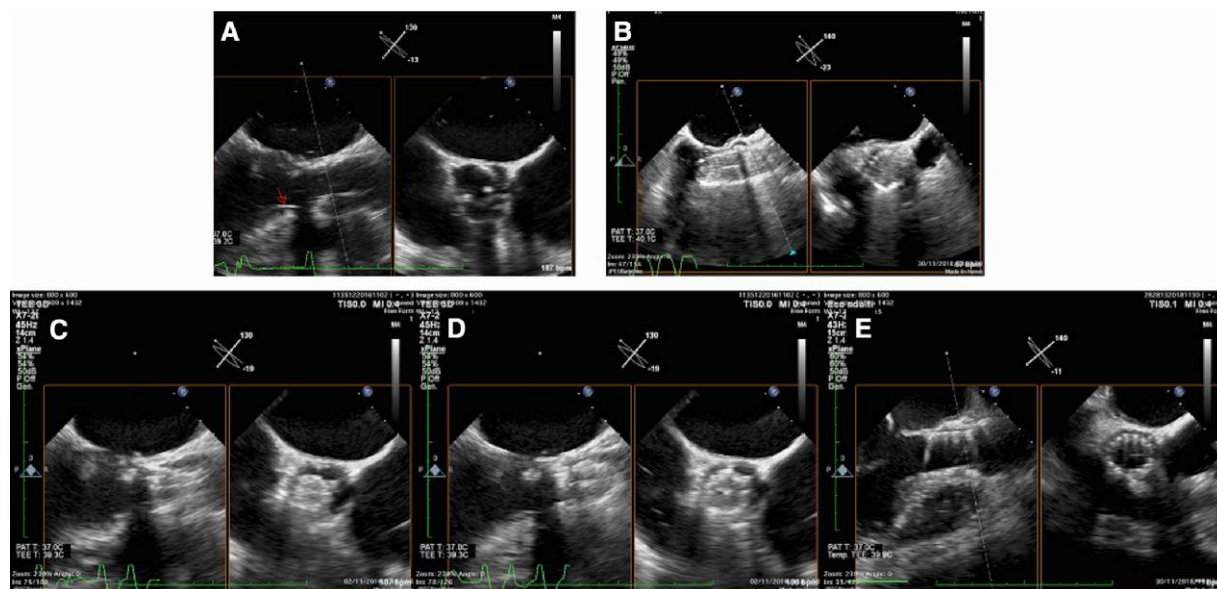
### Balloon valvuloplasty

Biplane TOE imaging is helpful as the balloon needs to be positioned in the middle of the valve for complete dilation of the calcified AV (Figure 15B). The presence of asymmetric calcification as opposed to regular calcification may predispose for post-implantation PVL. The valvuloplasty can be used for confirmation of the annular size and displacement of calcium during valve deployment. Rupture or

sliding of the balloon during valvuloplasty necessitates another attempt with a bigger balloon before valve implantation. In addition, balloon valvuloplasty may cause severe AR which may necessitate rapid valve deployment due to haemodynamic deterioration, especially in severely depressed EF.

### Device implantation

The device position is determined by TOE and fluoroscopy/angiography (Figure 15C–E). Every kind of device needs a specific placement in relation to the nadir of native aortic cusps. The interventional imager involved in TAVI guidance needs to familiarize with the structure of the implantable devices and their delivery systems to ensure that the specific landmarks are identified during the procedure. A possible complication during implantation is MV damage, as the delivery system can obstruct, distort, or perforate the anterior mitral leaflet causing severe regurgitation leading to rapid haemodynamic deterioration. Implanting



**Figure 15** TOE procedural monitoring. (A) Biplane view (LAX and SAX views of AV) showing the guidewire crossing the valve (arrow). (B) Biplane views during balloon inflation allow the accurate visualization of the balloon position. (C–E) Biplane views during step-by-step SE valve deployment.

fluoroscopic view is derived from pre-procedural CT: usually all three cusps of the AV are imaged in an orthogonal plane, typically with the right coronary cusp in the centre. A recent advance consists in the cusps overlaps projection that, by isolating the non-coronary cusp, unforeshortens and elongates the LVOT with more accurate assessment of implantation depth and commissural alignment.

*Device assessment after TAVI: confirm position, prosthetic performance in terms of gradients, and pathological regurgitation (either intra- or peri-prosthetic)*

Dedicated training or experience in post-TAVI echocardiographic evaluation is needed as many complications can be subtle<sup>1</sup>: careful echocardiographic examination after deployment is needed to fully evaluate valve function and screen for complications (Figure 16).

After evaluation of valve position and possible embolization, device performance should be evaluated. A multiwindow approach is indicated, including parasternal, apical, and sometimes subcostal views. Starting from an apical five-chamber view (or the TOE deep transgastric), as it is the least impacted by acoustic shadowing of the prosthesis, allows the evaluation of gradients and the easy detection of any kind of regurgitation. The three-chamber view and the short axis at the base (with up and down tilting), or the equivalent TOE views (ideally in combination using biplane imaging), are used to assess how well the valve is seated, its shape, and circularity and to rule out the presence of para/transvalvular leak; in particular, the short axis could locate the regurgitation, distinguishing intra- vs. para-prosthetic leakage. A multiwindow approach is extremely important in order to overcome acoustic shadowing, thus exploring all the portion of the prosthesis.

Typically, the leaflet's seating improves over the first minutes following implantation and the valvular regurgitation usually ameliorates.

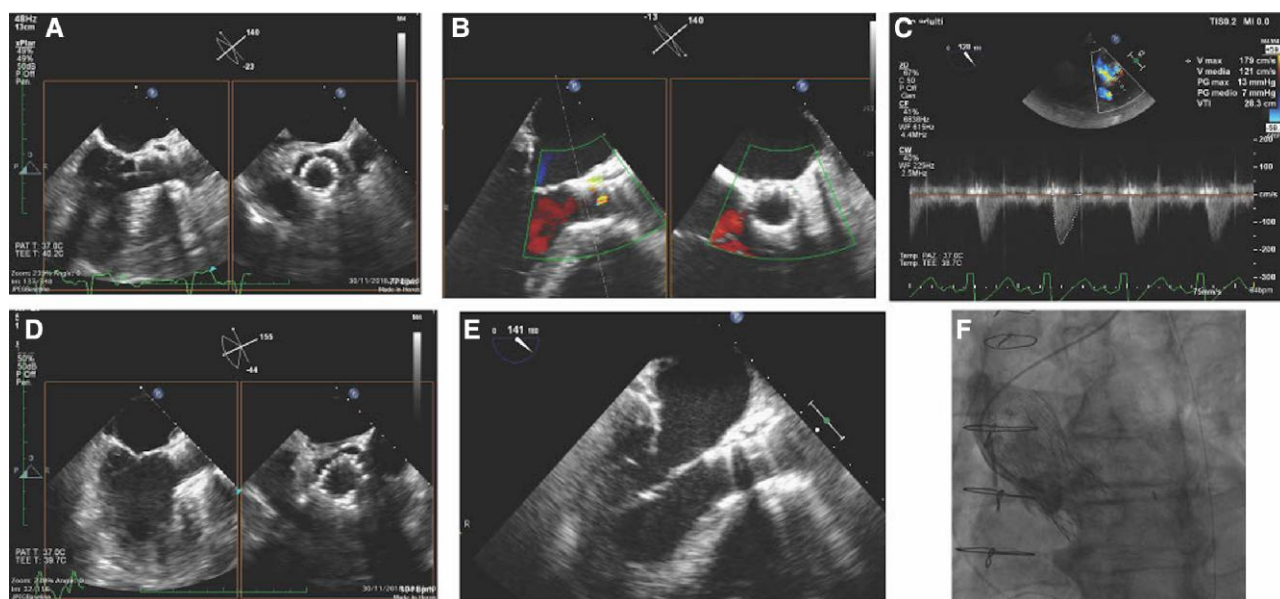
#### Assessment of PVLs

The Valve Academic Research Consortium (VARC) criteria have established the grading scheme for assessment of regurgitation after TAVI.<sup>76</sup> A five-class grading scheme (mild, mild–moderate, moderate, moderate–severe, and severe) or a three-class scheme (mild, moderate, and severe), as recommended by the American Society of Echocardiography and European Association of Cardiovascular Imaging guidelines,<sup>77</sup> can be used. Using the five-class scheme, assigning 'in-between' grades, has already been shown to reduce variability between echocardiography core laboratories.<sup>78</sup>

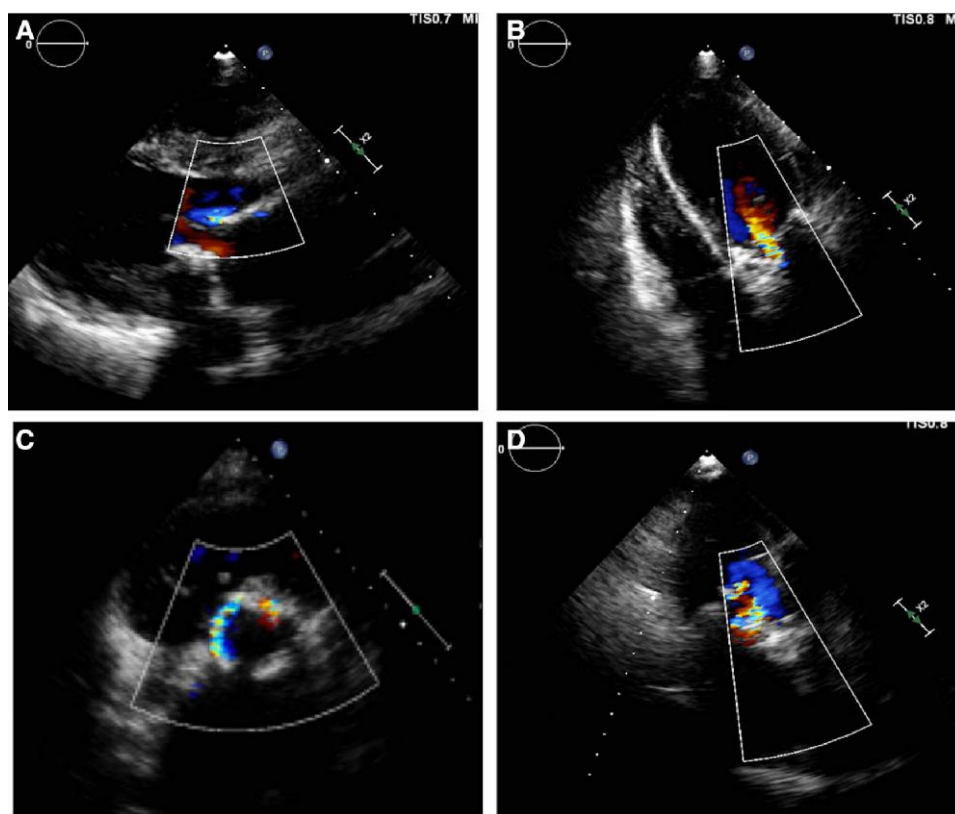
A multiwindow and multiparametric echocardiographic approach incorporates both qualitative and semi-quantitative parameters (Figure 17): the most accurate (semi)quantitative evaluation of the regurgitant jet(s) should be carried out, mainly based on continuous-wave (CW) Doppler density, path length of the paravalvular jet, vena contracta (VC) width, circumferential extension, and if feasible evaluation of diastolic flow reversal in thoracic/abdominal descending AO (Table 7).

Colour Doppler imaging in both SAX and LAX views of the AV, scanning through the entire valve and into the LVOT in order to trace complex jets, should be assessed, as regurgitant jets can occur around the perimeter of the valve and acoustic shadowing could be a problem. Owing to atypical nature of the jets (eccentric/multiple), colour Doppler is more beneficial in localizing (extent and origin) and assessing (multiple, width, eccentric, central, peripheral, and single) the jets compared with typical Doppler parameters (qualitative and semi-quantitative). Quantitative Doppler as effective regurgitant orifice area and 3D colour Doppler area of VC may prove helpful, although tedious to perform in the operating room.

A multimodality approach could be helpful, integrating angiographic and haemodynamic data, sometimes including also invasive assessment of the left ventricular end-diastolic pressure. Aortography provides a qualitative assessment of the residual AR, but it does not provide information on the mechanism of regurgitation (paravalvular vs. transvalvular), which has implications in deciding whether to re-expand the valve or if rescue valve-in-valve is needed.



**Figure 16** Evaluation after prosthesis deployment. (A) Biplane views show the correct shape of the device. (B, C) Functional evaluation of prosthesis. (B) Evaluation of possible presence of AR. (C) Transgastric view for gradient measurement across the valve. (D) Biplane views show the incomplete expansion of the device. (E, F) Incorrect position of the valve. LAX view (E) and fluoroscopy (F) show the protrusion of the valve in the LVOT.



**Figure 17** Example of PVL evaluation by transthoracic examination using multiwindow approach. (A) LAX view. (B) Five-chamber view. (C) Parasternal SAX view. (D) Three-chamber view.

**Table 7** Evaluation of severity of paravalvular regurgitation after TAVI

Severity of paravalvular regurgitation				Main limitation
Echocardiography				
Qualitative or semi-quantitative parameters	Mild	Moderate	Severe	
Jet length and width + number of jets and jet origins	Non-extensive, multiple jets possible	Extensive, multiple jets often present	Extensive, multiple jets often present	<ul style="list-style-type: none"><li>• Jets may not be visible due to acoustic shadowing of stent or calcifications</li><li>• Jet length and width only weakly correlated with severity</li></ul>
Circumferential extent jet	<10%	10–29%	≥30%	<ul style="list-style-type: none"><li>• Less reliable in the presence of multiple or eccentric jets</li><li>• Plane position dependent</li><li>• May be difficult to visualize</li></ul>
Ratio jet width at origin/LVOT diameter	5–30%	30–60%	>60%	
VC width	<3 mm	3–6 mm	>6 mm	<ul style="list-style-type: none"><li>• Often irregularly shaped</li><li>• May be difficult to visualize due to acoustic shadowing and in case of multiple jets</li></ul>
Signal intensity of jet (CW Doppler)	Faint/variable	Dense	Dense	
PHT (CW Doppler)	>500 ms	200–500 ms	<200 ms	<ul style="list-style-type: none"><li>• Heart rate and rhythm dependent</li><li>• Strongly influenced by the compliance of the LV and the AO</li></ul>
Diastolic flow reversal in descending AO [pulsed-wave (PW) Doppler]	Absent	Intermediate	Holodiastolic (>20 cm/s)	<ul style="list-style-type: none"><li>• Strongly influenced by the compliance of the LV and the AO</li></ul>
Quantitative parameters				
RV	<30 mL/beat	30–59 mL/beat	≥60 mL/beat	<ul style="list-style-type: none"><li>• Large inter- and intra-observer variability</li><li>• Cannot be assessed in the presence of &gt;mild mitral or pulmonary regurgitation</li></ul>
EROA	<10 mm <sup>2</sup>	10–30 mm <sup>2</sup>	≥30 mm <sup>2</sup>	
VC area	<10 mm <sup>2</sup>	10–30 mm <sup>2</sup>	≥30 mm <sup>2</sup>	<ul style="list-style-type: none"><li>• Technically difficult with large inter- and intra-observer variability</li></ul>
Ancillary findings			Dilated LV	<ul style="list-style-type: none"><li>• In chronic regurgitation</li></ul>
CMR imaging				
Regurgitant fraction	<20%	20–30%	>30%	<ul style="list-style-type: none"><li>• Variable cut-offs reported</li><li>• Inability to differentiate paravalvular from transvalvular regurgitation</li></ul>

Abbreviations as in the text.

### Complications

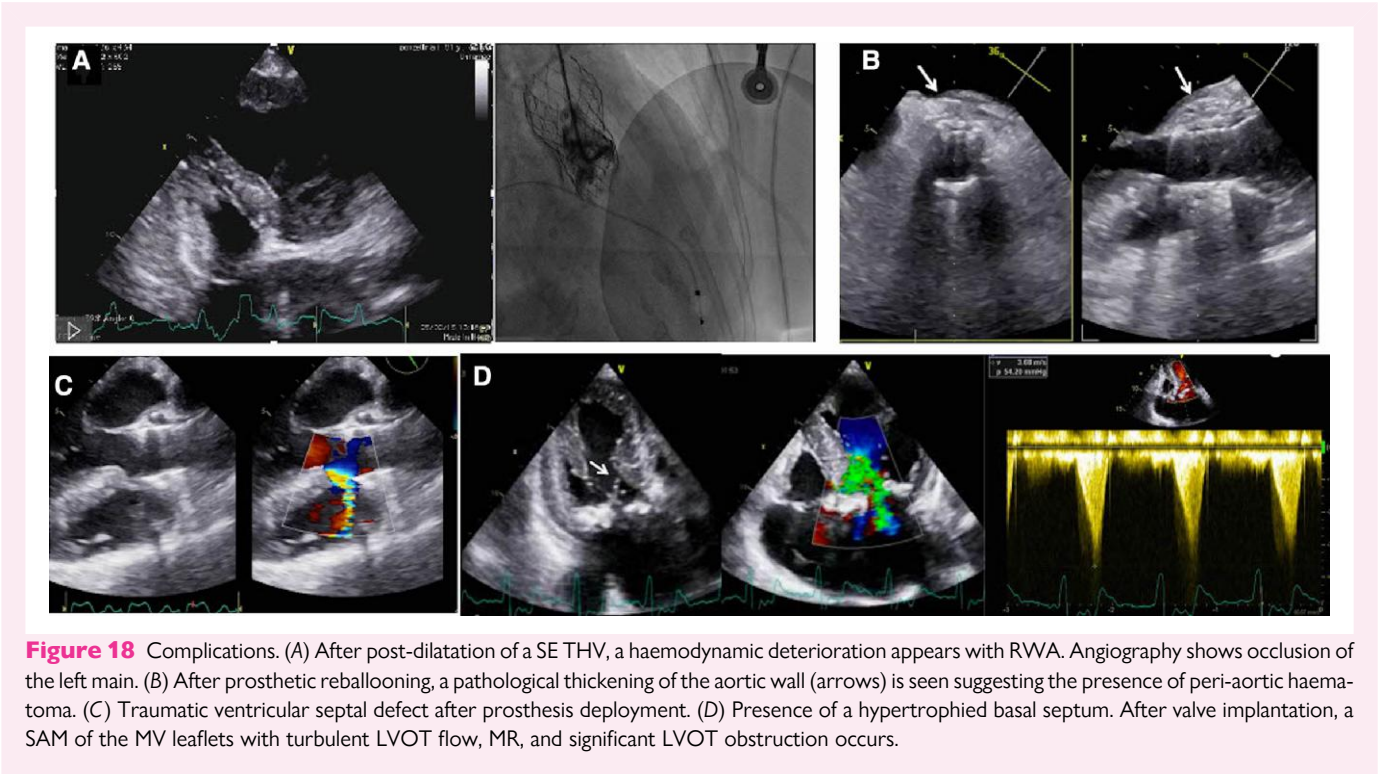
The occurrence of regional wall motion abnormalities (RWMA) (Table 8), as evaluated in different echocardiographic views, should alert the interventional echocardiographer for a possible occlusion of one or both coronary ostia, especially in cases of low-lying coronary ostia (Table 8). Although coronary occlusion can be easily identified with angiography, early RWMA can be quickly identified by TTE or TOE (Figure 18A). Ostial coronary obstruction commonly occurs as a result of displacement of the AV leaflets by the implantation of the device if

one or both coronary arteries originate below the projected tip of the deflected native or prosthetic aortic leaflet on CT, especially in narrow SOV or STJ. Bioprosthetic or native aortic leaflet intentional laceration to prevent iatrogenic coronary artery obstruction (BASILICA) is a recently developed technique to reduce the risk of ostial coronary obstruction in the setting of TAVI.<sup>79</sup> The role of peri-procedural TOE during BASILICA is not fully studied to date,<sup>80</sup> with a possible significant role of fusion imaging. The incidence of coronary ostia occlusion seems higher in case of TAVI in TAVI procedure.<sup>81</sup> As future coronary access could be troublesome, individual aortic cusp orientation and



Table 8 Complications of TAVI		
	Essential assessments	Imaging modalities
Haemodynamic instability		
Severe intra-prosthetic or paravalvular	Location of the jet (central vs. paravalvular) Position of the THV Severity of AR Embolization of the valve (into the LV or into the AO)	2D TTE, 2D/3D TOE 2D TTE, 2D/3D TOE, and angiography 2D TTE, 2D/3D TOE, and angiography Fluoro-angiography, 2D TTE, and 2D TOE
Severe MR	Severity of MR and mechanism	2D TTE and 2D/3D TOE
Pericardial effusion	Tamponade physiology and possible aetiology (i.e. chamber perforation and aortic dissection)	2D TTE and TOE
Ventricular dysfunction	Regional or global wall motion abnormalities of the LV or RV (i.e. coronary obstruction)	2D TTE and 2D/3D TOE Coronary angiography
Aortic rupture or dissection	Aortic root/ascending AO for peri-aortic haematoma, aortic dissection, or rupture Pericardial effusion/tamponade	2D/3D TOE 2D TTE and TOE
Major bleeding	Ventricular size and function (wall collapse due to hypovolaemia)	2D TTE and TOE
LVOT obstruction	SAM of the MV leaflets, turbulent LVOT flow, MR, and CW Doppler-derived LVOT gradient	2D TTE and TOE
Other procedural complications		
Fistula	Ventricular septal defect Aortocameral fistula (typically into the RV or RA)	2D TTE and 2D/3D TOE

Abbreviations as in the text.





**Table 9** Key anatomical and haemodynamic parameters for prosthetic valve assessment

Essential assessments and haemodynamic parameters	Description	How to assess	Comments
Valve position	Expected High Low	Parasternal long-axis (PLAX), apical five-chamber and three-chamber views	<ul style="list-style-type: none"> <li>Evaluation of proximal end of the stent relative to the anterior MA</li> <li>Optimal position should be &lt;8 mm from its proximal end to the aortic annulus and ≤4 mm for SE and BE THVs, respectively</li> </ul>
Valve structure	Stent shape <ul style="list-style-type: none"> <li>Normal</li> <li>Irregular</li> <li>Elliptic</li> </ul> Cusp mobility Cusp thickness Cusp calcification	SAX  Multiple views Multiple views Multiple views	<ul style="list-style-type: none"> <li>Stent shape should be perfectly circular</li> <li>Any stent irregularity should be described</li> <li>Cusps should have a normal motion, thin aspects, and be difficult to see with TTE</li> <li>Any thickening of the cusp is a warning for degeneration or endocarditis</li> <li>Any degree of cusp calcification is considered abnormal</li> </ul>
Haemodynamic parameters	Vmax  MG  EOA  DVI	Apical five-chamber and three-chamber views, right parasternal and suprasternal views  Apical five-chamber and three-chamber views, right parasternal and suprasternal views PLAX for LVOT diameter	<ul style="list-style-type: none"> <li>Normal cut-off value &lt;3 m/s</li> <li>Alignment with transvalvular flow to avoid underestimation</li> <li>The window from which Vmax has been recorded should be reported for comparison at follow-up</li> <li>Normal cut-off value &lt;20 mmHg</li> <li>See comments for Vmax</li> <li>Whenever an increase in MG is recorded, assessment of EOA by continuity equation is mandatory</li> <li>Measurement of LVOT diameter is critical</li> <li>PW Doppler sample volume should be placed just apically from the proximal end of the stent</li> <li>Placing PW Doppler sample volume inside the stent of the valve can overestimate SV due to flow acceleration inside the stent</li> <li>Normal cut-off value &lt;0.35</li> <li>&lt;0.35 raises suspicion of PPM or valve obstruction</li> </ul>
Valve obstruction	Thrombosis endocarditis SVD  PPM	PLAX, SAX, apical five-chamber and three-chamber, right parasternal, and suprasternal views  PLAX, apical five-chamber and three-chamber, right parasternal, and suprasternal views	<ul style="list-style-type: none"> <li>A MG &gt; 20 mmHg or an increase in MG &gt; 10 mmHg paralleled by a decrease in EOA as compared with the baseline is indicative of valve obstruction</li> <li>An indexed EOA &lt; 0.65 cm<sup>2</sup>/m<sup>2</sup> defines severe PPM and EOA &gt; 0.85 cm<sup>2</sup>/m<sup>2</sup> excludes PPM</li> <li>PPM should be ruled out after the first 'fingerprint' TTE at discharge</li> </ul>
Valve regurgitation	PVL Intra-prosthetic	Multiple views	<ul style="list-style-type: none"> <li>See <a href="#">Table 6</a></li> <li>Mild central jet can be considered normal</li> <li>Any intra-prosthetic jet more than mild should be described and followed-up</li> </ul>

Continued





in case of suspicion of endocarditis, significantly increasing diagnostic accuracy.

### Cardiac magnetic resonance

CMR can provide a non-invasive, radiation-free modality to evaluate both valvular and ventricular function, as flow-derived parameters are directly quantified using phase-contrast imaging.

If there is any uncertainty, CMR should be considered to assess the severity, especially if there are signs and symptoms of AR post-TAVI, although this technique is often limited by the stent frame artefacts and can miss very eccentric jets and outcome studies are needed to best validate cut-offs.

### Follow-up after TAVI: key points

- (i) TTE is the key exam for routine evaluation and follow-up after TAVI.
- (ii) Echocardiographic follow-up aims to assess valve morphology, function including haemodynamic parameters, and PVL, as well as cardiac chamber dimensions and function and concomitant valvulopathies.
- (iii) TOE and/or a cardiac CT/PET CT and/or CMR are second-level imaging techniques that should be performed if a complication is suspected or in case of doubts after the TTE assessment, depending on the type of complication identified.
- (iv) CMR should be considered to assess the AR severity in case of uncertainty.

## Transcatheter therapy for MV stenosis

### Assessment of MV stenosis

The most common cause of MS is rheumatic fever.<sup>98</sup> Echocardiography is the primary method for diagnosis and evaluation of patients with MS, the main goals being to establish disease severity and assess the consequences and the suitability for percutaneous mitral commissurotomy (PMC).

Quantification of MS severity includes measuring the mitral valve area (MVA) by planimetry or by pressure half-time (PHT) method, the mean transmitral gradient (MTG), and the sPAP.<sup>99</sup>

Planimetry is the reference method to determine the anatomical MVA, as it is relatively load independent. The MVA measured by 2D echocardiography correlates well with MS severity determined at cardiac catheterization or assessed on explanted valves<sup>100</sup>; however, it necessitates a careful upside-down scanning of the MV for the smallest orifice area. 3D echocardiography allows direct visualization of the MV orifice in multiple planes to ensure that the smallest orifice is being measured.<sup>101</sup> Therefore, multiplanar reformatting starting from a 3D zoom mode acquisition with high spatial and temporal resolution or direct 3D MVA planimetry from LV is the most accurate echo method to assess MS severity<sup>102</sup> and is considered the gold standard (Figure 19).

The PHT method is the simplest approach to estimate the functional MVA using Doppler echocardiography.<sup>103</sup> The more severe the obstruction, the longer the PHT. MVA derives from the PHT using the formula:  $MVA = 220/PHT$ .<sup>104</sup> The measured PHT is dependent on the compliance of both LV and LA. Thus, when PHT-derived MVA is non-severe but there are still doubts based on the clinical presentation, all the other complementary methods should be considered.<sup>105</sup>

MTG is highly flow- and rate-dependent, being influenced by heart rate, cardiac output, and associated MR.<sup>104</sup> Therefore, it is usually

used only as a supportive parameter of MS severity. Other indices of MS severity are rarely used in clinical practice.<sup>105</sup> From a practical point of view, MTG screens for MS: if  $>5$  mmHg, MVA defines severity. However, recently, low-gradient severe MS has been recognized.<sup>106</sup>

TTE usually provides sufficient information for routine management. Other imaging modalities are rarely used. CT scan may identify calcifications and exclude LA thrombosis,<sup>107</sup> and CMR may be used when Doppler echocardiographic data are not conclusive.<sup>105</sup>

Echocardiography is the preferred method for assessing the haemodynamic consequences of MS and associated valvular lesions. It provides information about LA size, the presence of LA spontaneous echo contrast or thrombus, RV and LV size and function, and pulmonary artery pressure. TOE may provide additional relevant information regarding MV morphology, MR severity, and the presence of thrombus inside LA.<sup>108</sup> TOE should always be performed to exclude thrombus into LA before PMC or after an embolic episode.<sup>109</sup>

Exercise echocardiography is recommended whenever there is a discrepancy between the clinical picture and the resting echo findings and may provide additional objective information by assessing changes in mitral gradient and pulmonary artery pressure.<sup>108,109</sup>

MS is considered significant when MVA is  $<1.5$  cm<sup>2</sup>.<sup>109</sup> When MVA is  $<1.5$  cm<sup>2</sup>, the decision to intervene is based on symptoms, suitability for PMC, sPAP values at rest, and presence of atrial fibrillation.<sup>108,109</sup>

Thus, echocardiography is essential in determining the timing and type of intervention in MS and it allows evaluation of the suitability for PMC.

### Assessment of MV stenosis: key points

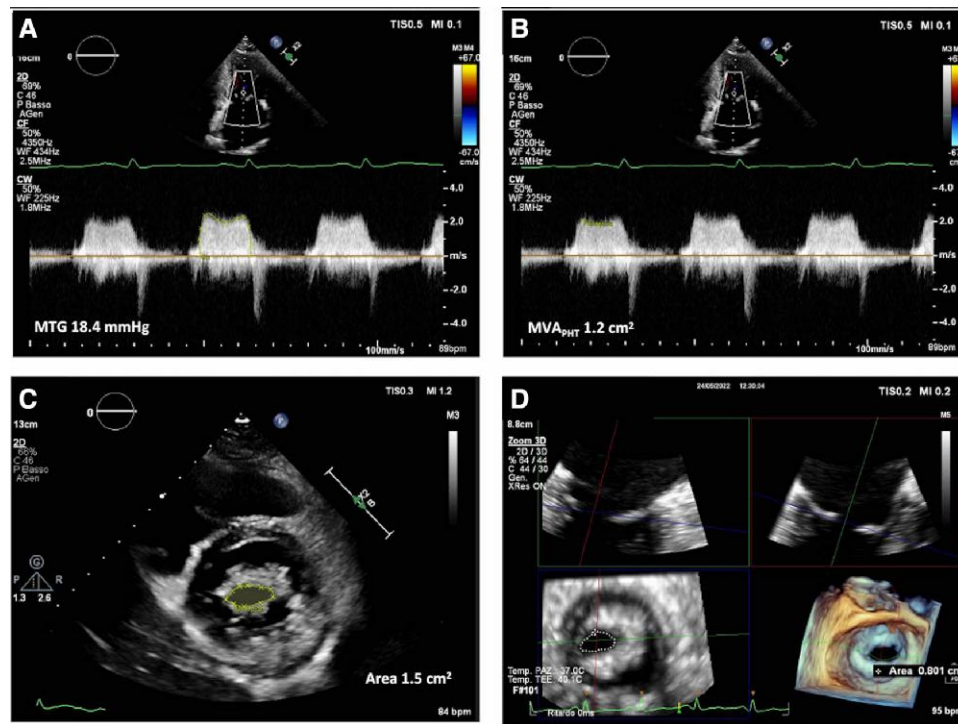
- (i) 2D/3D TTE is the primary imaging modality for assessing severity, anatomical features, the haemodynamic consequences and the suitability for PMC.
- (ii) 2D/3D TOE may be considered when TTE is suboptimal or inconclusive and should always be performed to exclude thrombus inside LA before PMC or after an embolic episode.
- (iii) MVA planimetry is the recommended reference method to determine the MS severity. 3D MVA is considered the gold standard to estimate the anatomical MVA.
- (iv) The PHT method is the simplest approach to estimate the functional MVA; however, it is dependent on the compliance of both LV and LA.
- (v) MTG is usually used as a screening parameter to define severity.
- (vi) Exercise echocardiography is indicated whenever there is a discrepancy between the clinical picture and the resting echo findings.

## Percutaneous balloon mitral valvulotomy

### Patient selection: Wilkins/Cormier scores

PMC was one of the first catheter-based therapies for SHD and has now become the treatment of choice for selected severe symptomatic MS with favourable anatomical characteristics, in the absence of contraindications: thrombosis into LA, more than mild MR, severe/bi-commissural calcifications, absence of commissural fusion (CF), concomitant coronary artery disease, or severe aortic/tricuspid disease requiring surgery.<sup>109</sup> In general, indications for intervention are limited to patients with clinically significant (moderate to severe/severe) MS (MVA  $<1.5$  cm<sup>2</sup>). However, PMC may be considered in symptomatic patients with MVA  $>1.5$  cm<sup>2</sup> if symptoms cannot be explained by another cause and if the anatomy is favourable.<sup>109</sup>

Echocardiography plays an essential role for the selection of candidates for PMC. As said, 2D TTE is the technique of choice to assess



**Figure 19** Quantification of MS severity. (A) MTG. (B) MVA by PHT. (C) MV area by 2D planimetry. (D) 3D MVA by MPR method.

the severity and consequences of MS, as well as the extent of anatomic lesions.<sup>110</sup> TOE may be useful if TTE provides suboptimal information and is required before PMC to exclude thrombus into LA.

Comprehensive TTE examination of valve morphology should assess leaflet thickening, mobility, calcification, subvalvular involvement, and commissural areas (Figures 20 and 21).

CF is one of the most important parameters to report because PMC may not be indicated in the absence of CF. CF is best assessed in parasternal SAX view using TTE. 3D TTE or TOE provides an even more comprehensive assessment of the completeness and extent of CF<sup>111</sup> (Figures 22 and 23): multislice or multiplanar format allows contemporary visualization of the valve at different levels.

One of the most useful ways to evaluate CF, the main target of the procedure, is from 3D LV perspective: after Carpentier's classification, Grade I is a partial CF, Grade II is complete CF with a visible delineation between leaflets, and Grade III is complete CF without visible delineation between leaflets.<sup>112</sup>

The extent and symmetry of commissural involvement predict commissural splitting post-PMC: if both commissures are symmetrically fused, bi-commissural splitting is likely, unless heavy fibrosis or calcification is present; if CF is asymmetric, the less fused commissure is predicted to split.<sup>113</sup>

Commissural assessment also allows to differentiate rheumatic MS from other causes of MS in which there is no CF (mainly degenerative MS with annular calcification, or MS due to radiation therapy or rheumatological conditions, such as systemic lupus) (Figure 24).

2D and 3D TTE/TOE should also assess the presence and extent of calcifications, involving or not the commissural areas (Figure 23).

Several scoring systems taking into account these morphologic features have been developed to assess suitability for PMC and to predict the success of the procedure. Two were shown to be predictive of both short- and long-term outcomes.<sup>114,115</sup> The most widely used is the Wilkins scoring system (Massachusetts General Hospital Score or

'splitability' score).<sup>114</sup> leaflet mobility, leaflet thickening, subvalvular thickening, and calcification are scored on a 1-to-4 scale and total score is obtained by adding each component of the score (Table 10).

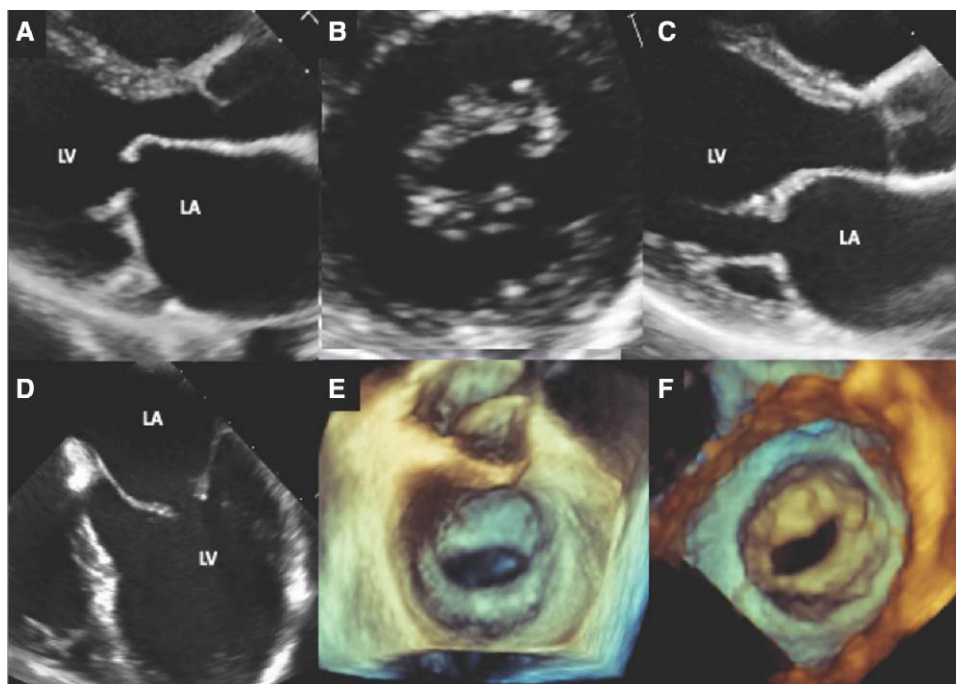
An unfavourable anatomy is defined by a score >8. An important limitation of this scoring system is the lack of information about commissural anatomy.<sup>116</sup>

Subvalvular involvement is best evaluated at TTE parasternal LAX view or TOE transgastric two-chamber view: multiple splitted jets of MV inflow suggest important subvalvular involvement.

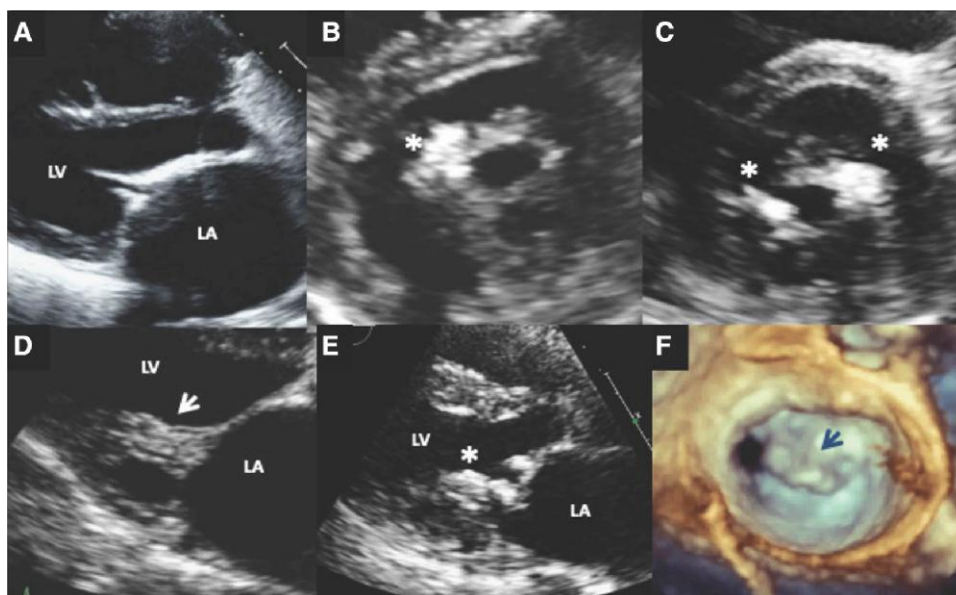
The Cormier score differentiates three groups according to the global MV anatomy assessed with TTE and fluoroscopy (for calcifications) (Table 11).

More recently, a new scoring system, incorporating quantitative parameters to assess leaflet displacement and asymmetry in commissural remodelling in addition to MVA and subvalvular thickening, has been shown to improve the prediction of early but not long-term outcomes after PMC (Table 12).<sup>117</sup>

All scoring systems have limitations, in particular as regards their predictive value of the immediate results and risk of procedural complications. Choice of treatment should be individualized and take into account the multifactorial nature of the prediction of the short- and long-term results of PMC.<sup>115,118</sup> Recent data from large series indicate that the long-term outcome following PMC depends not only on morphological characteristics of the valve but also on a number of clinical and procedural variables, such as age, history of commissurotomy, advanced functional class, final valve area and gradient, severe pulmonary hypertension, and the presence of atrial fibrillation.<sup>118</sup> Although PMC is definitely the preferred treatment in patients with favourable valve anatomy (i.e. with a Wilkins score  $\leq 8$  or a Cormier Class 1), good immediate and midterm results can also be achieved in patients with unfavourable anatomy even with calcified valves in selected patients who have otherwise favourable characteristics.<sup>115,119</sup> There are also reports on the use of

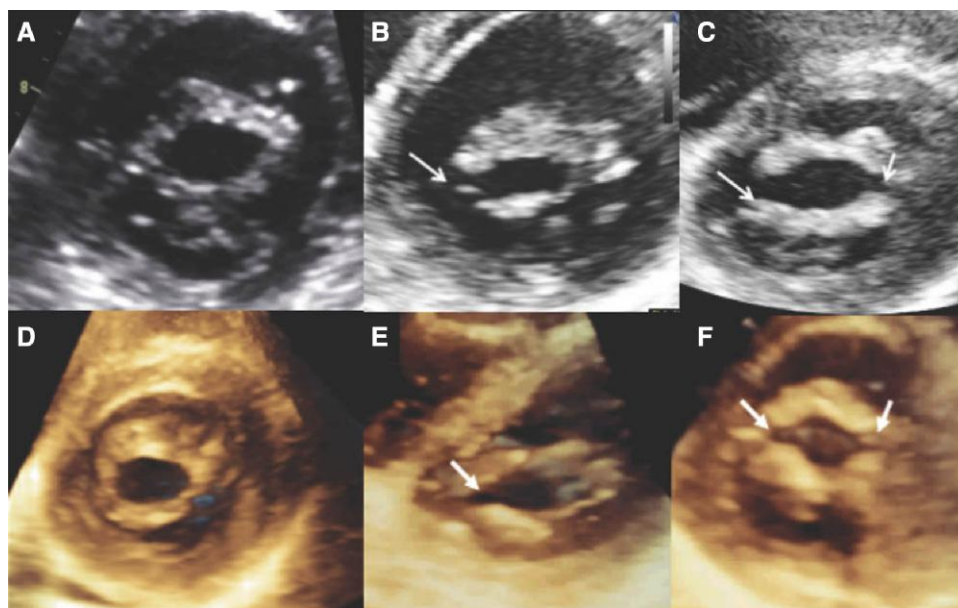


**Figure 20** Valve morphology in MS: favourable characteristics for PMC. (A) Diastolic doming of the anterior leaflet, due to fibrotic involvement of the base with sparing of the free margin, is a marker of pliability of the valve, while the movement of the shorter posterior leaflet is often more restricted, as it is involved from the base to the free margin (TTE LAX view). (B) Fusion of both commissures (TTE SAX view). (C) Moderate subvalvular involvement with mild thickening and shortening of the chordae (TTE LAX view). (D) TOE four-chamber view showing doming appearance of the MV. (E) 3D TOE en face view of MV from the LA perspective showing CF, the fish-mouth appearance of a symmetric MV orifice without calcification; the fusion of indentations between scallops of posterior leaflet is one of the earliest pathological findings of rheumatic MS. (F) 3D TOE en face view from the LV showing fusion of the commissures.

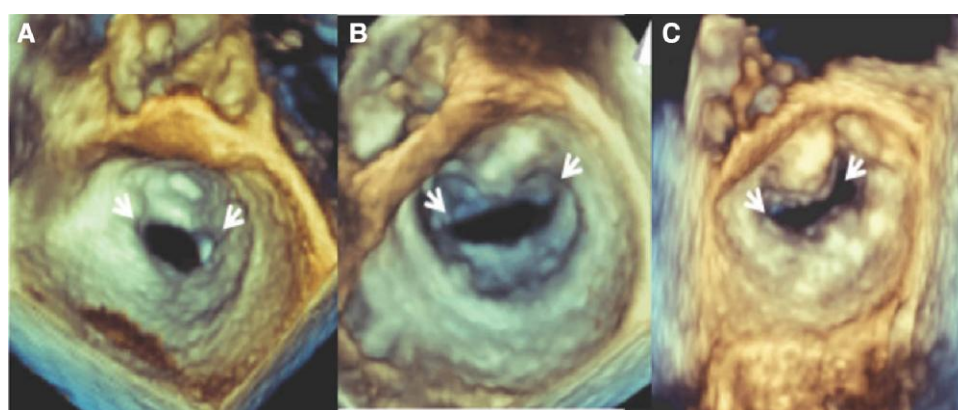


**Figure 21** Valve morphology in MS: unfavourable characteristics for PMC. (A) Thickening and rigidity of the MV (TTE LAX view). (B) Asymmetric orifice with commissural calcification (asterisk, TTE SAX view; note characteristic increased echogenicity and acoustic shadowing). (C) Bi-commissural calcification (asterisks, TTE SAX view). (D) Severe subvalvular involvement with severe shortening and fusion of chordae (white arrow, TTE LAX view). (E) Severe subvalvular involvement with calcifications of chordae (asterisk). (F) 3D TOE 'en face' view from the LA showing the extent of calcifications and asymmetry of the orifice.





**Figure 22** MS: TTE assessment of CF. (A, D) 2D and 3D TTE SAX views of the MV showing complete bi-CF. (B, E) 2D and 3D TTE SAX views of the MV showing absence of CF of the medial commissure (white arrow, a clue to asymmetrical CF is eccentric mitral inflow as a consequence of an asymmetrical orifice). (C, F) 2D and 3D TTE SAX views of the MV showing absence of fusion at both commissures (white arrows).



**Figure 23** MS: 3D TOE en face view from the LA. (A) Rheumatic MS: symmetric fusion of both commissures (white arrows). (B) Rheumatic MS: restenosis after PMC without fusion of the commissures (white arrows). (C) Degenerative MS: calcified MA without CF (white arrows).

Lithotripsy system to modify valvular calcium without causing tissue injury as a pre-treatment before PMC.<sup>120</sup>

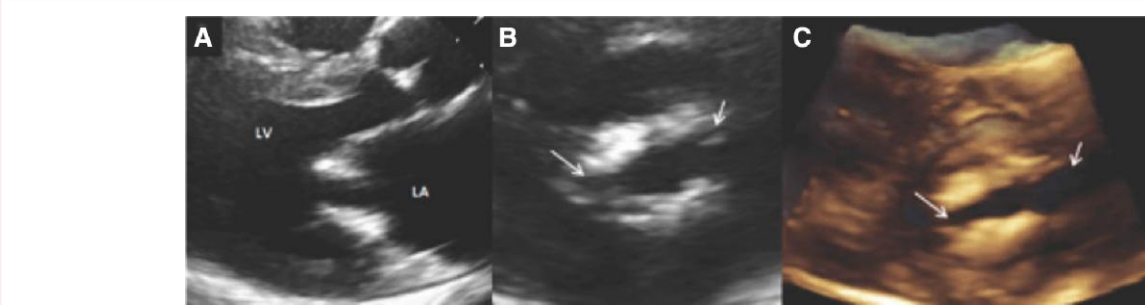
Echocardiographic screening should also exclude contraindication to PMC.<sup>121</sup>

The main contraindication is the presence of left atrial thrombosis, usually but not exclusively located in the left atrial appendage (LAA), which must be excluded by the systematic performance of TOE immediately before PMC. More than mild MR is a contraindication to PMC, especially if commissural, as there is a risk of worsening. Severe or bi-commissural valve calcifications contraindicate the PMC, as these increase the risk of procedural complications. Absence of CF, such as usually in patients with restenosis after previous balloon or surgical commissurotomy, is an indication for valve replacement.

### Patient selection for PMC: key points

- (i) Echocardiography is the essential imaging modality for the selection of candidates for PMC.
- (ii) 2D/3D TTE is the technique of choice to assess the extent of anatomic lesions: leaflet thickening, mobility, calcification, subvalvular involvement, and commissural areas.
- (iii) TOE is mandatory before PMC to exclude thrombus inside LA.
- (iv) Scoring systems are supportive to assess suitability for PMC and to predict the success of the procedure.





**Figure 24** MV stenosis due to valve rigidity. (A) Parasternal 2D TTE LAX view showing thickening and reduced opening of the leaflets. (B, C) Parasternal 2D and 3D TTE SAX views of the MV showing absence of fusion of commissures (white arrows; at 3D imaging, calcifications have a bulging appearance, as the shades of colour provide perception of depth).

**Table 10** MS: assessment of MV anatomy according to the Wilkins score

Grade	Mobility	Thickening	Calcification	Subvalvular thickening
1	Highly mobile valve with only leaflet tips restricted	Leaflets near normal in thickness (4–5 mm)	A single area of increased echo brightness	Minimal thickening just below the mitral leaflets
2	Leaflet mid- and base portions have normal mobility	Mid-leaflets normal, considerable thickening of margins (5–8 mm)	Scattered areas of brightness confined to leaflet margins	Thickening of chordal structures extending to one of the chordal lengths
3	Valve continues to move forward in diastole, mainly from the base	Thickening extending through the entire leaflet (5–8 mm)	Brightness extending into the mid-portions of the leaflets	Thickening extended to distal third of the chords
4	No or minimal forward movement of the leaflets in diastole	Considerable thickening of all leaflet tissue (>8–10 mm)	Extensive brightness throughout much of the leaflet tissue	Extensive thickening and shortening of all chordal structures extending down to the papillary muscles

Abbreviations as in the text. The total score is the sum of the four items and ranges between 4 and 16. From Wilkins et al.<sup>114</sup>

**Table 11** MS: assessment of MV anatomy according to the Cormier score

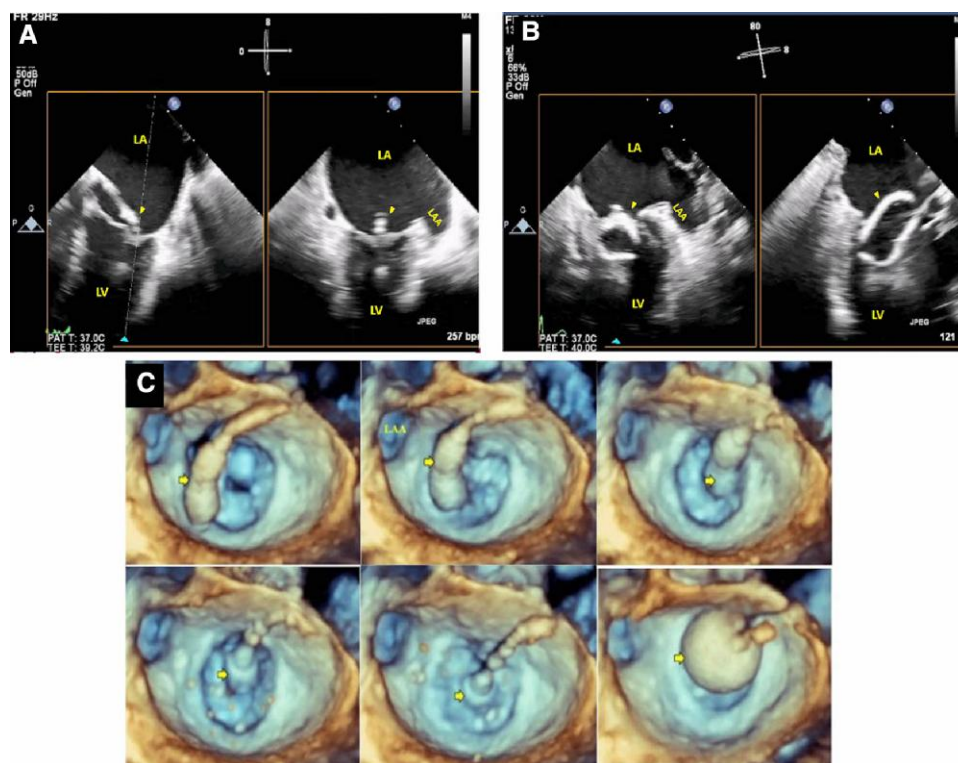
Echocardiographic group	MV anatomy
Group 1	Pliable non-calcified anterior mitral leaflet and mild subvalvular disease (i.e. thin chordae ≥10 mm long)
Group 2	Pliable non-calcified anterior mitral leaflet and severe subvalvular disease (i.e. thickened chordae <10 mm long)
Group 3	Calcification of MV of any extent, as assessed by fluoroscopy, whatever the state of subvalvular apparatus

Abbreviations as in the text. From lung et al.<sup>115</sup>

**Table 12** MS: assessment of MV anatomy according to the modified echocardiographic score

Morphologic features of MS	
• MVA ≤ 1 cm <sup>2</sup> : 2 points	
• Maximum apical leaflet displacement relative to the annulus ≤ 12 mm: 3 points	
• Commissural area ratio (accounting for symmetry/asymmetry) ≥ 1.25: 3 points	
• Subvalvular involvement: 3 points	
Low risk score	Score of 0–3
Intermediate risk score	Score of 5
High risk score	Score of 6–11

Abbreviations as in the text. From Nunes et al.<sup>117</sup>



**Figure 25** Biplane TOE and 3D rendering. (A) Biplane TOE ME view, showing the balloon (arrow head) crossing the stenosed MV. (B) Balloon inflation (arrow head) into the MV. (C) 3D TOE anatomically oriented zoom view of MV from the LA perspective showing serial images of the movement of the balloon (arrow) inside the LA while crossing the stenosed MV and during balloon inflation.

## Procedural guidance

### TTE vs. TEE

TTE could seldom be used for procedural monitoring. The apical four-chamber<sup>122</sup> and the subcostal views<sup>123</sup> were used as adjuncts to fluoroscopy mainly during TSP and for evaluation of the results. However, TTE may lead to interruptions of the procedure, potential hazards related to the sterile technique, and not always capable of providing adequate images.

2D/3D TOE was shown to add value during many of the procedural steps.<sup>124</sup>

### Baseline evaluation

At the starting of the procedure, we have to exclude the presence of any thrombi within the LA and/or LAA, reevaluate MVA and measure the baseline MTG, associate MR, and exclude/document the presence of any degree of pre-existing pericardial effusion.<sup>125</sup>

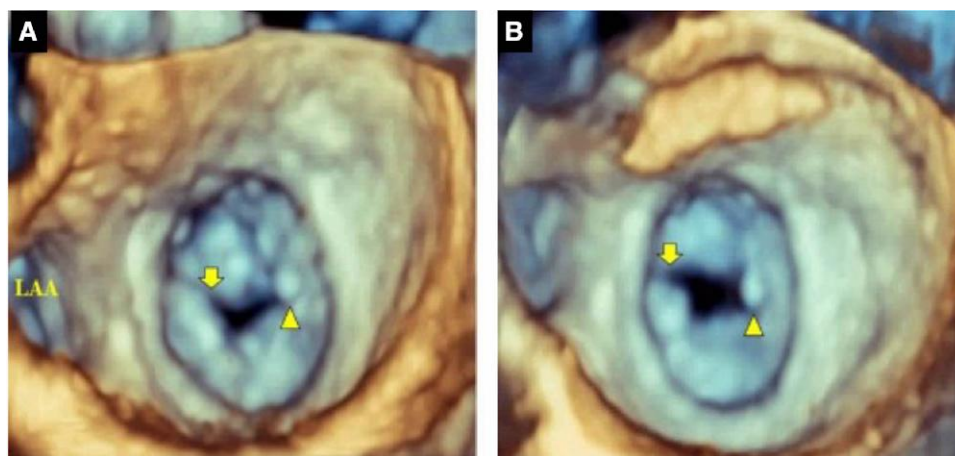
### TSP

TSP does not need to be perfectly tailored: the preferred TSP site is the infero-posterior part of the fossa but usually a mid-posterior puncture provides a favourable working height in the LA and a coaxial plane with the MV.<sup>126</sup> See chapter on TSP.

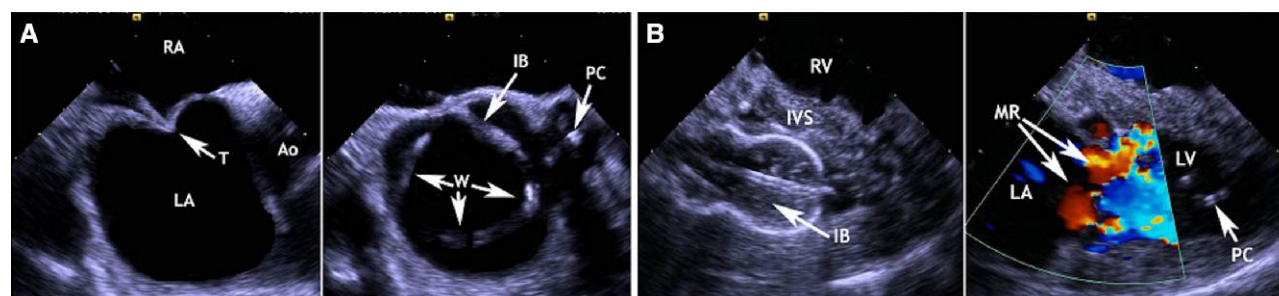
**Balloon positioning and inflation.** It is important to make sure that the balloon is well seated within the MV orifice and neither in the LAA nor within the subvalvular apparatus. 2D TOE and X-plane imaging are very useful

(Figure 25A and B), as they can monitor if the balloon is properly seated across the MV, showing both the distal and the proximal parts of the balloon. In addition, fluoroscopy allows visualization of balloon inflation and typical indentation. The 3D zoom anatomically oriented view of the MV from the LA perspective is useful for monitoring, guiding balloon positioning and inflation(s) (Figure 25C).<sup>127</sup> A 3D live longitudinal perspective of LA and LV starting from the mid-oesophageal commissural (MEC) view highlights the depth of the balloon across the stenosed MV inside the LV.

**Procedural assessment of the results and complications.** After balloon withdrawal, the interventional imager has to assess procedural results in terms of MTG, MVA, and commissural splitting (Figure 26A and B) which is the main target of the procedure, assess the degree of MR if any and its mechanism, exclude MV leaflet tear, assess the residual shunt through the IAS, and exclude pericardial effusion. Assessment of commissural splitting using 3D TOE is more accurate than with 2D TOE, and it has an important prognostic value of the clinical success of the procedure: partial splitting results in a triangular appearance while complete commissural opening results in complete leaflet separation at commissure.<sup>128</sup> Using the PHT method for MVA calculation is not recommended as it was shown to be inaccurate immediately after PMC<sup>129</sup>; MVA planimetry is more-or-less load independent and hence it is the recommended method for MVA assessment post-PMC. 3D TOE provides superior estimation of MVA using the multiplanar reformatting, compared with 2D TOE, in the immediate post-procedural setting.<sup>130</sup> It is also feasible to measure the MVA with direct planimetry



**Figure 26** 3D TOE anatomically oriented zoom view of MV from the LA perspective showing (A) the MV diastolic opening before balloon inflation and (B) after balloon inflation, with a clear increase in the diastolic opening with splitting of the lateral commissure (arrow), while the medial calcified commissure (arrow head) did not show significant splitting.



**Figure 27** (A) Transatrial ICE view for safe TSP (left panel) and for advancing wires and the 'Inoue' balloon into the LA (right panel). (B) Transventricular longitudinal view for monitoring balloon inflation (left panel) and for evaluation of the result (right panel). Ao, AO; IB, 'Inoue' balloon; LA, left atrium; PC, pigtail catheter placed in the AO; RA, right atrium; T, tenting; W, wire; IVS, interventricular septum; LV, left ventricle; MR, mitral regurgitation (mild); PC, pigtail catheter placed in the LV; RV, right ventricle.

over the 3D image, especially from ventricular perspective, if the commissures are at the same plane of the mitral leaflet tips.

### Intracardiac echocardiography

ICE is rarely used for procedural guidance of PMC and just single cases have been reported. Even though TOE was established decades ago and has shown its benefits in PMC,<sup>131</sup> ICE may represent an alternative guiding tool in those individuals who could not undergo general anaesthesia and in those who cannot tolerate the TOE probe during MAC. ICE is capable of monitoring each step of the procedure<sup>132,133</sup> using right atrial and RV windows. For guiding TSP, the ICE catheter is advanced into the RA with the miniaturized probe interrogating the IAS and the FOV in particular. ICE images display the puncture needle, the 'tenting', and the distance of the potential puncture site to the

Ao and all other left atrial borders (Figure 27A). ICE clearly shows transeptal passage of the catheter and its advancement over the looped wire (Figure 27A). The ICE catheter is then repositioned and introduced in the RV with the probe aligned with and aimed to the interventricular septum for interrogating the LA and the LV in a longitudinal axis. This approach is also called transventricular longitudinal view<sup>134</sup> (Figure 27B). Optimal cut plan shows the MV opening. ICE monitors distal and proximal balloon inflation and displays the result immediately after balloon deflation. Particularly, any significant MR can be excluded or displayed. Unfortunately, the Doppler angle is not favourable to read pressure gradients using the transventricular longitudinal view. Transeptal ICE is technically feasible but might be considered not indicated just for reading the pressure gradient. However, all descriptions on how to use ICE in PMC are based on single-centre experiences and case reports. There are no strong data available, yet.

## Procedural guidance during PMC: key points

- (i) 2D/3D TOE is the standard modality for procedural guidance.
- (ii) TTE and ICE are rarely used.
- (iii) Baseline evaluation (LA thrombosis, MVA, and MTG), results, and possible procedural complications are an integral part of procedural monitoring.
- (iv) Assessment of commissural splitting using 3D TOE is more accurate than with 2D TOE.
- (v) MVA planimetry (3D MPR is the preferred method of measurement) is the highly suggested method for MVA assessment post-PMC.

## Follow-up

A comprehensive clinical and TTE examination at the end of the index hospitalization is key and will serve as a reference for the follow-up. It is essential to use an integrative approach to assess the final results.<sup>109</sup>

The echocardiographic assessment will (i) estimate the presence, location, and degree of commissural opening, (ii) measure the MVA using planimetry, (iii) quantify and locate any MR, (iv) assess MTG, and (v) evaluate the level of systolic pulmonary pressure.<sup>118,135</sup>

- If there is a clear commissural opening resulting in large valve area associated with a low gradient and zero or mild MR together with a decrease in pulmonary pressure, the results are undisputedly good and the management is similar to that of mild stenosis, i.e. a cardiology visit every year initially and every second year thereafter in the absence of symptoms.<sup>118,135</sup>
- When PMC is not acutely successful (final MVA  $<1.5 \text{ cm}^2$  and/or MR  $>2/4$ ): in cases with mixed mitral disease or significant residual stenosis, surgery should be considered. The indications and the date of surgery will depend on the symptoms and the surgical risk. A close follow-up is needed and exercise evaluation is helpful to determine the timing of surgery.<sup>136</sup>

If there is a severe traumatic MR, early surgery is recommended, especially when it is associated with severe pulmonary hypertension.

- In case of 'intermediate' or discordant results, reevaluation after few months is necessary. It will take into account the presence of symptoms, further evaluated by exercise echocardiography if there are doubts, and the evolution of the main echocardiographic parameters including the level of pulmonary pressures. The decision of surgery is related to the surgical risk.

During longer term follow-up, the clinical and echocardiographic assessment will search for the occurrence of restenosis. Even if there is no uniform definition, restenosis after PMC has generally been defined as a loss of more than 50% of the initial gain with MVA  $<1.5 \text{ cm}^2$ . The mechanism of restenosis must be determined by 2D and 3D TTE. The predominant mechanism of restenosis is commissural refusion, if both commissures are fused, and valve rigidity in the other cases. A careful comparison between follow-up examinations and immediate post-procedural examination is useful.

Reintervention is indicated when symptoms or pulmonary hypertension occurs. Re-PMC can be proposed in selected patients with (i) an initially successful PMC, (ii) restenosis occurring after several years, (iii) favourable characteristics for PMC, and (iv) the predominant mechanism of restenosis being commissural refusion.

In the other cases, including those with uni-commissural refusion where the other commissure remains open, surgery should be considered.

In patients with restenosis who remain asymptomatic, follow-up should be closer (twice a year). Here again, exercise evaluation is recommended in case of doubt.

In conclusion, the follow-up after PMC mainly relies on a comprehensive examination early after PMC and a timely and appropriate indication for subsequent reintervention which is largely guided by clinical examination and echocardiographic evaluation.

## Follow up after PMC: key points

- (i) A comprehensive TTE examination at the end of the index hospitalization will serve as a reference for the follow-up.
- (ii) A successful PMC is defined in the presence of final MVA  $>1.5 \text{ cm}^2$  and MR  $<2+$ .
- (iii) Timing of follow-up examinations is based on procedural results and symptoms.

## Transcatheter therapy for MR

MR is the second-most frequent valvular heart disease in Europe and is an important cause of morbidity and mortality.<sup>137,138</sup>

Open surgical correction, using MV repair or replacement, is currently accepted as the best available treatment option. However, percutaneous MV therapies are emerging as an alternative option in patients with contraindications for surgery or high operative risk.

Imaging techniques are essential for assessment of mitral functional anatomy to select patients who can benefit from percutaneous intervention and to tailor the therapeutic strategy. 2D TTE and TOE are the primary modalities used to accurately assess the MV morphology.<sup>139</sup> 3D imaging provides a comprehensive evaluation of the MV morphology and should be used when available (TTE or TOE if necessary). This technique is superior for describing mitral pathology. CMR can be used as an alternative tool when TTE/TOE images are suboptimal. CT may also be helpful in assessing MV anatomy but its major role is for planning of intervention, to assess the presence and extent of MV calcifications, mitral annular size, and presence of coronary artery disease.<sup>139</sup>








## Patient selection

Both primary MR (PMR) and secondary MR (SMR) can be suitable for percutaneous valve repair or replacement. For patients with PMR, transcatheter edge-to-edge repair (TEER) is the most evidenced, while the safety and efficacy of other techniques have been demonstrated in smaller series.<sup>140–142</sup> In patients with PMR, TEER may be considered in symptomatic patients who fulfil the echocardiographic criteria of eligibility, judged inoperable or at high surgical risk by the Heart Team and for whom the procedure is not considered futile (IIb, LOE B recommendation).<sup>98</sup>

In patients with SMR, two randomized trials (MITRA-FR and COAPT)<sup>143,144</sup> comparing MitraClip and optimal medical therapy have provided conflicting results in terms of heart failure hospitalization and a survival benefit in patients with MitraClip treatment. The MITRA-FR trial demonstrated that among patients with severe SMR, the rate of all-cause mortality or unplanned hospitalization for heart failure at 1 year and 2 years did not differ significantly between patients who underwent percutaneous MV repair in addition to optimal medical therapy and those who received optimal medical therapy alone. In the COAPT trial, MitraClip implantation substantially reduced the rate of the primary endpoint of cumulative hospitalization heart failure and the all-cause mortality within 24 months of follow-up than medical



**Table 13** Current available devices for percutaneous MV therapy with CE mark

	Device (manufacturer)	Anatomic target	Approach	Mechanisms
	MitraClip (Abbott)	Leaflets	Transfemoral	Edge-to-edge
	Pascal (Edwards Lifesciences)	Leaflets	Transfemoral	Edge-to-edge
	Cardioband (Edwards Lifesciences)	Annulus	Direct annuloplasty (transfemoral)	Plicating adjustable band on atrial side of the annulus
	Carillon Mitral Contour System (Cardiac Dimensions)	Annulus	Indirect annuloplasty (transjugular)	CS reshaping
	NeoChord (NeoChord, Inc., St. Louis Park, MI)	Chordal apparatus	TA	Artificial chordal implantation
	Harpoon (Edwards Lifesciences)	Chordal apparatus	TA	Artificial chordal implantation
	Tendyne (Abbott)		TA	MV replacement

therapy alone. The rate of freedom from device-related complications exceeded a pre-specified safety threshold.

These diverging results might be partially explained by effect size of the trials, differences in trial design, patient selection, echocardiographic assessment of SMR severity, use of medical therapy, and technical factors. Patients in COAPT demonstrated greater severity of SMR and less LV dilatation than those enrolled in MITRA-FR.

Therefore, TEER should be considered in selected symptomatic patients, not eligible for surgery and fulfilling the COAPT inclusion criteria suggesting an increased chance of responding to the treatment (IIa, LOE B recommendation).<sup>98</sup>

In addition, in selected symptomatic cases in whom the COAPT criteria are not fulfilled, TEER or other transcatheter valve therapy if applicable may be considered after careful evaluation for ventricular assist device or heart transplant with the aim of improving symptoms and quality of life (IIb, LOE C recommendation).<sup>98</sup>

## Devices for MV regurgitation

In recent years, multiple technologies and approaches for percutaneous valve repair or replacement have been developed. Conventionally, the devices are classified according to the anatomical and pathophysiologic target (*Table 13*):

- (i) Annular repair: direct or indirect annuloplasty aiming to reduce annular dimensions, thus improving leaflets coaptation.
- (ii) Chordal repair: adjustable TA beating-heart artificial chordal implantation.

- (iii) Leaflet repair: TEER by approximating MV leaflets together at the site of regurgitation.
- (iv) MV replacement.

However, it should be noted that this is a rapidly changing field with the introduction of new devices and withdrawal/redesign of existing ones.

## Percutaneous MV annuloplasty

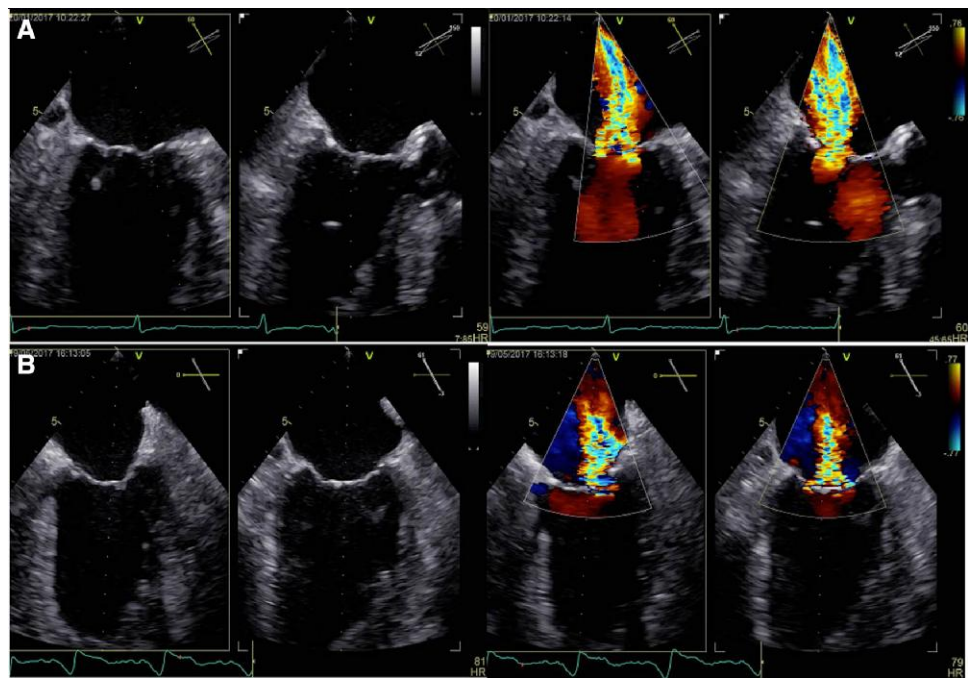
The goal of surgical mitral annuloplasty is to restore the normal ratio between the leaflet surface area and the annular area and to improve coaptation. Since transcatheter annuloplasty devices have become clinically available, they may be an alternative to surgery in selected patients. It can be performed as a stand-alone procedure or in combination with TEER/chordal implantation.<sup>145,146</sup>

Moreover, one of the most appealing features of this approach is that it preserves the native valve anatomy, thus keeping the option for future valve treatment open.<sup>145,147</sup>

There are two available different catheter-based annuloplasty devices ([Table 13](#)): (i) direct annuloplasty and (ii) indirect annuloplasty.

## Patient selection

Proper patient selection based on pre-operative echocardiography is the major determinant of technical feasibility and long-term outcomes.



**Figure 28** (A) Type I MR due to annular dilation/deformation. (B) Type IIIb MR with symmetric leaflet tethering and low degree of MV remodelling.

The echocardiographic analysis of the MR mechanism, according to Carpentier's classification, is crucial when selecting patients for annuloplasty. Considering the surgical annuloplasty experience, common MR mechanisms that might be corrected by percutaneous annuloplasty include Type I (incomplete coaptation due to annular dilatation/deformation) or Type IIIb (symmetric leaflet tethering with low degree of MV remodelling) (Figure 28). The anatomic criteria for percutaneous annuloplasty are summarized in Table 14.

TTE provides baseline information regarding functional anatomy of MR and annular dimension. The mitral annulus (MA) may be assessed using the 2D approach with TTE apical LAX view (three-chamber) and TOE ME view for the minor axis (AP or septolateral) (Figure 29A). The major axis (intercommissural) annulus diameter can be measured using a modified TTE two-chamber apical view or a commissural ME TOE view (Figure 29A). Integrated analysis of annulus shape, using CT and 3D TOE, provides additional information on the feasibility and planning of annuloplasty therapy (Figure 29B–D). Using 3D TOE reconstruction models, the functional anatomy and dynamics of the MA can be quantitatively assessed (Figure 29C and D). The following annular parameters may be useful to plan mitral annuloplasty: area, circumference, AP and intercommissural diameters, and sphericity index (AP/intercommissural diameter ratio).

**Table 14** Morphological suitability criteria for percutaneous annuloplasty

Ideal morphology	Unsuitable morphology
Carpentier I: annular dilatation/deformation	Carpentier II or IIIa
Carpentier IIIb: symmetric leaflet tethering	Carpentier IIIb: asymmetric leaflet tethering with: (a) Tethering angle of posterior leaflet >45° (b) Distal tethering of anterior leaflet >25°
Coaptation depth <1 cm	Coaptation depth >1 cm
Tethering angle of posterior leaflet <45°	Heavily calcified annulus or leaflets
Distal tethering of anterior leaflet <25°	
Lack of annular calcification	
Anatomically normal mitral leaflets	

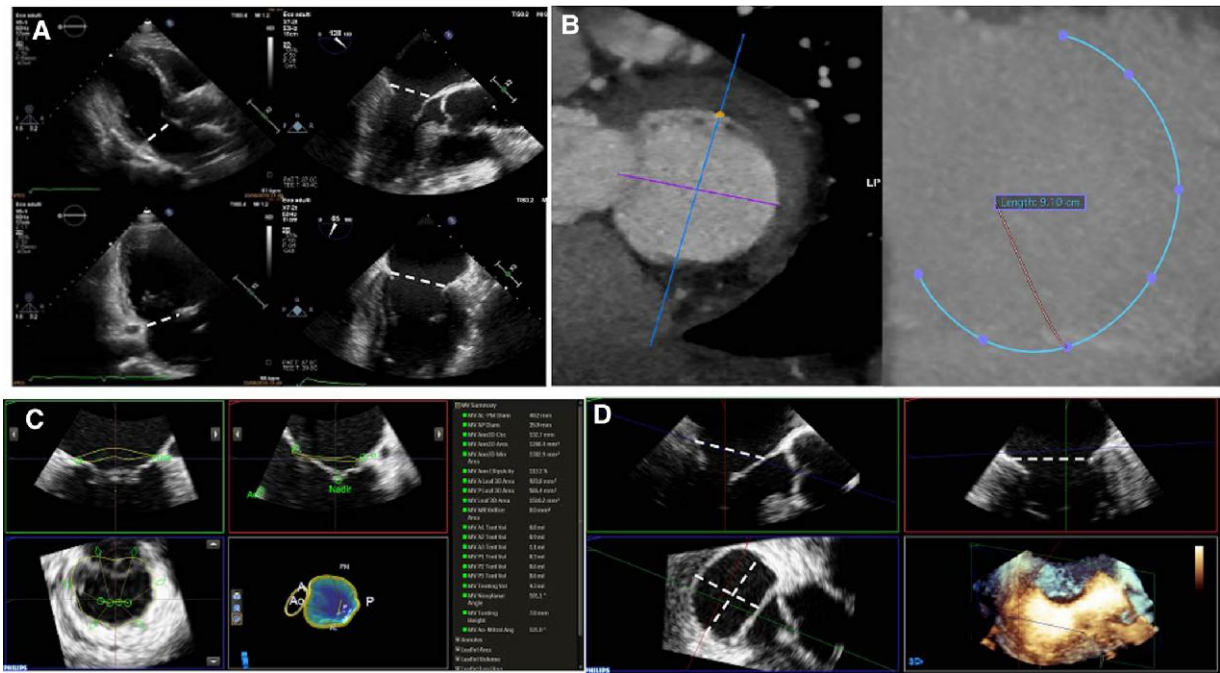
**Key points**

- (i) The 2D/3D TTE/TOE echocardiographic evaluation defining the functional anatomy of MR is crucial for patient selection.
- (ii) CT provides additional information on the feasibility and planning of annuloplasty therapy.

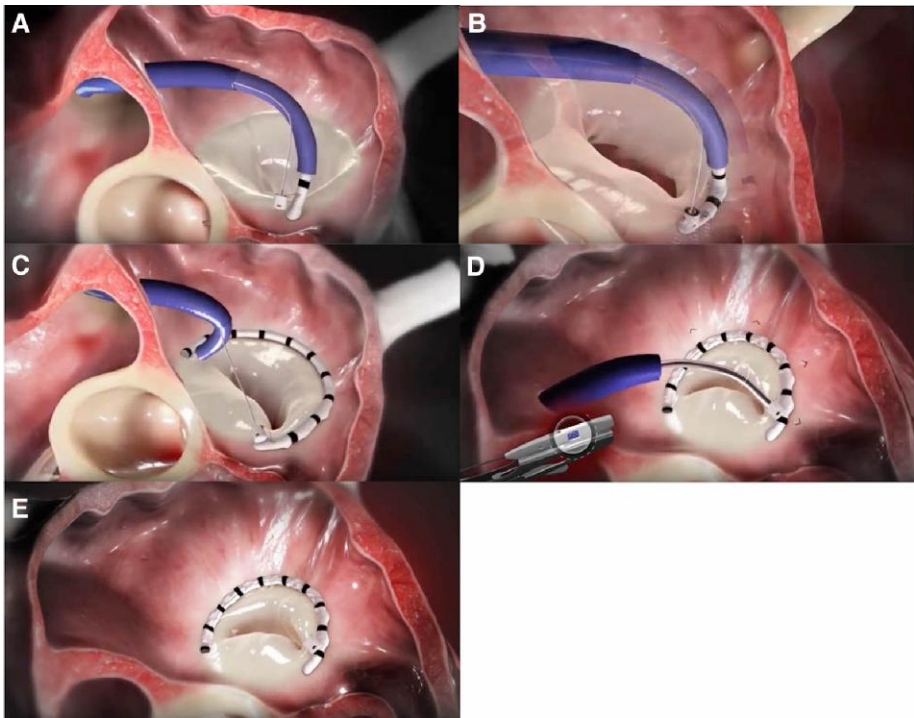
**Direct annuloplasty**

**Cardioband**

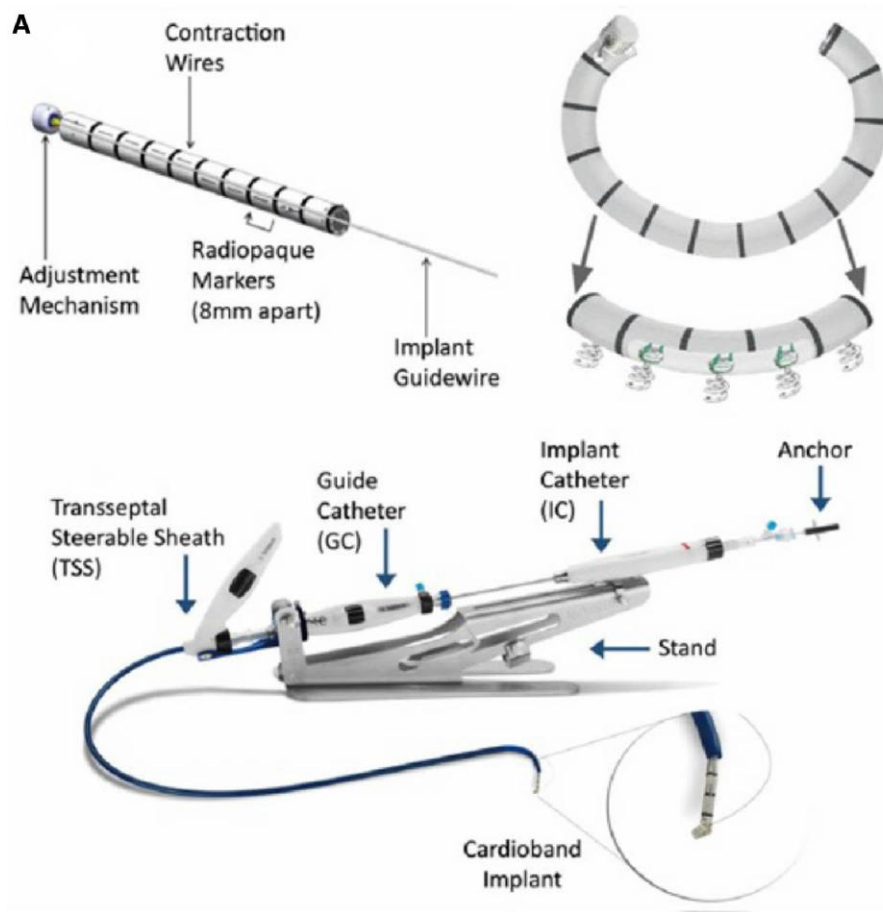
The Cardioband™ (Edwards Lifesciences, Irvine, CA, USA) is an incomplete adjustable surgical-like Dacron band delivered from transseptal approach and implanted in posterior annulus from anterolateral to



**Figure 29** (A) AP diameter (minor axis): transthoracic apical LAX view (left upper panel) and ME LAX view (right upper panel). Inter-commissural diameter (major axis): transthoracic apical two-chamber view (left bottom panel) and MEC view (right bottom panel). (B) CT reconstruction of MV annulus and sizing. (C) 3D parametric reconstruction and analysis of the mitral apparatus. The software provides quantitative parameters of the MA, the leaflets, and the remodelling indices (tenting, coaptation depth, etc.). (D) MPR of the MA. Left upper panel: AP diameter; right upper panel: inter-commissural diameter; left bottom panel: axial plane of the MA in which both diameters, perimeter, and area can be measured.



**Figure 30** Cardioband procedure. (A–C) Dacron band delivered in posterior annulus from anterolateral to posteromedial commissure. (D) Implant size cinching. (E) Final result.



**Figure 31** Components of the Cardioband system.

posteromedial commissure under echocardiographic and fluoroscopic guidance (Figure 30).

In the feasibility trial in symptomatic patients with SMR, the Cardioband was effective in reducing MR and the septolateral dimension and was associated with improvement in heart failure symptoms and demonstrated a favourable safety profile.<sup>148,149</sup> At 1 year, overall survival, survival free of readmission for heart failure, and survival free of reintervention were 87%, 66%, and 78%, respectively.<sup>150</sup> In the overall population, MR grade at 12 months was moderate or less in 61% and moderate or less in 95% of the 39 patients who underwent TTE at 1 year.<sup>149</sup> Functional status [79% vs. 14% in New York Heart Association (NYHA) Class I/II], quality of life, and exercise capacity improved significantly.<sup>149</sup>

The system includes (Figure 31) the following:

- (i) The implant, that is a polyester sleeve with radiopaque markers spaced 8 mm apart.
- (ii) The transfemoral delivery system: the Cardioband delivery system (CaDS) consists of the 25 F transseptal steerable sheath (TSS) and the implant delivery system (IDS).
- (iii) Implantable metal anchors and anchor delivery shafts.
- (iv) The size adjustment tool (SAT).

## Patient screening and procedural planning

The procedure is dependent on pre-interventional screening based on echocardiography and CT scan, in order to assess the following:

- (i) the proximity of circumflex artery from annulus to avoid the injury of the artery, (ii) annulus sizing, (iii) the anatomy of MA, LA, and IAS, and (iv) transseptal puncture. Pre-procedural CT also provides the coordinates for the procedure and the expected fluoroscopic projections

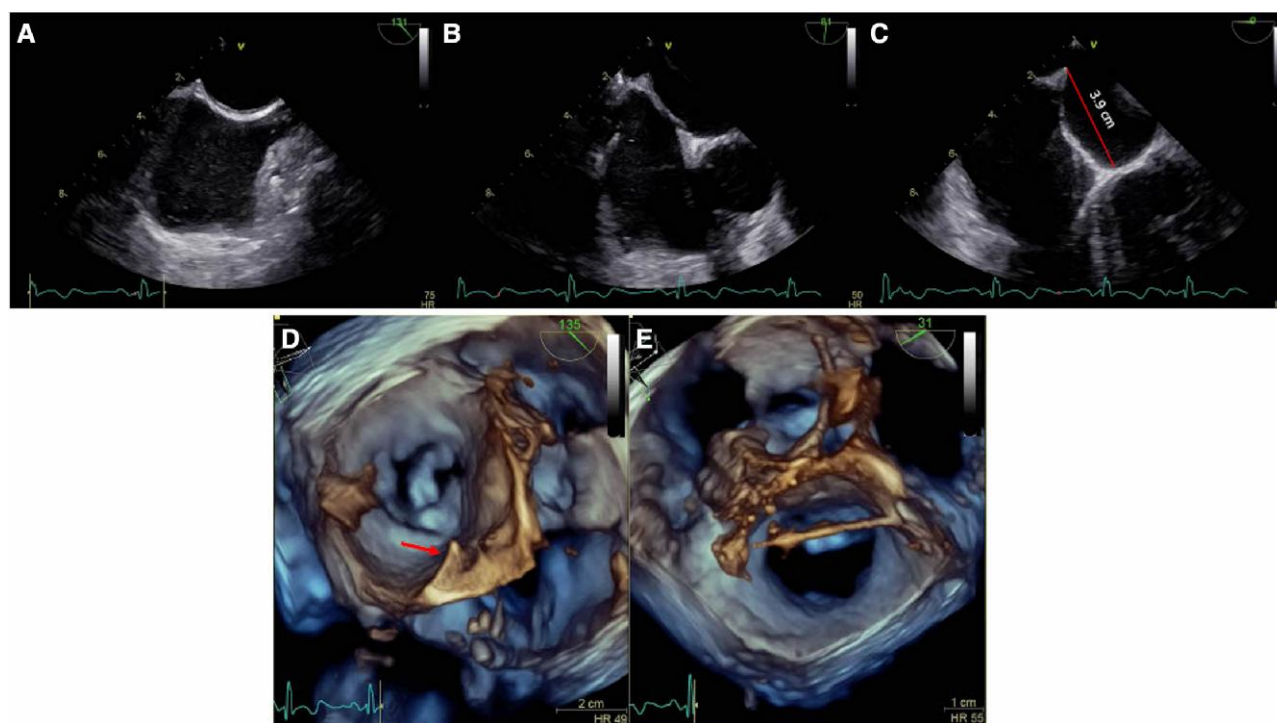
### Key points: screening and procedural planning

- (i) The echocardiographic assessment of functional anatomy and the determination of the mechanism of MR are mandatory for patient selection.
- (ii) The procedural planning is based on CT that provides a tailored planning based on patient's heart anatomy.

## Procedural monitoring

The procedure consists of several steps that need to be monitored using a combination of different imaging modalities: 2D and 3D, fluoroscopy, and angiography.





**Figure 32** TSP. (A) Bi-caval view. (B) SAX view at base. (C) Four-chamber view. Measurement of the height of the TSP. (D) Posteromedial commissural perspective. The TSP (tenting) is located above the posteromedial commissure. (E) 3D overhead perspective of LA showing the guidewire inside the LA.

The optimal TSP site is pre-defined by CT planning. Two issues are of utmost importance: (i) the puncture (tenting) must be above the posteromedial commissure and the minimum height must be no <3.5 cm from the annular plane (Figure 32A–D). The TSS is advanced over a super-stiff guidewire inside the LA (Figure 32E). The steering and navigation of IDS along the posterior annulus is guided by different 3D perspectives and fluoroscopic LAO caudal view. After reaching the target point, RAO projection, several 2D and biplane views, or MPR are used to assess the distance from the hinge point of posterior leaflet (PL) and the device angulation for fine adjustment and for checking anchoring via a push-and-pull test. Coronary angiography rules out the risk of injury to the circumflex artery. The first anchor should be positioned as anterior as possible in the annulus, close to the anterior commissure. The IC tip is then navigated along the posterior annulus using echocardiographic guidance until reaching the posterior commissure. After last anchor deployment and disconnection of the device, the SAT is inserted and connected to the spool of the implant that is then contracted while reduction of MR severity and annulus size are monitored (Figure 33).

### Key points: procedural guidance

- (i) The procedural monitoring relies mainly on 2D/3D TOE. The different echocardiographic modalities (2D, 3D perspectives of MV, MPR, and simultaneous biplane views) must be used appropriately in specific procedural steps.
- (ii) The fluoroscopy and angiography are used together with TOE and are fundamental in individual procedural steps.

## Indirect annuloplasty

### Coronary sinus annuloplasty

Coronary sinus (CS) annuloplasty attempts to reshape the AP annular dimension to correct the mitral leaflet apposition and restore coaptation. The rationale of this approach is based on the anatomical relationship between the CS/great cardiac vein (GCV) and the posterior annulus. Several techniques have been proposed that involve placing a device within the CS/GCV to attempt septal–lateral diameter reduction and/or MA ‘cinching’.

### Carillon

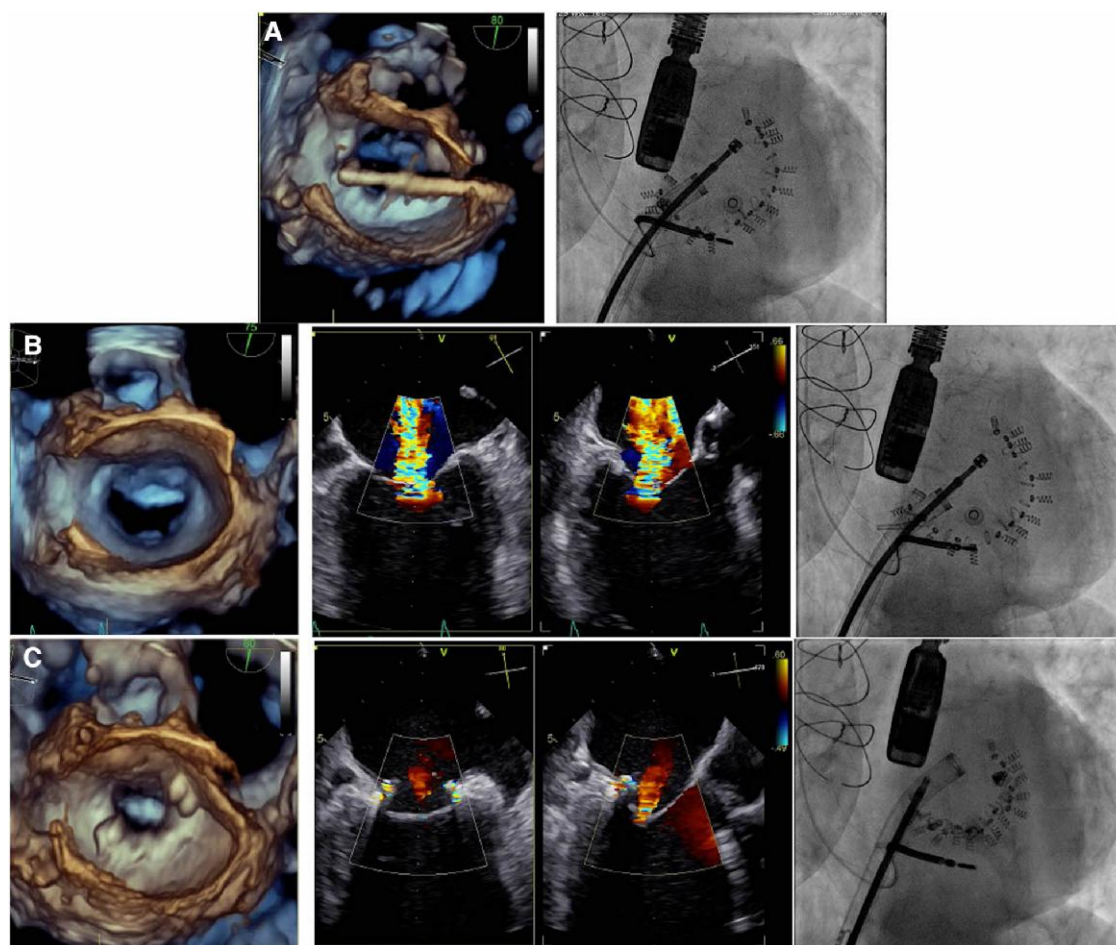
The Carillon™ Mitral Contour System (Cardiac Dimensions, Kirkland, WA, USA), which consists of two helical anchors interconnected by a nitinol bridge, is the most clinically tested device (Table 13).

The clinical experience of CARILLON includes the AMADEUS study, which reports an implantation feasibility in 30 of 48 patients without significant MR improvement and a moderate risk of coronary complications (15%) and death (1 patient),<sup>150</sup> and the TITAN trial, which reports a successful implantation in 36 of 53 enrolled patients, leading to MR reduction and concomitant LV remodelling.<sup>151</sup>

Using right internal jugular access, the distal anchor is positioned in the GCV, and subsequent manual traction is applied to approximate the lateral and septal portion of the MA improving leaflet coaptation.

### Pre-procedural screening

Indirect mitral annuloplasty via the CS requires additional anatomic considerations regarding CS anatomy. Patency, diameter, and



**Figure 33** (A) 3D overhead perspective of LA showing the SAT connected to the spool and fluoroscopy. (B) Baseline 3D en face view of MV, biplane color Doppler, and LAO fluoroscopic view before cinching. (C) 3D en face view of MV after SAT removal showing the implant like to an incomplete surgical annuloplasty and a consistent reduction of the annulus. Biplane color Doppler after SAT detachment. LAO projection. The distance among the radiopaque anchors is reduced.

tortuosity of the coronary venous system, location and extent of the Thebesian and Vieussens valves, and proximity of the CS to the MA and to the left circumflex artery are important factors due to a high patient variability. A close relation between the CS and the left circumflex artery may limit the use of percutaneous annuloplasty via the CS due to the risk of arterial impingement.<sup>152</sup> Furthermore, in the majority of patients, the CS is located superior to the level of the MA, often in direct contact with the LA wall.<sup>153</sup> This relation may result in annular deformation through secondary tension from the LA wall and may lead to a suboptimal annuloplasty result. The distance between the CS and the MA should therefore be taken into consideration in pre-interventional planning.

Post-processing of 3D TOE data sets with dedicated software has been shown to allow reconstruction of the MA and the CS. Venography is the gold standard for the assessment of CS anatomy and should not only be performed during the procedure as a roadmap but also routinely for pre-interventional evaluation to assure CS accessibility, patency, and sufficient diameters.<sup>154</sup> Simultaneous coronary angiography further allows assessment of the relation of the coronary venous system to the coronary arterial tree. MultiSlice Cardiac Tomography (MSCT) offers a non-invasive evaluation of the CS and its relation with the MA and the coronary arteries with high spatial

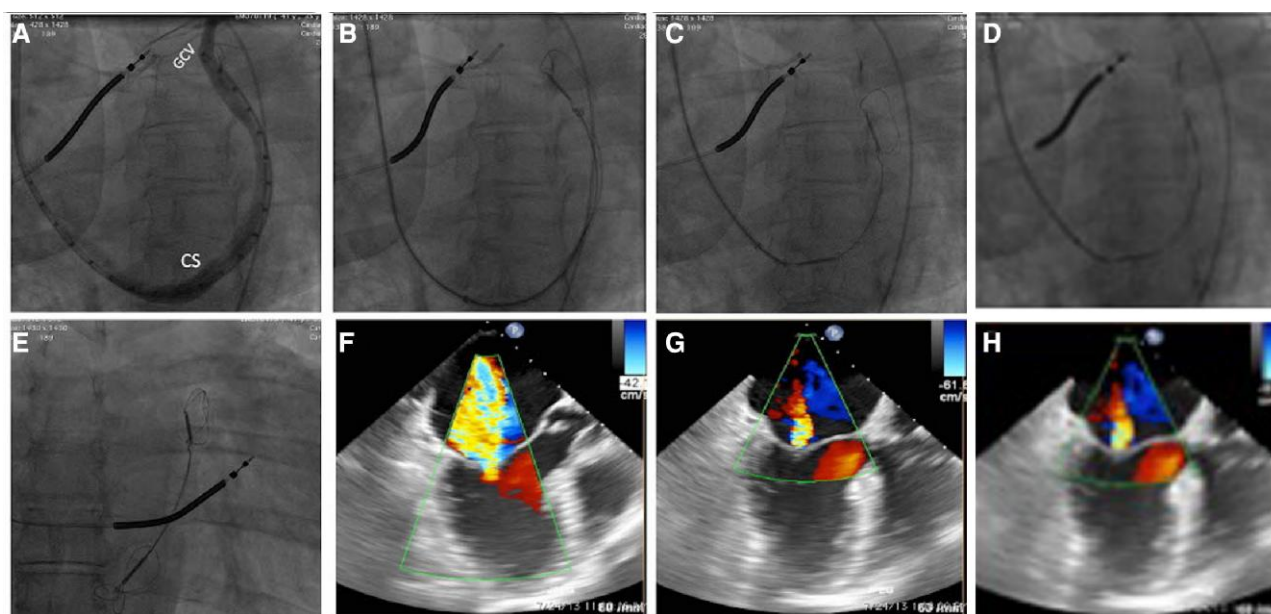
resolution and should therefore also be used for pre-interventional evaluation.<sup>153,155</sup>

### Pre-procedural screening for indirect annuloplasty: key points

- (i) 3D TOE allows reconstruction of the MA and the CS.
- (ii) CT offers a non-invasive evaluation of the CS and its relation with the MA and the coronary arteries.
- (iii) Venography is the gold standard for the assessment of CS anatomy.

### Procedural guidance

The procedural steps are monitored by fluoroscopy and TOE using a ME LAX view/biplane views (commissural and LAX views) or by trans-thoracic monitoring only. The choice of the fluoroscopic view is of particular importance. A LAO caudal projection offers visualization of the



**Figure 34** (A) The CS is cannulated and a 9 F delivery catheter is positioned distal in the GCV. (B) Occlusive venography providing a roadmap of the CS. (C) Distal anchor deployment. (D) Proximal anchor deployment. (E) Left coronary angiography showing the left circumflex artery coursing inferiorly to the CS. (F) Final deployment. (G) Baseline color Doppler evaluation. (H) Color Doppler after system release showing significant reduction of MR. CS, coronary sinus; GCV, great cardiac vein.

CS surrounding the posterior segment of the MV. 3D analysis can help to appreciate the annular modification.

For the procedure, patients are either sedated or anaesthetized depending on site preference. The CS is cannulated with standard techniques, and a 9 F delivery catheter is positioned distal in the GCV, near the anterior commissure of the MV (Figure 34). Afterwards, occlusive venography is performed to provide a roadmap of the CS tributary for insertion of catheter and to characterize the length of the CS/GCV and the diameter of the vein in the target location of the GCV and CS anchors (Figure 34). A coronary angiography is performed to assess for underlying coronary arterial disease. Once the arteriovenous anatomy was characterized, an appropriately sized implant is selected. Deployment of the helical distal anchor involved two steps: retraction of the delivery catheter to allow passive expansion of the nitinol wire forms and advancement of the delivery catheter to expand the anchors to their maximum diameter. After the distal anchor of the device is deployed (Figure 34), manual traction is placed on the delivery system to plicate the peri-annular tissue. A combination by TOE and fluoroscopy is used to determine the final position of the proximal anchor (Figure 34). Ultimate device size and position are determined by maximal geometric reduction of the posterior–anterior MA dimensions with accompanying reduction of MR as assessed by fluoroscopy and TOE. Before the implant is decoupled, coronary arteriography is performed to confirm that coronary flow is not significantly compromised (Figure 34), and echocardiography is performed to confirm that a quantitative reduction in MR is achieved (Figure 34). In the event of coronary artery compromise or insufficient MR reduction, the implant is recaptured by advancing the delivery catheter forward to collapse first the proximal anchor and then the distal anchor.

The variable distance between the CS and the MA may affect procedural success. In some patients, the CS is located above the annular level in contact with the LA wall. Annular devices in these patients

theoretically would chinch the LA wall without annular reshaping and therefore might not reduce MR. An additional concern of indirect annuloplasty is the risk of coronary ischaemic events due to the close but variable relationship between the CS and the left circumflex artery.<sup>156</sup> Finally, these devices cause at least a theoretical risk of CS thrombosis or rupture.

### Procedural guidance for indirect annuloplasty: key points

- (i) The procedural monitoring is performed by fluoroscopy and TOE or by transthoracic monitoring only.

## Chordal implantation

Percutaneous leaflet repair has been proposed in the treatment of MV prolapse using adjustable TA beating-heart chordal implantation systems.

The ideal anatomical criteria to this procedure are as follows:

- (i) P2 prolapse or flail.
- (ii) The prolapsing segment overriding the opposite leaflet by at least 9 mm suggests the presence of coaptation leaflet reserve (CLR) and correlates with a successful outcome of the procedure. The measurement can be obtained as the difference between leaflet length and annulus width in the three-chamber view (Figure 35).
- (iii) Absence of significant annular dilatation, as defined by a leaflet-to-annulus index  $\geq 1.25$ , the ratio between the sum of anterior and PL length over AP length measured in 2D LAX view at TOE.<sup>157</sup>



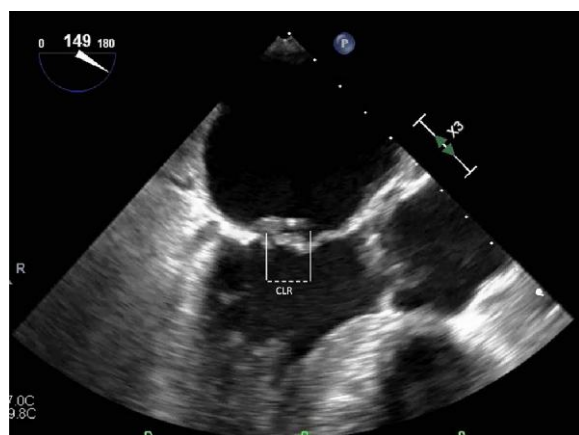
- (iv) Absence of severe LV dilatation with leaflets tethering with central regurgitant jet and/or calcification of leaflet segments.

The procedure is performed under general anaesthesia by a mini-thoracotomy TA approach. Using TOE guidance, the expanded polytetrafluorethylene (ePTFE) chords attached to the leaflets are subsequently adjusted to optimize MR reduction, then tightened to the LV myocardium and fixed to the apex. Optimal TOE imaging systems are mandatory because the procedure relies on imaging quality.

## NeoChord

The procedure is performed using the NeoChord DS1000 system (NeoChord, Inc., Eden Prairie, MN) consisting of<sup>158–160</sup> (Figure 36):

- (i) a single-use, hand-held instrument designed to load and deploy commercially available ePTFE sutures through exchangeable cartridges and (ii) a tethered leaflet verification display that enables confirmation of leaflet capture in the distal clamp of the device through four fibre optic lights. These lights reflect the tissue in between the device jaws.

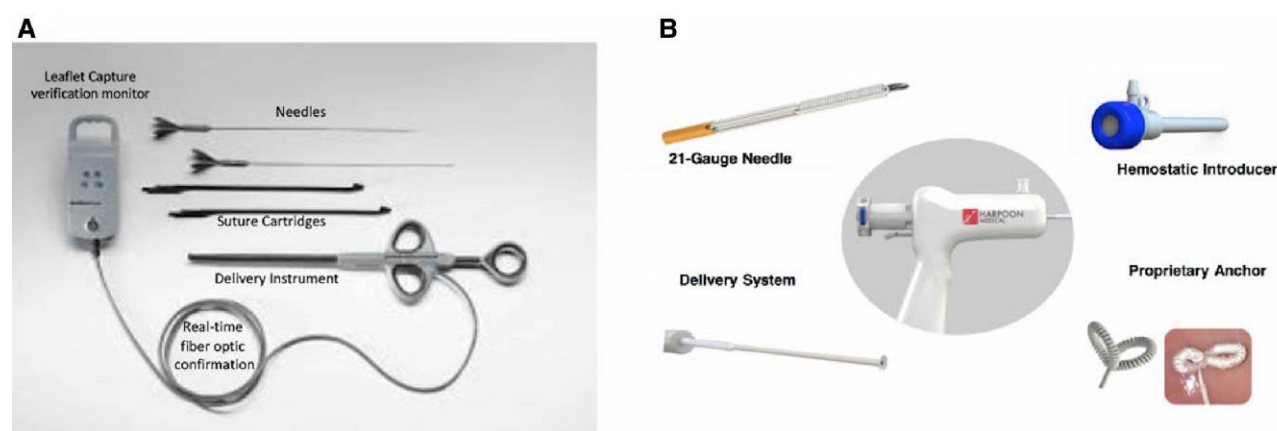


**Figure 35** ME LAX view showing P2 flail and the measurement of CLR.

A standard left lateral mini-thoracotomy is performed in the fifth intercostal space to access the LV apex. The system is directed towards the LA on 2D TOE guidance (simultaneous multiplane ME LAX + MEC views) avoiding native subvalvular apparatus entrapment (Figure 37). The key point is to maintain the device under the A2-P2 segments to stay free from the native chordae during systole and cross the valve during opening (Figure 37). Once the MV is overcome, echocardiographic imaging is switched to 3D surgical view of MV and the device is shifted towards the prolapsing segment. When an appropriate position has been achieved, the jaws of the device are opened and the leaflet is grasped. The leaflet is correctly captured when all four fibre optic monitor lights turn from red to white. At this time, the needle is pushed forward to puncture the valve segment. Then, the distal tip of the needle is retracted and the Gore-Tex suture loop exits the instrument. When the Gore-Tex suture has been engaged and retraction of the needle starts, the mosquito must be released. The device is finally pulled out from the ventricle with the jaws opened while the two ends of the suture are gripped manually. Tension is applied to the neochorda and if it significantly reduces the MR under TOE monitoring (Figure 37), a girth hitch knot is secured to the leaflet, locking one head of the suture on the valve segment while two ends remain outside the chest for final fixation on the apex. Additional neochordae are implanted by repeating the procedure to achieve maximal MR reduction. When a satisfactory number of chordae are deployed, the apical purse strings are tied.

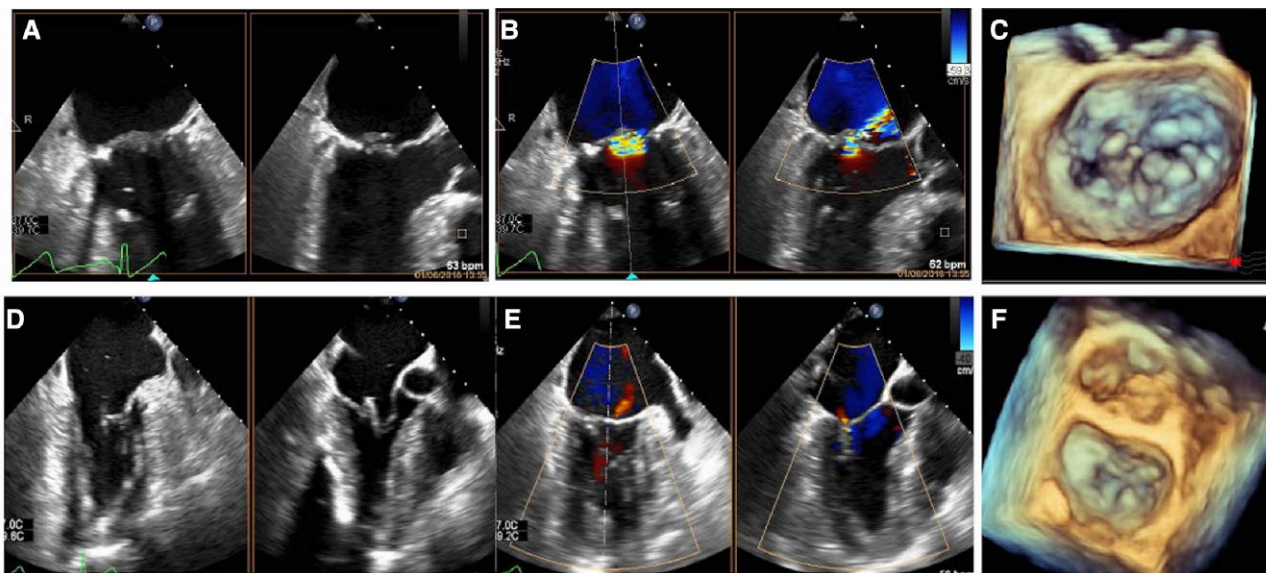
## Harpoon

The MV repair system (Edwards Lifescience, Irvine, USA) consists of two parts: a haemostatic introducer and a delivery system<sup>161</sup> (Figure 38). The end effector on the tip of the delivery system shaft is positioned on the targeted segment of the mitral leaflet; afterwards, the device is deployed, causing the needle and ePTFE wrap to penetrate the leaflet tissue. The needle is withdrawn and the coil of ePTFE is tightened to form a double-helix knot on the atrial surface of the leaflet. Simultaneous 2D images (ME LAX + MEC views) are required for device guidance. Once the delivery system is steered to the targeted location on the leaflet, the knot is deployed (Figure 38). After each knot deployment, the delivery system is withdrawn from the heart, leaving two ePTFE strands exteriorized through the introducer lumen. The ePTFE suture pairs are then threaded individually through a stiff ePTFE pledget and are tightened simultaneously and incrementally by using TOE guidance to optimize coaptation and minimize MR (Figure 38).

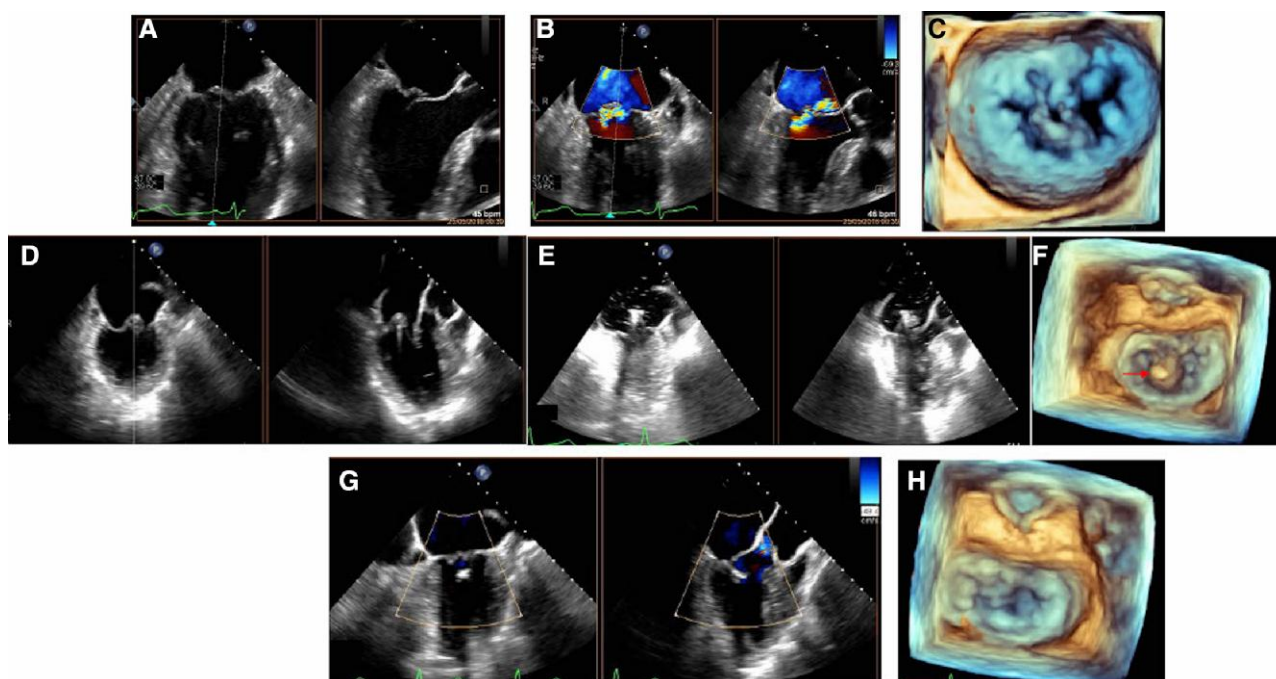


**Figure 36** Components of NeoChord (A) and harpoon systems (B).

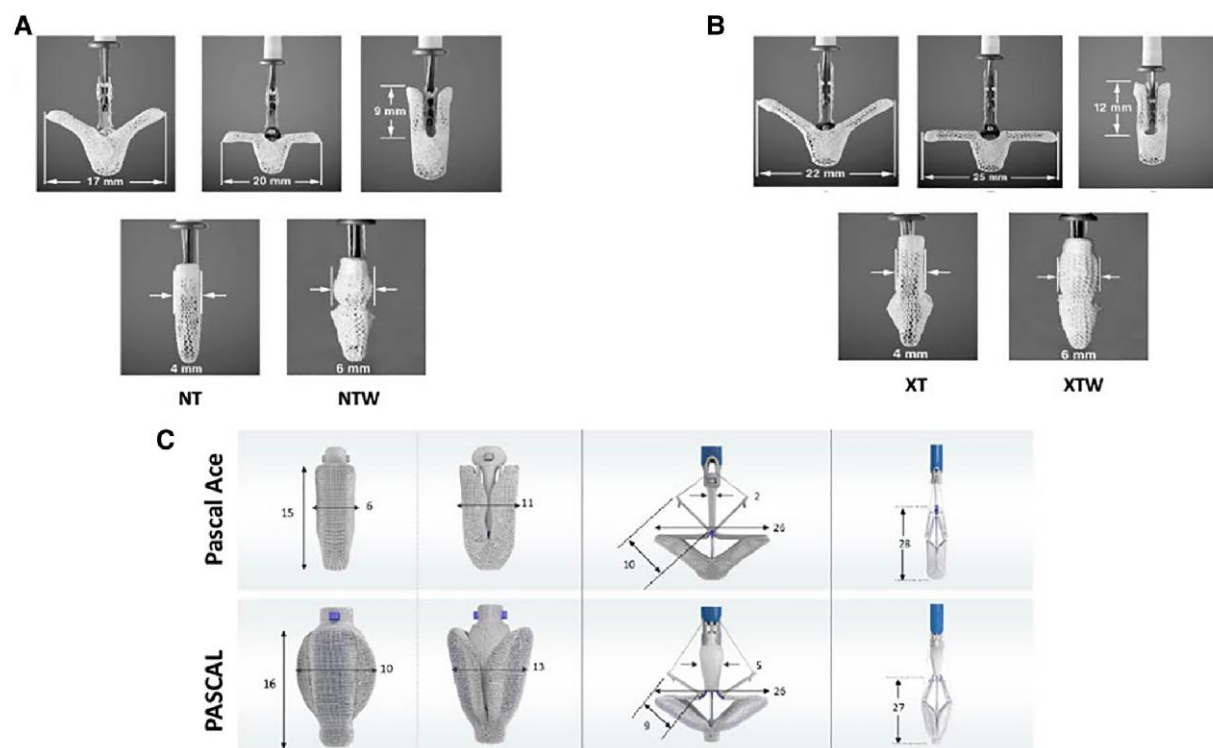




**Figure 37** P2 flail treated with NeoChord. Step-by-step description. (A) Biplane ME view showing P2 flail. (B) Biplane ME color Doppler. (C) 3D surgical view of the MV showing P2 flail with chordal rupture. (D) The system is directed towards the LA on 2D TOE simultaneous multiplane guidance avoiding subvalvular apparatus entrapment and under the A2-P2 segments. (E) The tension is applied to the NeoChord; as a consequence, the prolapse is significantly reduced. (F) 3D surgical view of the MV showing the correction of the prolapse.



**Figure 38** P2 flail treated with harpoon. Step-by-step description. (A) Biplane views showing P2 flail. (B) Biplane color Doppler. (C) 3D surgical view of the MV showing P2 flail with multiple chordal rupture. (D) The system is directed towards the LA under TOE guidance. (E) The knot is deployed. (F) 3D surgical view showing the knot in LA (arrow). (G) The tension is applied to the ePTFE and fixed on the apex with concomitant reduction of MR. (H) 3D surgical view demonstrates the prolapse correction.



**Figure 39** (A) MitraClip G4 NT and NTW. (B) MitraClip G4 XT and XTW. (C) Pascal and Pascal Ace.

### Chordal implantation: key points

- (i) The ideal candidate is a patient with P2 prolapse or flail, with the prolapsing segment overriding the opposite leaflet by at least 9 mm without annular dilatation.
- (ii) The procedure is performed under TOE guidance using 2D simultaneous biplane views and 3D en face MV perspective.

## Transcatheter edge-to-edge repair

Percutaneous mitral leaflet repair aims to reproduce edge-to-edge Alfieri surgical technique improving leaflet coaptation and reducing/eliminating MR.<sup>162</sup> At present, there are two available devices for TEER: the MitraClip system (Abbott Vascular Inc, Menlo, CA, USA) and PASCAL system (Edwards Lifescience, Irvine, USA). The devices are proven safe and effective both in PMR and SMR.<sup>142,163–165</sup>

The MitraClip system is a polyester fabric-covered cobalt–chromium implant with two arms which can be opened and closed with a steerable-guiding mechanism. The latest iteration of the device is the MitraClip G4 system (Generation 4), which was released in 2019. The clip is offered in four sizes (NT, NTW, XT, and XTW) (Figure 39A and B). In addition, the G4 system permits controlled gripper actuation (the grippers can be dropped independently to capture the leaflets one at a time) and the real-time left atrial pressure monitoring.

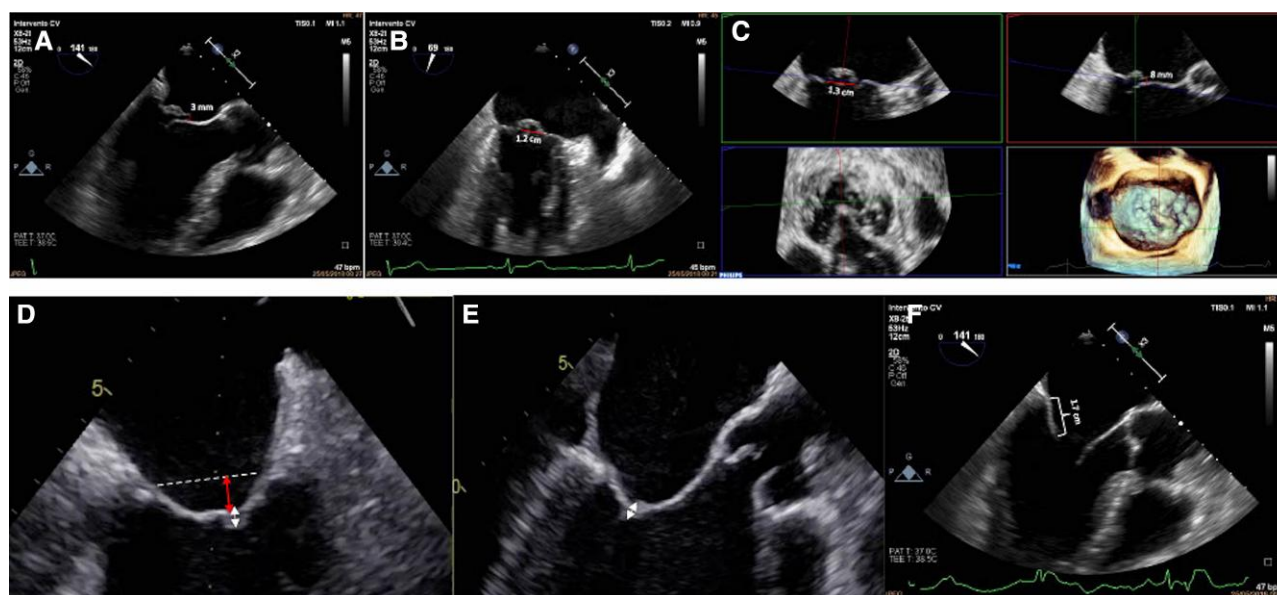
The Edwards Pascal transcatheter valve repair system also works on the principle of leaflet repair but has some additional design features. The Pascal implant has a central spacer designed to reduce the tension on the leaflets and fill the regurgitant orifice area. The spring-loaded paddles and clasps can be operated either simultaneously or independently to facilitate leaflet capture. The flexible delivery system allows navigation in three planes, and the Pascal device can be elongated, making it less prone to get stuck in the chords. Two implants are available: Pascal and Pascal Ace (Figure 39C).

In degenerative MR, the device anchors the flail and/or prolapsed segments, whereas in patients with SMR, it improves coaptation of the tethered leaflets reducing the time and force required to close the valve. Additionally, the device over time creates a tissue bridge between the two mitral leaflets. As a result, it limits annular dilatation and supports the durability of the repair. Finally, the device restrains the LV wall by restricting LV dilatation and induces reverse LV remodelling, which in turn may further reduce tethering and resultant regurgitation.

### Patient selection

TTE is the first-line imaging technique to rule out potential candidates for TEER. 2D/3D TOE is essential for assessment of mitral functional anatomy to select patients for TEER. Indeed, 2D/3D TOE is crucial to confirm the severity and to precisely define the mechanism of MR as well as the anatomic suitability for TEER. It is crucial to assess the MV anatomy at the origin of MR (target lesion) and to confirm that leaflet tissue quality and length are adequate in this area to allow for a secure device placement.

For patients with degenerative MV prolapse/flail, the following features should be addressed:



**Figure 40** ME LAX and MEC views showing the measurement of flail gap (A) and flail width (B). (C) 3D multiplane reconstruction allowing accurate measurement of both measurements. (D) Four-chamber and (E) ME LAX depicting measurement of the coaptation length (white arrow) and coaptation depth (red arrow). (F) Measurement of the length of the PL in P2 region (supposed target zone).

- (i) Number and localization of diseased segments. This issue can be addressed by multiple 2D TOE views and 3D TOE. 3D TOE enables the identification of leaflet abnormalities that can impact the feasibility of a device implantation (i.e. clefts or perforations).<sup>166</sup> 3D TOE colour Doppler is more accurate in localizing the MR jet origins than 2D TOE providing a direct visualization of the true proximal flow convergence region.<sup>166,167</sup>
- (ii) Evaluation of the extension of the prolapse/flail using multiple 2D TOE views, 3D TOE, and multiplane reconstruction of 3D data sets. The TOE view should be aligned to demonstrate the maximal excursion of the flail segment. Two main anatomic measurements are required: (a) the flail gap (distance separating the tip of the flail segment from its opposing normally coapting leaflet) measured by 2D TOE in ME LAX, four-chamber, or MEC views and (b) the flail width derived from the MEC view and/or transgastric SAX view (Figure 40). 3D TOE using the surgical view or MPR can also be very helpful in determining the flail width and gap (Figure 40).

For patients with functional/ischaemic MR, the presence of sufficient leaflet tissue for mechanical coaptation and the degree of restriction of PL constitute the most important features. Two measurements are essential: the coaptation depth measured by 2D TOE in a four-chamber view and the coaptation length measured in four-chamber and ME LAX views (Figure 40).

In addition, the measurement of the length of the PL in target zone is required for both degenerative and functional/ischaemic MR (Figure 40).

Based on morphologic characteristics of MV, the suitability for TEER implantation can be classified as ideal, challenging, and unsuitable. The suitability criteria are mostly derived from experience with the MitraClip system (Table 15 and Figures 41–43). The ideal morphology is well suited for implantation and initial institutional experience. It is also possible to successfully treat challenging morphologies. Such cases should only be

attempted by experienced centres in the absence of therapeutic alternatives.

### Patient selection for TEER: key points:

- (i) TTE is the first-line imaging technique to rule out potential candidates for TEER.
- (ii) 2D/3D TOE is essential for confirming the suitability for TEER.
- (iii) The characterization of the mechanism of MR and the anatomy of MV are crucial features to define the suitability of TEER.

## Procedural guidance

The procedural guidance of TEER procedures relies on 2D TOE, 3D TOE, and fluoroscopy.

### MitraClip procedure

#### TSP

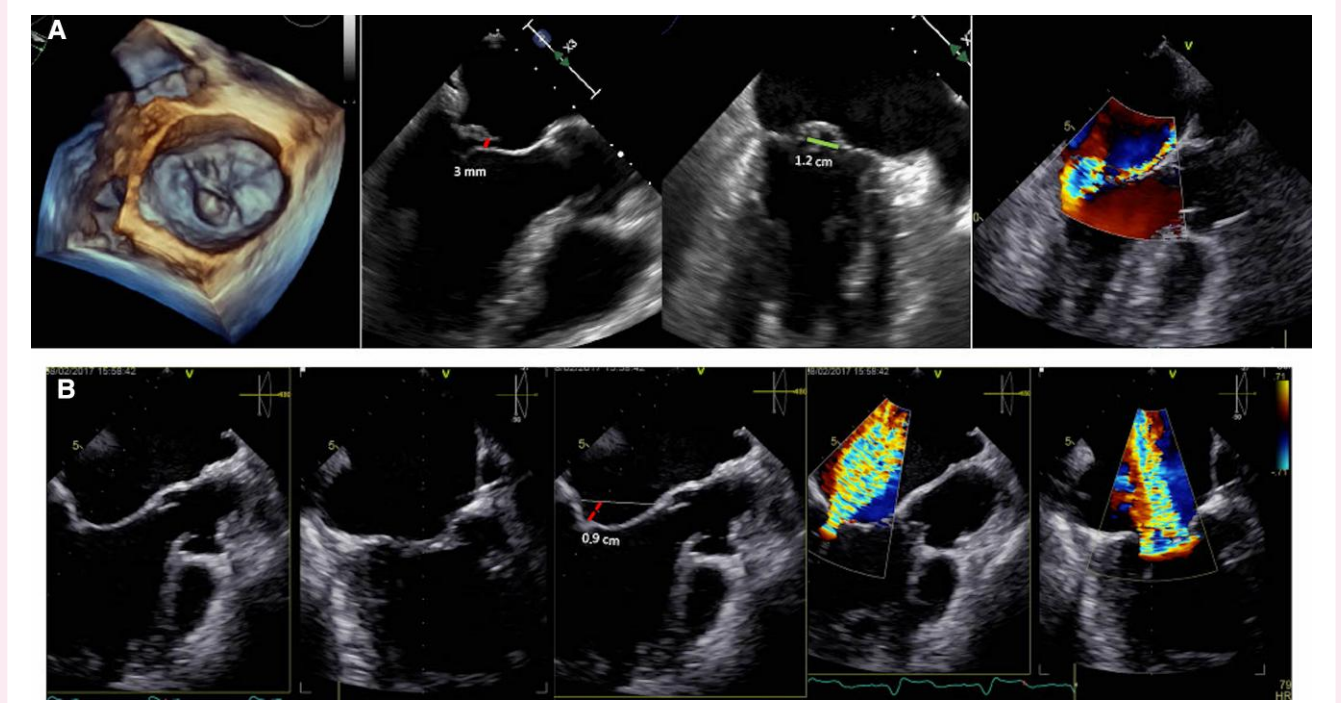
The determination of the optimal TSP site is fundamental for a MitraClip procedure. A suboptimal TSP puncture often requires additional steering manoeuvres to correct the position of the MitraClip delivery system. The optimal TSP is located in the superior–posterior part of the FO and the height should be  $\geq 4.0$  cm above the annular plane. However, the optimal height above the MV differs for degenerative and secondary MR. In patients with prolapse/flail, the puncture site should be 4–5 cm above the MA, thus providing enough space to adequately manoeuvre the MitraClip delivery system within the LA. In patients with secondary MR and extensive tethering, the coaptation is usually shifted below the annular plane. In these cases, the puncture site 3.5–4.0 cm above the annular plane could be acceptable. A patent foramen ovale cannot be recommended for access to the LA. Even if the entry into the LA would be superior, it is too anterior and therefore



**Table 15** Morphological suitability criteria for TEER

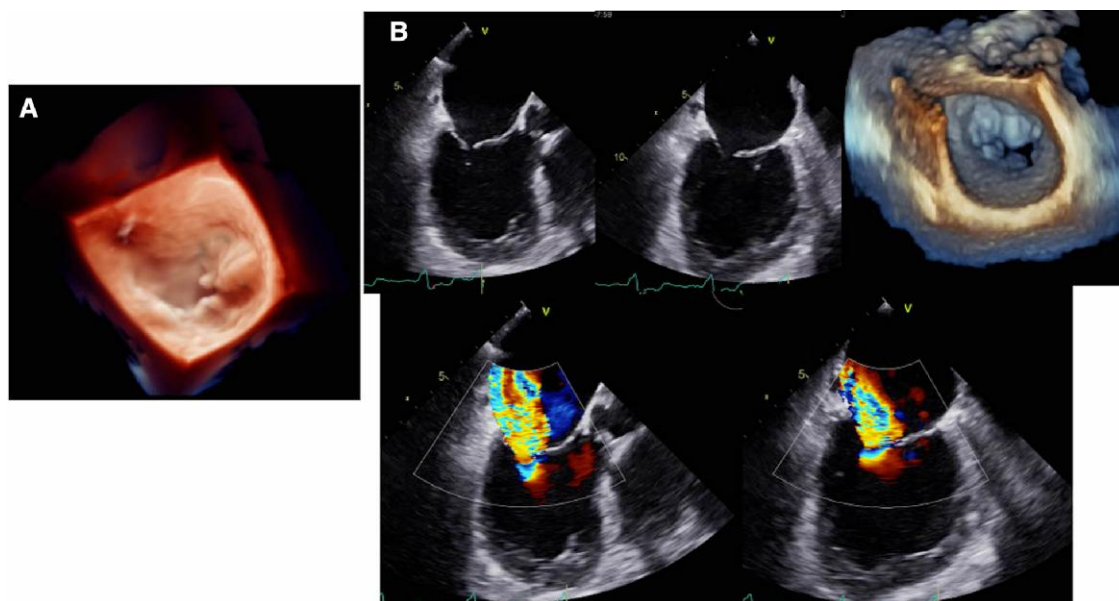
Ideal morphology	Challenging morphology	Unsuitable morphology
Central A2-P2	P1/A1 or P3/A3 lesions	Calcifications in the grasping area or hinge point
Absence of calcifications in the grasping zone	Calcifications not in the grasping zone	Barlow's disease with multisegment flail leaflets
MVA >4 cm <sup>2</sup>	MVA ≥3 ≤4 cm <sup>2</sup> with preserved leaflet mobility	MVA <3 cm <sup>2</sup> or MG >5 mmHg
Flail gap <10 mm	PL length ≥6–7 ≤10 mm	PL length <6 mm
Flail width <15 mm		
Coaptation length ≥2 mm	Carpentier IIb	Carpentier IIa
Tenting height ≤11 mm		
PL length >10 mm	Flail width >15 mm	Significant cleft
Good imaging quality	Tenting height >11 mm	Perforation or laceration
Large LA volume	Important annular dilatation (end-systolic AP or IC diameter >40.5 mm) <sup>192</sup>	Endocarditis
Large FO	Loss of systolic leaflet coaptation	Anatomic characteristics of IAS precluding TSP: very small FOV or previous ASD closure
	Multiple prolapsing/flail segments	Very poor imaging quality
	Cleft/indentation	
	Suboptimal imaging quality	
	Small FO	
	Previous surgical correction of IAS	
	Previous MV repair	
	Small LA	

Abbreviations as in the text.

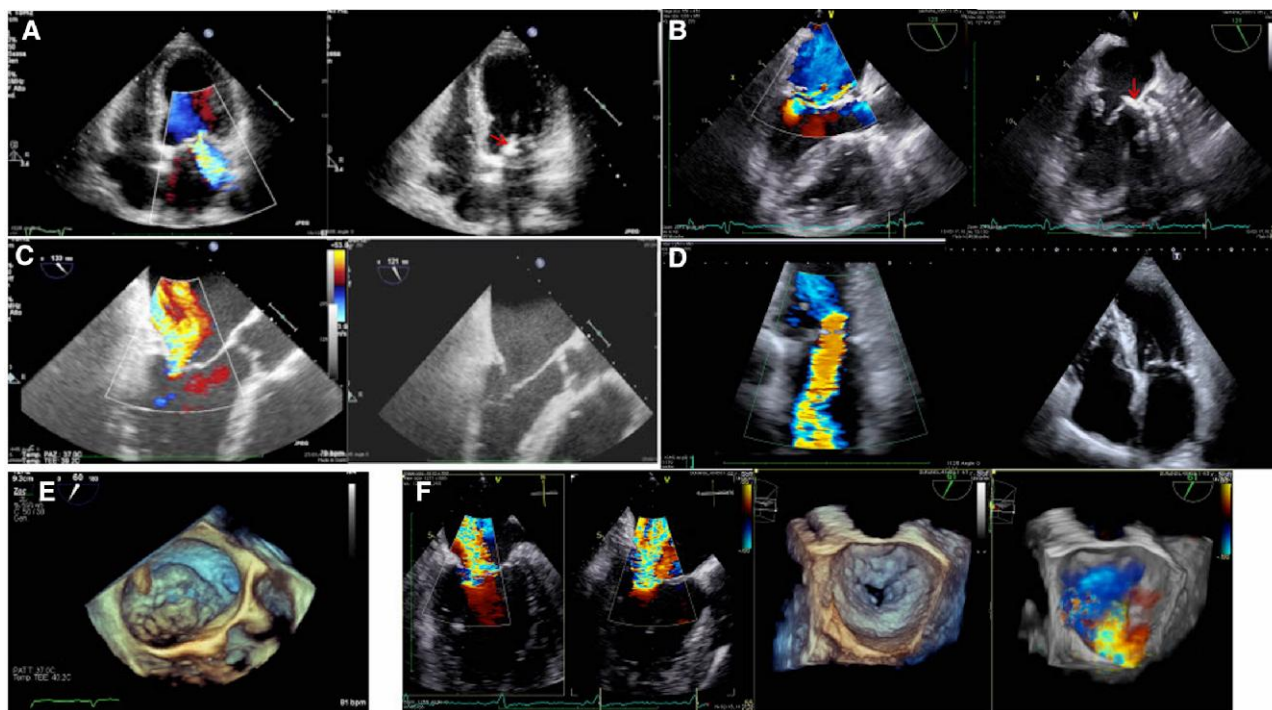


**Figure 41** Ideal morphology for TEER procedure. (A) Degenerative aetiology. 3D en face of MV showing the P2 flail (central lesion). Biplane view shows the flail leaflet. Biplane color Doppler demonstrating the single central jet. Flail gap = 0.3 cm (red line); flail width = 1.2 cm (green line). (B) Functional MR. Biplane view shows the symmetric tethering. Tenting height: 0.9 cm (dotted red line). Biplane color Doppler demonstrating a wide central jet.

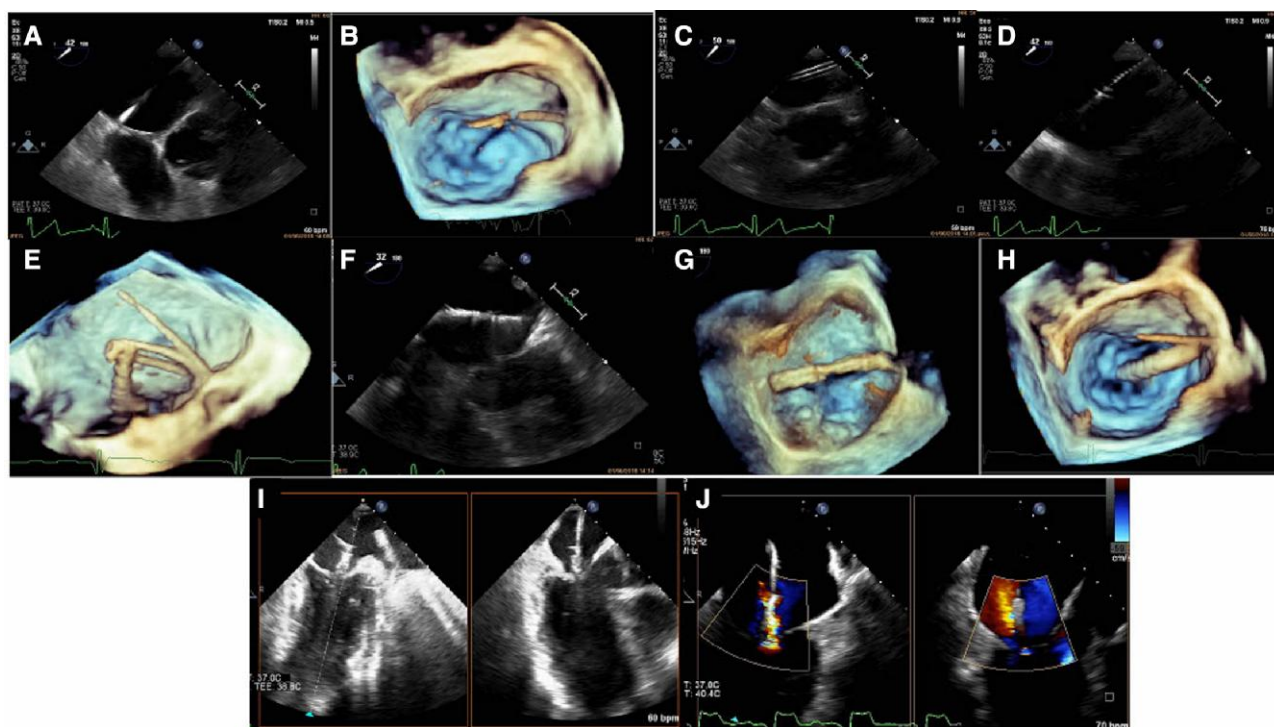




**Figure 42** Challenging morphology for TEER procedure. (A) Degenerative aetiology. 3D en face perspective of MV showing wide prolapse of P3. (B) Functional MR with lack of leaflet coaptation. LAX and 90° views show a huge coaptation defect in central and medial regions of the valve, respectively. 3D en face view confirms the gap in these regions. LAX and 90° views with color Doppler demonstrating a large jet originating from the central and medial region of the valve.



**Figure 43** Unsuitable morphologies for TEER. (A) Calcifications in the grasping zone in anterior leaflet (arrow). (B) Calcifications in the hinge point (arrow). (C) Short PL. (D) Restrictive morphology. Rheumatic disease (Carpentier IIa). (E) Barlow's with multisegment flail leaflet disease. (F) Cleft in PL.



**Figure 44** MitraClip procedural guidance. (A) SAX view. The guidewire crosses the septum. (B) 3D overhead of LA showing the transseptal sheath and the guidewire inside the LA. (C) The guidewire in LUPV. (D) The dilator can be identified by a typical echogenic coil. (E) The SGC appears in 3D as a railroad-shaped artefact. (F, G) CDS advancement into LA: 2D ME view (F) and 3D overhead perspective of the LA (G). (H) 3D overhead perspective of LA showing the steering of CDS towards the centre of the valve. (I, J) Biplane views (commissural and LAX view) without (I) and with colour Doppler (J) allow to perform medial–lateral and anterior–posterior clip adjustments.

suboptimal for this procedure. Access via an atrial septal defect (ASD) is also not recommended as the size of the defect generally does not match the size of the steerable guide catheter (SGC) whose position is therefore not stable. Furthermore, in most cases, the septum is fragile and does not provide enough support for a stable position of the SGC and the risk of IAS rupture is increased.

#### SGC insertion into LA

After septal crossing, the SGC and dilator assembly are gently advanced into the LA over a super stiff exchange length guidewire which is preferably placed in the left upper pulmonary vein (LUPV) (Figure 44A–C). The dilator can be identified by a typical echogenic coil (Figure 44D). The insertion of the SGC should be carefully monitored with the aid of 2D and 3D TOE (SAX and four-chamber views are recommended) and fluoroscopic imaging to avoid injuries of the LA wall. The tip of the SGC is marked with a radiopaque echo bright double ring structure and can be identified by 2D TOE and 3D TOE. Once the SGC is in place and secured (2–3 cm within the LA cavity), the wire and the dilator will be removed. After removing the wire and dilator, the SGC appears in 2D and 3D as a railroad-shaped artefact (Figure 44E).

#### Clip delivery system advancement through the catheter into LA

The clip delivery system (CDS) is then advanced into the LA through the SGC under fluoroscopic and TOE guidance (Figure 44F). 3D overhead perspective of the LA offers the best view for appreciating the spatial relationship among structures and device (Figure 44G). However, 3D does not offer enough spatial resolution to confirm if

the clip is not interacting with LA or valve structures as 2D and simultaneous multipane views. At this stage, 2D TOE view (usually in between SAX and bi-caval views) is used to confirm that the SGC is maintained in the LA.

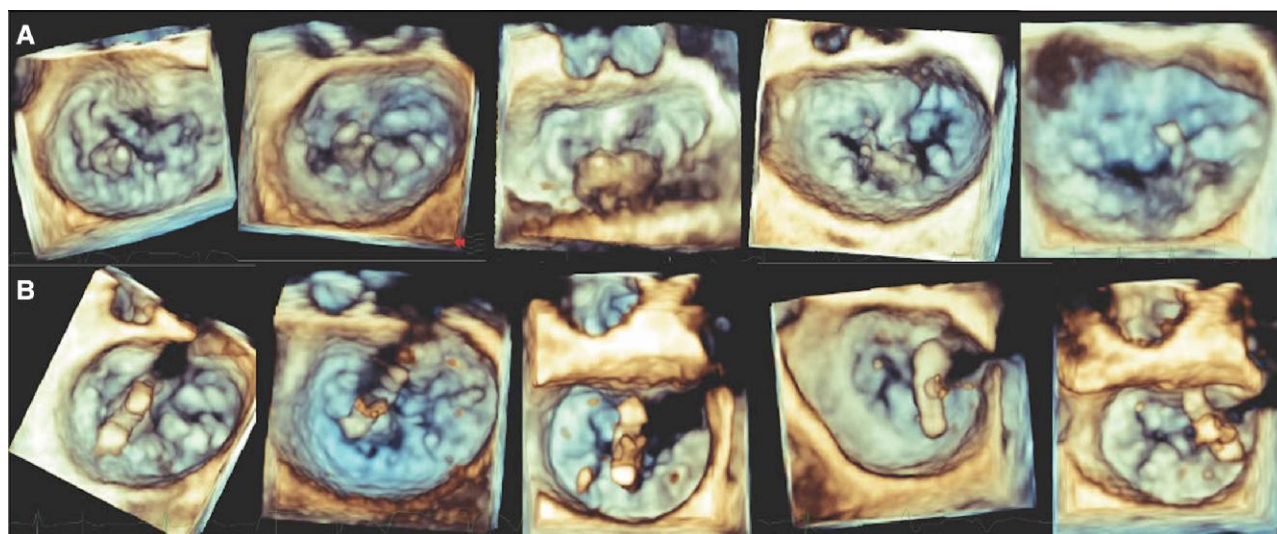
#### Steering and positioning the MitraClip in the LA

The CDS is steered towards the MV over the target lesion [the tip of the clip should point towards the largest proximal isovelocity surface area (PISA)]. The medial deflection and posterior torque of the system are needed. A series of steering manoeuvres is generally needed to achieve a position of the clip over the MV target lesion with respect to anterior–posterior and medial–lateral directions. This step is usually monitored by 3D overhead perspective of the LA and simultaneous biplane views overlapping the colour Doppler (Figure 44H). Two orthogonal 2D TOE imaging views are used: MEC view ( $\sim 60^\circ$ ) in which both commissures can be adequately identified to perform medial–lateral clip adjustments and LAX view at  $120\text{--}150^\circ$  to monitor anterior–posterior clip adjustments. Colour Doppler should be used in addition to confirm the adequate clip alignment over the regurgitant jet. The clip should split the regurgitant jet indicating a correct position above the target lesion.

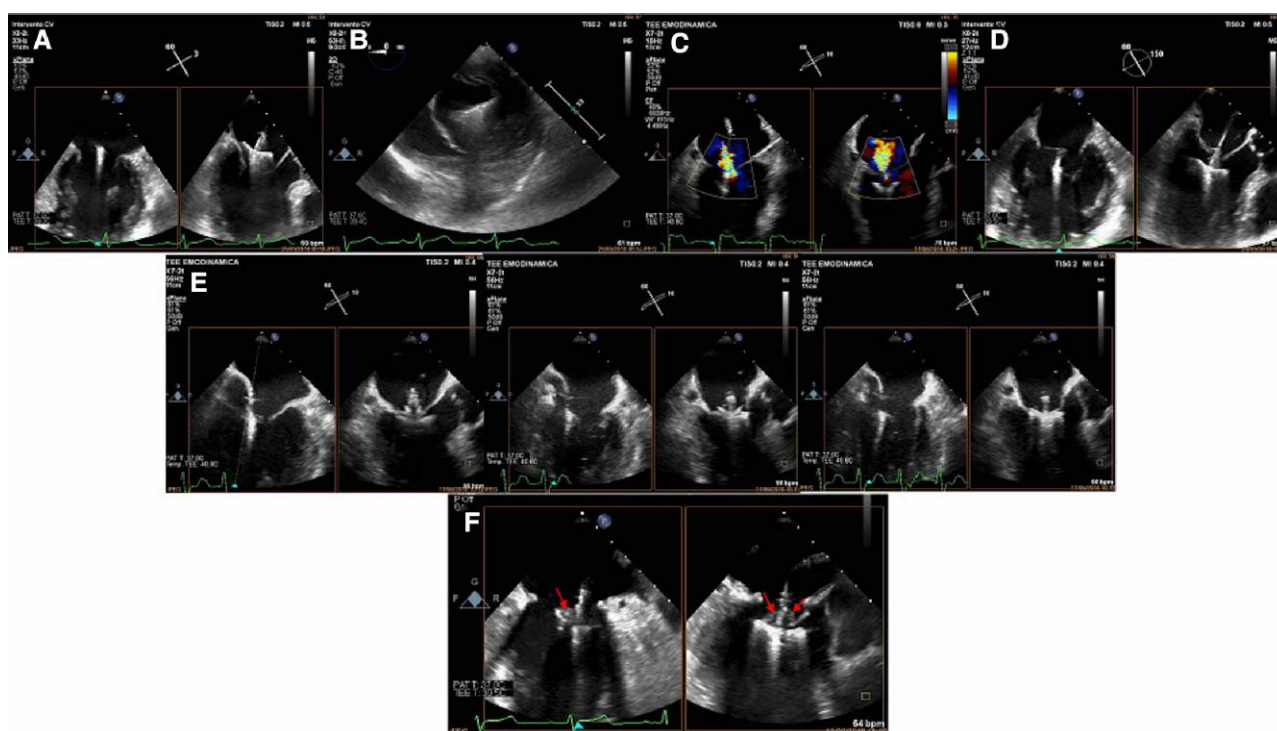
#### Axial alignment of the CDS

The trajectory is tested with gentle advancement of CDS towards the MV plane avoiding to overcome the leaflets (Figure 44I and J). The trajectory should be perpendicular to the MV plane and not slanting because a misalignment can affect an incorrect advancement of CDS

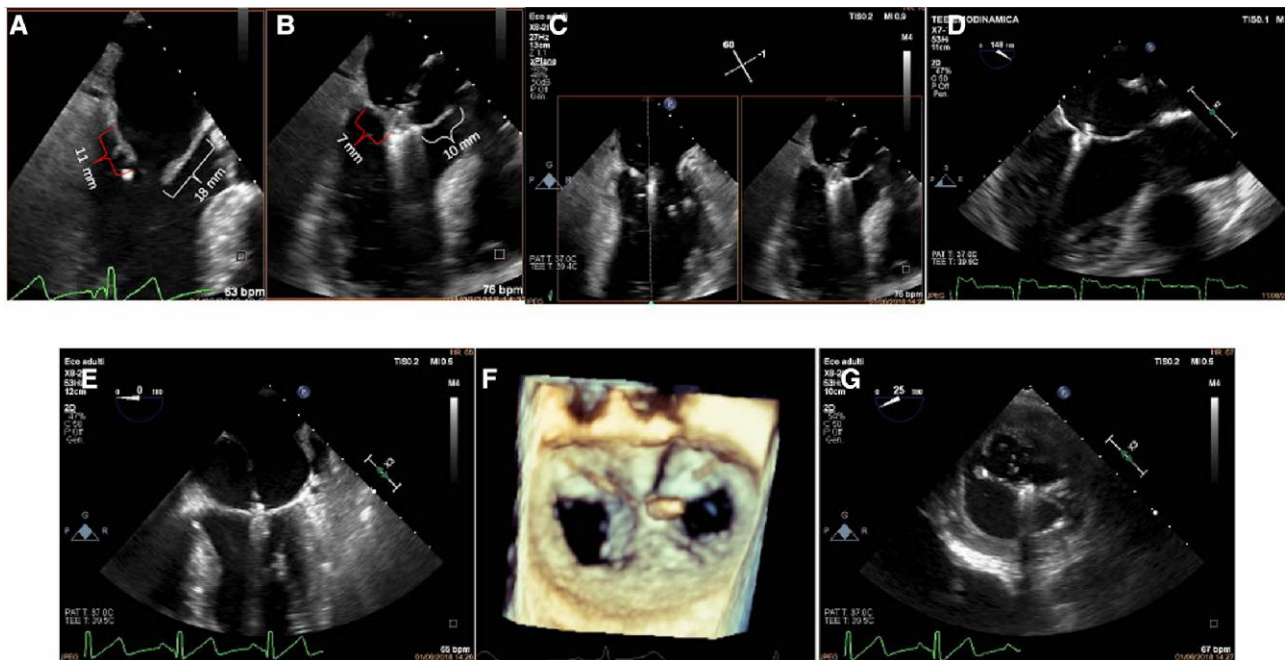




**Figure 45** (A) Different lesions of the PL. Left to right panel: P1, P2M2, P2 central, P2M2, and P3 lesions, respectively. (B) 3D en face views of the different clip orientations according to the localization of specific lesion.



**Figure 46** (A, B) Clip arm orientation. (A) Biplane views. In commissural view, the clip arms are not visible, whereas in LAX view, the arms are fully opened. (B) SAX transgastric view shows the arms perpendicular to the coaptation line in central position. (C) Biplane colour Doppler: the clip partially closed splits the jet during advancement into the LV. (D) Biplane views showing the clip in LV in the central position with correct arm orientation. (E) Leaflet grasping. (F) Entrained chordae tendineae between grippers and shaft (arrows).



**Figure 47** The free lengths of AL (in white) and PL (in red) before grasping (A) and after grasping (B). Differences in lengths denote lengths of respective leaflet captured inside the MitraClip. (C) Multiplane views. (D) LAX view used for assessing the PL insertion. (E) Four-chamber view used for assessing the anterior leaflet insertion. (F) 3D en face view before clip release showing the double orifice and the bridge of tissue. (G) SAX transgastric view showing the double orifice.

into LV and the efficacy of the grasping (e.g. distortion of the coaptation line). This aspect is of the utmost importance in the commissural lesion to avoid chordal entrapment. This can be assessed mainly by simultaneous biplane views (MEC and LAX views).

#### *Alignment of the clip arms to the coaptation line*

Clip locations at the lateral (P1) and medial (P3) scallops of the PL are defined as lateral and medial, respectively. A clip location in the central scallop (P2) is defined as central or if the clip is located in P2M1 or P2M2 as centrolateral and mediocentral, respectively. The clip arms must be oriented perpendicularly to the coaptation line. When the clip is positioned in the central region of the valve, the anterior arm must be oriented at 12 o'clock, while if the clip is placed lateral, the anterior arm is oriented in slightly clockwise direction or if it is placed medial, the anterior arm is oriented in slightly counterclockwise direction. The clip's orientation is monitored by en face 3D view of the MV (Figure 45). If the clip is positioned centrally, the clip arms are not visible in the MEC view while both clip arms are visible in full length in the orthogonal LAX view (Figure 46A). In the RAO cranial fluoroscopic projection, the clip arms are not visible. If the clip is positioned in lateral or medial region of the valve, the clip's arms can be partially visible in the MEC view. Additionally, SAX transgastric view can be used to confirm that the clip arms are perpendicular to the coaptation line (Figure 46B).

#### *Advancement into LV*

The CDS is then advanced distally across the MV, commonly with a fully opened clip (180°) using the NTR system and partially closed (60°) with XTR system, into the LV to a position ~2 cm below the MV under fluoroscopic and simultaneous biplane (MEC and LAX views) guidance (Figure 46C and D). In order to prepare for a successful grasp perpendicular to the coaptation line, the correct positioning should be verified by

ensuring that both mitral leaflets move freely above the clip arms and that the clip splits the MR jet. As the clip may rotate during the passage across the MV, it is important at this step to reconfirm the correct clip orientation by simultaneous biplane views and/or 3D en face view reducing progressively the gains until deleting the MV leaflets, so looking at the clip arms in transparency or alternatively using the 3D display from LV. Clip arm adjustment (>90° in each direction) in the LV should be avoided as this may lead to an entanglement of the clip in the chordae tendineae and may make it difficult or even impossible to remove the clip.

#### *Leaflet grasping*

Once the MitraClip is in a good position, leaflet grasping is done by slowly retracting the system back towards the LA to allow the leaflets to come to rest on the clip arms. If the grasp appears satisfactory, then the grippers are lowered onto the leaflets (Figure 46E). This step is usually monitored with a 2D LAX view. It is important to visualize continuous leaflet insertion while grasping to avoid rolling leaflets/chordae (Figure 46F). Initial closure of the clip until the clip arm angle is ~60° is recommended. Fluoroscopically, the clip should maintain a distinct 'V' shape. When the clip position, as well as leaflet insertion and MR reduction without inducing MS, appears satisfactory, the clip can be fully closed.

#### *Assessment of leaflet insertion*

The acquisition of a longer loop is helpful as the grasp can be reevaluated whenever needed. The leaflet insertion measurements are taken in diastole using MEC and LAX views in a simultaneous biplane. Leaflet lengths at baseline are measured from hinge point to leaflet tip. Leaflet length outside the clip is measured either between the hinge point and the contact point of the leaflet with the clip. The length of leaflet captured inside the clip is determined by subtracting the leaflet length outside the clip from the corresponding leaflet length at baseline. 'Adequate leaflet



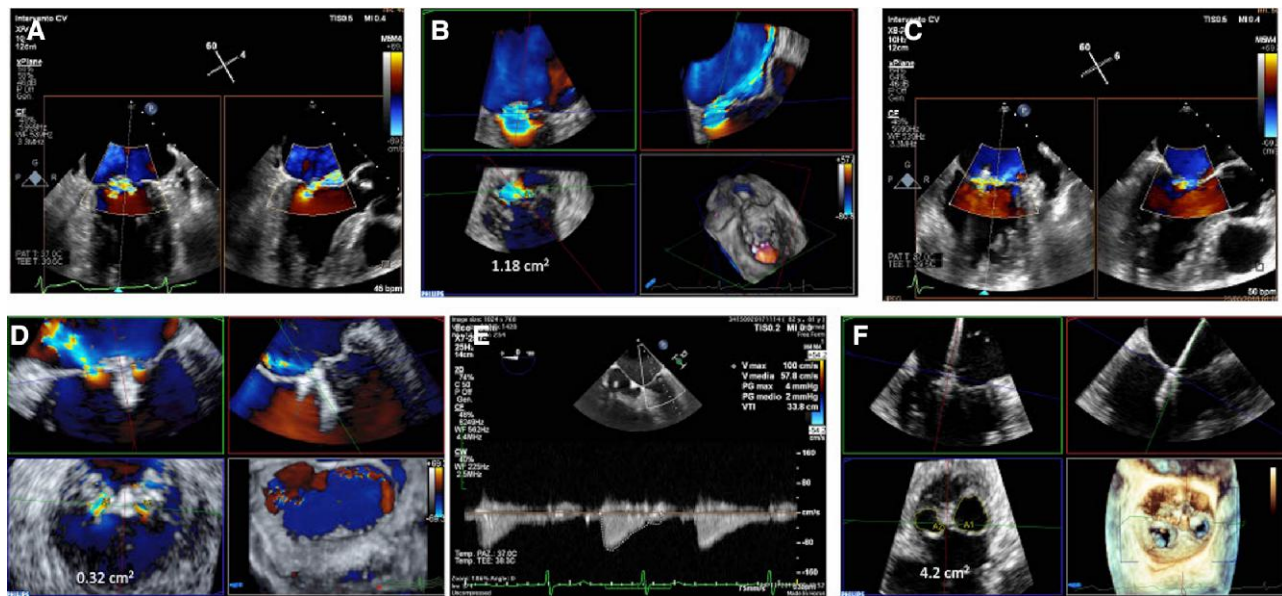
**Table 16** Echocardiographic and haemodynamic parameters for grading MR severity in TEER procedure

Parameter		Comments	
Haemodynamic parameters			
Left atrial pressure (LAP)	Reduction of a regurgitant V-wave/reduction of LAP	<ul style="list-style-type: none"><li>• Load dependent</li><li>• Affected by other haemodynamic factors (e.g. anaesthetic drugs)</li></ul>	
Systolic peripheral arterial pressure (sBP)	Increase in sBP	<ul style="list-style-type: none"><li>• Load dependent</li><li>• Affected by other haemodynamic factors (e.g. anaesthetic drugs)</li></ul>	
Echocardiographic parameters			
Qualitative	MR reduction	Mild MR	
Color Doppler jet <ul style="list-style-type: none"><li>• Size</li><li>• Number</li><li>• Eccentricity</li></ul>	Reduction of numbers and size of jets	Few small, narrow jets	<ul style="list-style-type: none"><li>• Multiple jets can lead to overestimation</li><li>• Device artefacts/shadowing may mask jets</li><li>• Eccentric jets difficult to evaluate</li><li>• Affected by technical and haemodynamic factors</li></ul>
Flow convergence size (at a Nyquist limit 25–40 cm/s)	Reduction of flow convergence	None or small	<ul style="list-style-type: none"><li>• Device artefacts/shadowing may mask jets</li><li>• Influenced by technical and haemodynamic factors</li></ul>
Mitral inflow pattern	Decrease E-wave velocity/ decrease inflow VTI	A-wave dominant	<ul style="list-style-type: none"><li>• Affected by multiple factors: relative MV obstruction, LV filling pressure, and atrial fibrillation</li></ul>
Pulmonary vein flow pattern	Increase in forward systolic component	Systolic dominant	<ul style="list-style-type: none"><li>• Influenced by many factors: LV diastolic function, atrial fibrillation, and LA pressure</li></ul>
CW Doppler of MR jet (density and contour)	Decrease in density and modification of the shape	Faint, parabolic contour	<ul style="list-style-type: none"><li>• Angle dependency</li><li>• Difficult for eccentric jets</li></ul>
PW LVOT (SV)	Increase in VTI LVOT		<ul style="list-style-type: none"><li>• Affected by multiple haemodynamic factors</li></ul>
LASEC	Appearance/increase		<ul style="list-style-type: none"><li>• Not specific/not frequent</li></ul>
Semi-quantitative			
VC width	Not specific/not frequent	≤0.3 cm	<ul style="list-style-type: none"><li>• Not validated for multiple jets</li><li>• Difficult for eccentric jets</li></ul>
Quantitative			
3DVCA	VCA reduction	<0.2 cmq	<ul style="list-style-type: none"><li>• Likely a preferred method but limited studies available</li><li>• Technical dependence/artefacts</li></ul>
RV	RV reduction		<ul style="list-style-type: none"><li>• Requires excellent LV endocardial definition ≥ best with 3D echo or contrast echo</li><li>• Cannot use MA site for flow because of MV devices (except MV annuloplasty)</li><li>• Multiple measurements may compound errors ≥ technically difficult</li><li>• Not accurate if &gt;mild AR or VSD present</li></ul>
Regurgitant fraction (RF)	RF reduction	<30%	

Adapted from Agricola et al.<sup>170</sup> Abbreviations as in the text.

insertion' is considered present if the length of leaflet captured inside the clip is ≥5 mm and both leaflets inserted into the atrial aspect of the closed clip arms (Figure 47A and B). The quality of leaflet insertion and satisfactory grasp is verified by observation of other direct signs such as leaflet immobilization, the limited leaflet mobility relative to the tips of the clip arms, and the presence of a double MV orifice, and the indirect signs, for instance the adequate MR reduction and the appearance of spontaneous echo contrast in LA, whereas the presence of jet through the clip suggests little amount of leaflet tissue insertion into clip arms. The leaflet motility can be assessed by simultaneous biplane modality

using the MEC view as the main view and moving the elevation plane along the MV from the posterior–medial orifice to the anterior–lateral one (Figure 47C). The quality of insertion of PL is usually best seen in a LAX view and of anterior leaflet insertion in four-chamber view (Figure 47D and E). In addition, MPR allows to evaluate the leaflet insertion in any desired planes without anatomic restrictions. The 3D en face view of MV from LA or LV perspectives as well as the 2D SAX transgastric view of MV is helpful to assess the geometrical changes of the MV, which presents a double MV orifice in most cases and the quality of the tissue bridge between the leaflets (Figure 47F and G).



**Figure 48** Baseline colour Doppler: (A) biplane views. (B) 3D VC measured by MPR. After clip placement and closure: (C) biplane colour Doppler. (D) 3D VC. (E) Transmittal pressure gradient. (F) MVA calculated with MPR by planimetry of the both orifices.

#### Assessment of result before clip deployment

To make results comparable regarding MR grading, it is of the utmost importance to perform measurements pre- and post-Clip implantation under similar haemodynamic conditions. The evaluation of residual MR after edge to edge is challenging.

Quantitative Doppler evaluation cannot be used reliably after clip placement. Although the 3D colour Doppler VC area seems promising, a multiparametric approach and a classification in a four-grade system (1+ to 4+) should be used (Table 16 and Figure 48A–D).<sup>168–171</sup> In addition, the risk of MS has to be evaluated after the placement of each clip. For this purpose, the MTG is usually assessed by CW Doppler (Figure 48E). It has been demonstrated that MTG has the same validity in assessing double-orifice MV as a single-orifice MV.<sup>172</sup> A limitation is that Doppler measurements are highly influenced by heart rate, cardiac output, and residual MR.<sup>172</sup> In addition, planimetry of the MV should be performed, preferably by using 3D echocardiography, which allows for MPR of the MVA (Figure 48F).<sup>173</sup> Alternatively, 2D planimetry should be performed in mid-diastole in SAX transgastric view. The edges of the MV leaflets should be clearly seen. The inner edge of each orifice is then traced and the areas combined to calculate the total MVA. A MVA  $\leq 1.5$  cm<sup>2</sup> and a MTG  $\geq 5$  mmHg were considered criteria to indicate significant MS.<sup>174</sup>

The final geometry of the MV and the assessment of the final size of the newly created orifices have also to be judged and are best evaluated by using 3D TOE en face views. It should be ensured that each clip is placed symmetrically on both leaflets and that the clip is not biased towards one of the leaflets. Excessive distortion of the leaflets should be avoided as this may lead to unbalanced traction on the leaflets which can potentially cause partial clip detachment or leaflet rupture during follow-up.

#### Clip release

In case of a satisfactory clip position and effective MR reduction without creating relevant MS, the clip is detached from the catheter shaft. A stable clip position has to be reconfirmed and the grade of residual MR should be reassessed. The final clip deployment is then performed by removing the gripper line. This step is monitored with 2D, 3D, and fluoroscopy.

#### System removal

After release, the CDS is withdrawn into SGC. This step is potentially dangerous because the traumatic tip of DC can damage the LA structures, and it is usually monitored by 2D multiple views. At this stage, 2D TOE view (usually in between SAX and bi-caval views) is used to confirm that the SGC is maintained in the LA that can be used for a second clip placement. If no additional clip is needed, the SGC is withdrawn back across the atrial septum and out the femoral vein access.

#### Second clip procedure

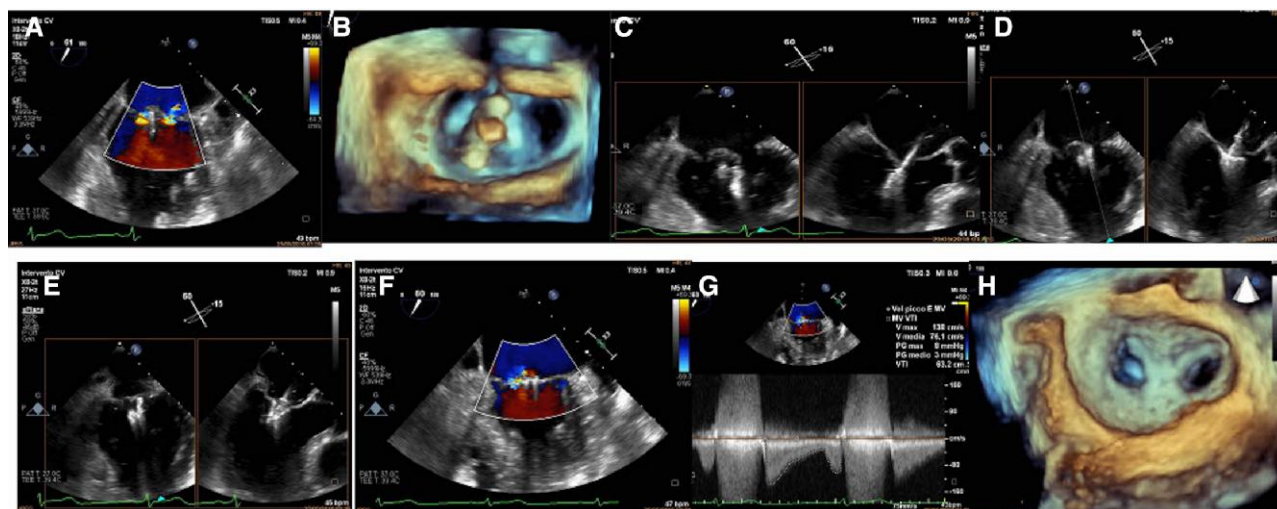
In the presence of residual significant MR, additional clip(s) may be deployed as necessary to minimize residual MR while avoiding stenosis. With PMR, in particular with highly mobile leaflets, excessive clip movement is often seen despite adequate grasping and reduction of MR. In such cases, a second clip placed immediately adjacent to the first clip can stabilize and reduce the leaflet tension of the prior clip and minimize the risk of subsequent leaflet detachment.<sup>175</sup> The procedural steps are the same as for the first clip implantation. Firstly, the main target lesion should be identified. Usually, in the presence of multiple residual jets, the tip of the clip should be pointed towards the largest PISA (Figure 49A). The 3D overhead view of the LA and the simultaneous biplane view using the MEC view as the main view and positioning the elevation plane on the target lesion to get LAX view are used to guide the steering of the CDS towards the target lesion, the trajectory of CDS, and the grasping (Figure 49B–H). The clip is advanced into LV with arms closed. Before releasing the second clip, the results in terms of reduction of MR and gradient have to be assessed.

#### ASD evaluation

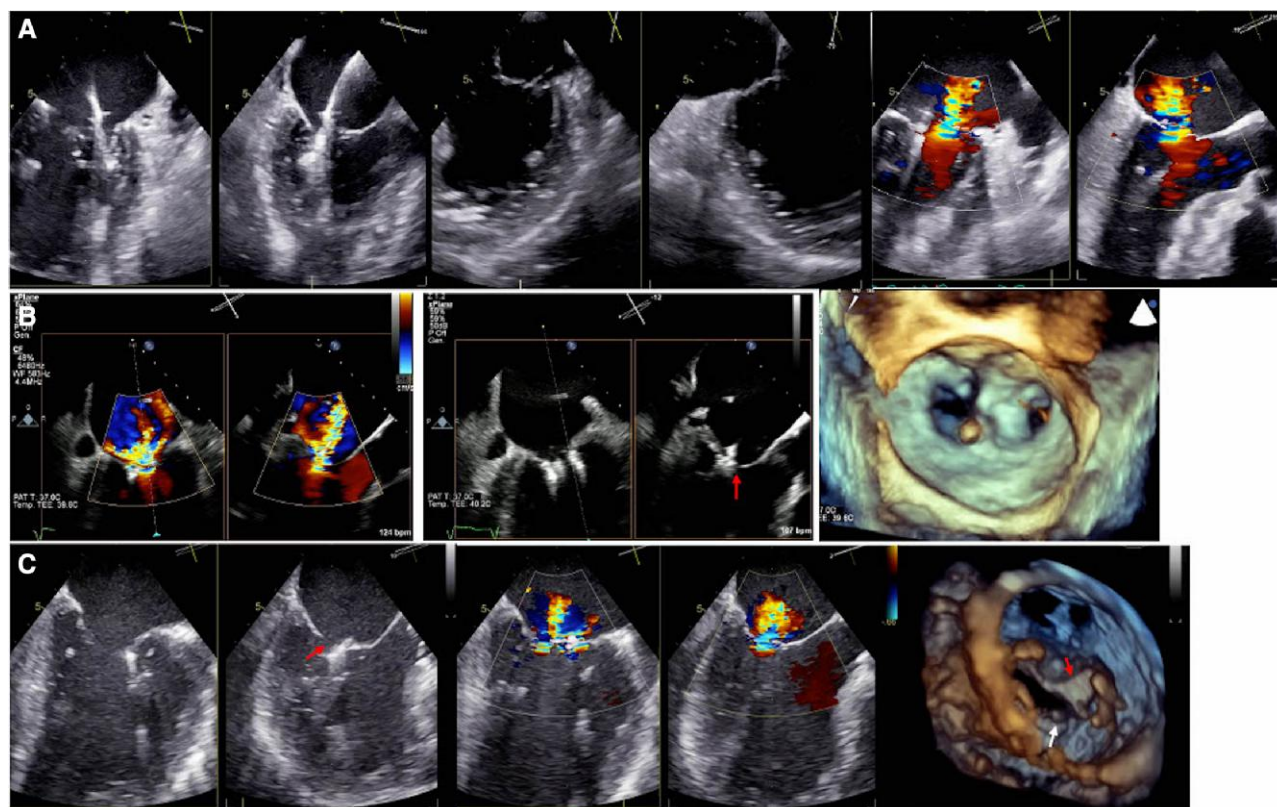
After system removal, the residual shunt and the dimension of the iatrogenic ASD should be evaluated.

## Complications

MitraClip implantation is a safe procedure with good haemodynamic tolerance even in high-risk patients and is associated with only a few

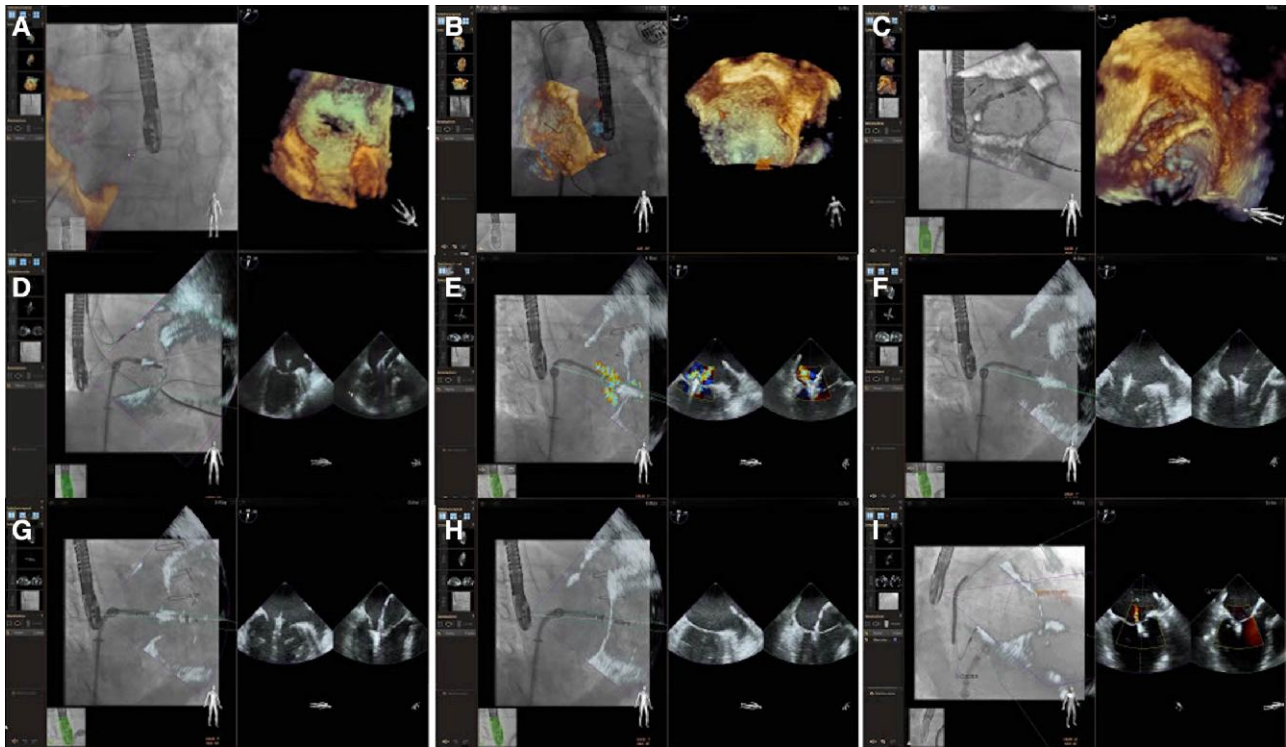


**Figure 49** (A) Results after the first clip deployment. The jet is split into two parts. The jet originating from the lateral orifice has the larger PISA (target lesion for the second clip implantation). (B) Clip arm orientation. (C) Clip advancement into LV. (D, E) Grasping. (F) Final result. (G) Final MTG. (H) 3D en face view showing the final double orifice.



**Figure 50** (A) Clip entangling in the lateral commissure with rupture chordae. (B) LLI and leaflet tear/perforation. The distal tip of anterior leaflet appears to connect with the clip (arrow) a few millimetres towards the ventricular end of the clip, indicative of leaflet tear/perforation as confirmed by 3D en face view (arrow). (C) Partial clip detachment. Complete disconnection of PL from the clip (arrow). 3D of MV from LV perspective showing the absence of the double orifice and the detachment of the clip (red arrow) from PL (white arrow).





**Figure 51** (A, B) TSP. 3D volume rendering superimposed to LAO fluoroscopic projection. The 3D data set is sliced to identify the tenting (A). The needle crosses the FO (B). (C) Navigation into the LA. Commissural view of MV including part of LA is displayed in partial-thickness modality. (D, E) Steering and positioning the clip in the LA. 2D commissural view superimposed to RAO CRA (D). The jet is displayed on fluoroscopic screen and is used as a reference marker (target lesion) (E). (F) Axial alignment of the CDS. Green plane and white line are coincident. The fluoroscopic plane results exactly perpendicular to the MV plane. (G, H) Grasping. (I) Final result.

major complications.<sup>163,164,176,177</sup> However, serious complications may occur and can be identified accurately and promptly by TOE.

Potential complications related to the nature of an interventional procedure can occur such as new intracardiac thrombus on guidewires and/or delivery sheaths.

Acute severe hypotension may be caused by cardiac tamponade, acute deterioration of LV dysfunction, or sudden worsening of MR. Pericardial effusion and cardiac tamponade may occur due to a perforation of the LA free wall or aortic puncture during TSP.

Three main mechanisms may lead to MR aggravation:

- (i) Acute worsening of LV dysfunction.
- (ii) Leaflet or chordal damage: Clip deployment out of the chordal free area between A2/P2 increases the risk of entangling and rupturing chordae (Figure 49A); multiple grasping attempts in addition to MitraClip potentially can cause leaflet perforation or laceration.
- (iii) Loss of leaflet insertion (LLI) and single leaflet detachment (SLD) that may be the consequence of insufficient leaflet grasping, which predisposes the affected leaflet to slip out of the clip if only a few millimetres of leaflet tissue are captured. LLI is conceivable as a consequence of leaflet tear or perforation.<sup>178</sup> LLI is established if a leaflet inserted no longer into the atrial aspect of the clip, but is seen during diastole to move along the clip arm towards its ventricular tip, with a regurgitant jet originating from the leaflet tip. If the leaflet tip does not deviate by >2 mm from the edge of the MitraClip, leaflet tear/perforation is diagnosed (Figure 50B). In case of complete diastolic disconnection of one of the leaflets from the clip, SLD is diagnosed (Figure 50C).

Depending on the underlying cause, acute MR may require emergency circulatory support and/or bail-out MV surgery.

The creation of MS is uncommon and may be prevented by a careful assessment of the MVA and MTG after implantation of each clip. A MTG  $\leq 5$  mmHg and a MVA  $\geq 2.5$  cm<sup>2</sup> are generally well tolerated. A post-interventional MTG of  $\geq 5$  mmHg best predicted elevated trans mitral pressure gradient (TMPG) at discharge.<sup>179</sup> Persistent ASD flow at the septal puncture site is frequent and does not represent a true complication as it is usually not haemodynamically significant.<sup>175</sup>

## Fusion imaging during MitraClip procedure

Although the MitraClip implant is effectively guided using 2D/3D TOE and fluoroscopy, echocardiographic–fluoroscopic fusion imaging may be potentially useful.<sup>180,181</sup>

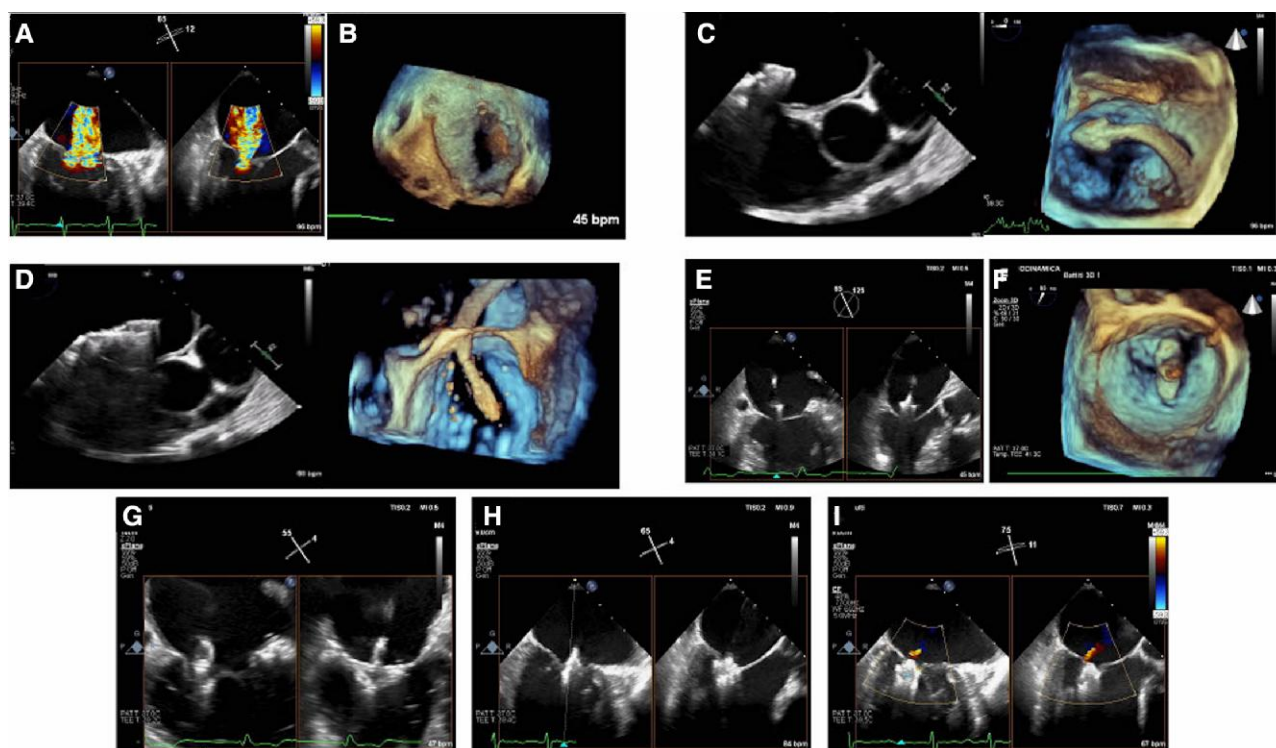
### Transseptal puncture

TSP is performed using the echocardiographic–fluoroscopic RAO projection (10–30°) or AP projection, which, respectively, show an ‘en face’ 3D and an oblique perspective of the FO, allowing the 3D spatial perception of catheter movement. Then, the tenting is visualized by either slicing the same 3D data set or displayed 2D bi-caval view in oblique anterior projection (20–40°), in order to display the FO in a sagittal view (Figure 51A and B).

### Navigation into the LA

The navigation within the LA is monitored using a single fluoroscopic projection only, usually RAO cranial, superimposing the 3D overhead





**Figure 52** Pascal procedure. (A) Baseline evaluation. (B) Parallelism test to ensure guide sheath tip flexes parallel to MV (3D en face view of the septum). (C, D) Implant system insertion: (C) implant elongated and (D) implant closed. (E) Implant trajectory and positioning. (F) Implant orientation. (G) Leaflet capture. (H) Implant closing. (I) Final result.

of LA. In the fused imaging, usually the commissural view of MV including part of the LA is displayed in partial-thickness modality or 2D image (Figure 51C). In particular, the visualization of soft tissue, together with the visualization of metallic material onto fluoroscopy, allows for compensating the lack of depth perception in 3D images improving the evaluation of the distances between catheters and LA structures. Under this echocardiographic–fluoroscopic projection, the SGC insertion into LA and CDS advancement through the catheter into LA are monitored.

### Steering and positioning the MitraClip in the LA

The delivery system is steered towards the MV over the target lesion. This step is usually monitored using the same echocardiographic–fluoroscopic projection used for the navigation into LA or the RAO CRA superimposing the 2D commissural view overlapping the colour Doppler (Figure 51D and E). Localizing with colour Doppler the site(s) of regurgitation into the fluoroscopic screen rather than using 2D/3D TOE monitoring alone may facilitate the advancement of the CDS towards the origin of the jet.

### Axial alignment of CDS

Once the valve plane is achieved, 2D ME bi-plane views of the MV (MEC view as a reference view and LAX view the derived one) are obtained and superimposed to RAO CRA fluoroscopic projection (Figure 51F). The LAX view in the fluoroscopy represents the ‘reference plane’ perpendicular to the MV plane. The ‘reference plane’ represents a sort of ‘track’ to follow that allows to get a fine perpendicular trajectory of CDS with respect to MV plane. The target lesion then is identified

superimposing the colour Doppler. The next steps are usually monitored using conventional 2D and 3D approaches as previous described (Figure 51G–I).

### System removal

After release, the CDS is withdrawn into SGC. This step is usually monitored using the same echocardiographic–fluoroscopic projection used for the navigation into LA displayed paying attention to include the IAS in the 3D data set.

### Procedural guidance during TEER: key points

- (i) The procedural monitoring is based on 2D/3D TOE. The different echocardiographic modalities (2D, 3D, and simultaneous bi-plane views) must be used properly in specific procedural steps.
- (ii) The fluoroscopy is used together with TOE.
- (iii) The results evaluation should be performed using a multiparametric approach including the invasive haemodynamic assessment.
- (iv) Complications can be accurately and quickly identified by TOE.

### Pascal procedure

The Pascal procedure is quite similar to MitraClip one, and the procedural steps are monitored with the same 2D/3D TOE views (Figure 52).

The main additional procedural features are as follows: (i) the desired TSP location is mid-fossa and posterior and the optimal height is  $\geq 4.5$  cm; (ii) after guide sheath and introducer insertion, use 3D view of septum to ensure guide sheath tip flexes parallel to MV; and (iii) check for clasp(s) bouncing which indicates leaflet is under clasp(s).

### Outpatient follow-up

TTE is generally sufficient for follow-up examination after TEER.<sup>182</sup> An additional TOE is indicated in cases in which further information are needed.

Although the reduction in MR severity achieved by TEER has been shown to persist in the majority of patients, recurrence of significant MR has been reported.<sup>163,183</sup> Different mechanisms may account for MR recurrence. On the one hand, progression of the underlying disease that originally gave rise to (primary or secondary) MR may lead to recurrent regurgitation despite initially successful TEER therapy.

TTE should assess the presence, number, location, and extension of regurgitant jets. Although small MR jets generally correspond to mild MR, semi-quantitative assessment based on regurgitant jet dimensions is limited by factors affecting the size of the regurgitant area. Quantitative 2D parameters such as VC and effective regurgitant orifice area (EROA) by the PISA method have not been validated for post-procedural double-orifice MV morphology.<sup>184</sup> A promising new approach for the evaluation of MR severity is the assessment of MR regurgitant volume (RV) by colour Doppler 3D TOE as the product of VC areas defined by direct planimetry of each orifice and velocity time integral using CW Doppler.<sup>184</sup> Currently, the most reliable method to assess the severity of MR after TEER is an integrative approach based on qualitative and quantitative parameters such as colour Doppler area size, pulmonary vein flow, and VC and categorized as 0 (none), 1+ (mild), 2+ (moderate), 3+ (moderate to severe), or 4+ (severe).<sup>185,186</sup>

MS is a rare event following MitraClip therapy. However, assessment of MVA and MV gradients should be performed systematically during TTE follow-up examination. MVA can be assessed with 2D TTE by measuring the planimetry of each orifice, and 3D TTE or 3D TOE MV planimetry is nowadays considered the gold standard. The pressure half-time method is not validated. After successful clip implantation without creating significant MS, it has been demonstrated that patients did not develop clinically relevant MS during 2 years of follow-up. This result was independent of the number of clips (one or two) and the aetiology of MR (40). At 2 years, a MTG  $>5$  mmHg was shown to be a significant predictor of poor outcome both in patients with PMR and SMR.<sup>179</sup> However, among patients enrolled in the COAPT trial, higher TMPG on discharge did not adversely affect clinical outcomes following MitraClip. These findings suggest that in patients with SMR and COAPT criteria, the benefits of MR reduction may outweigh the effects of mild-to-moderate MS after MitraClip.<sup>187</sup>

2D and 3D TTE assessment of LV volumes should be performed during follow-up to assess positive LV reshaping effects and improvements in LV size and function after TEER (46). Finally, RV dimensions and function, pulmonary pressure, and the presence and the evolution of tricuspid regurgitation should be evaluated as well.

### Follow-up after TEER: key points

- (i) TTE is the first imaging technique to follow-up patients after TEER.
- (ii) TOE is indicated when TTE is inadequate to clarify specific issues.
- (iii) The essential elements to assess during follow-up are residual/recurrent MR and its mechanism, TMPG, LV remodelling and function, stability of the device, RV dimension and function, tricuspid regurgitation, and pulmonary pressure.

## Transcatheter mitral valve replacement

TMVR offers theoretical advantages over MV repair. By replacing the entire valve itself, it offers a more predictable and complete resolution in MR severity, especially in anatomies unsuitable for repair.<sup>188,189</sup>

However, the MV anatomy is complex and heterogeneous, and the development of a TMVR device to target all anatomic variations and patient risk profiles is difficult and presents several challenges such as the use of delivery catheters with higher profile, the risk of LVOT obstruction, access route issues, no standardized anticoagulation therapy, adequate anchoring and sealing to prevent PVL, concerns with durability, valve thrombosis, and structural degeneration over time.

To date, a number of devices have been used in clinical settings. They differ for sealing mechanism (dedicated intra-annular skirts vs. wider atrial sealing skirts), anchoring system (radial force, anchors, apical tether, external annular synching, etc.), and access route (TA and transseptal).

At present, the only device which received the CE mark is the Tendyne prosthesis (Abbott Vascular, Santa Clara, CA, USA). It has a wide atrial skirt, is anchored by an apical tethering system, and is delivered via TA approach.

### Patient selection and pre-procedural planning

TMVR should be considered as alternative option to repair in the presence of calcification of the grasping zone, leaflet retraction, leaflet perforation, MV stenosis, rheumatic disease, multiple jets, and functional/ischaemic MR with severe leaflet tethering.

The procedure strongly relies on pre-procedural planning based on 2D/3D TTE/TOE and CT imaging, aiming to characterize:

- (i) MR grade and mechanisms.
- (ii) MV apparatus: annular size, presence, severity, and localization of calcium.
- (iii) Optimal site of the TA access.
- (iv) Prediction of neo-LVOT<sup>190</sup> (Figure 53): LVOT obstruction is the most dreaded complication of TMVR. The risk of LVOT obstruction and systolic anterior motion (SAM) of the native MV leaflet is particularly concerning because the prostheses are implanted in the fully open native MV; thus, the native anterior leaflet becomes the posterior boundary of the new LVOT.

### Patient selection for TMVR: key points

- (i) 2D/3D TTE/TOE are the first-line imaging techniques to assess the suitability for TMVR.
- (ii) CT is mandatory to confirm the suitability and for the procedural planning.

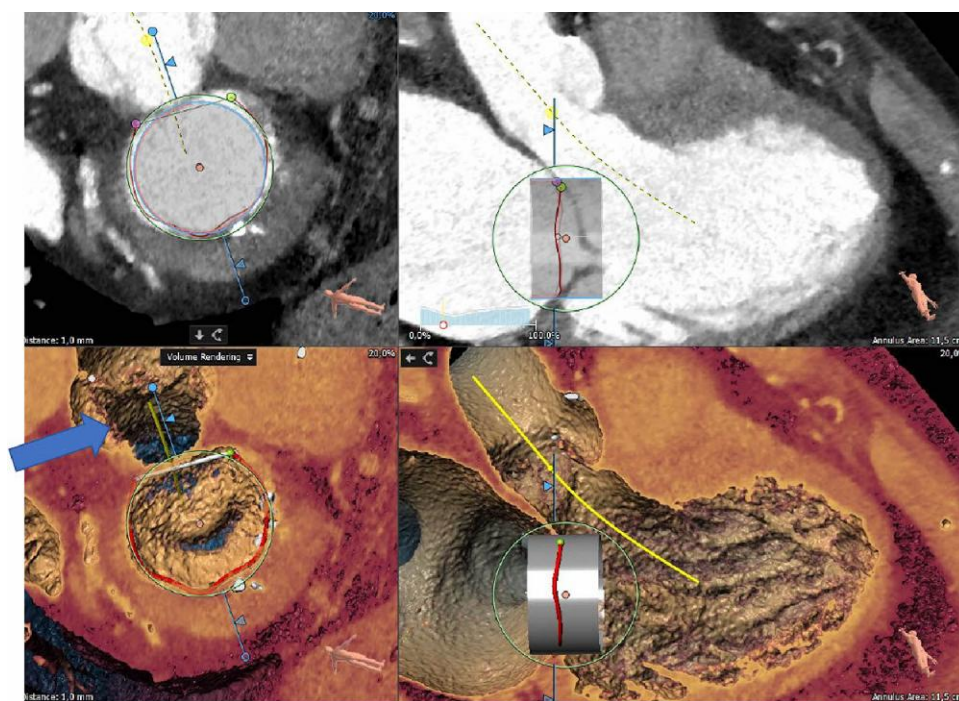
### Procedural guidance

The procedural guidance relies on 2D/3D TOE and fluoroscopy.

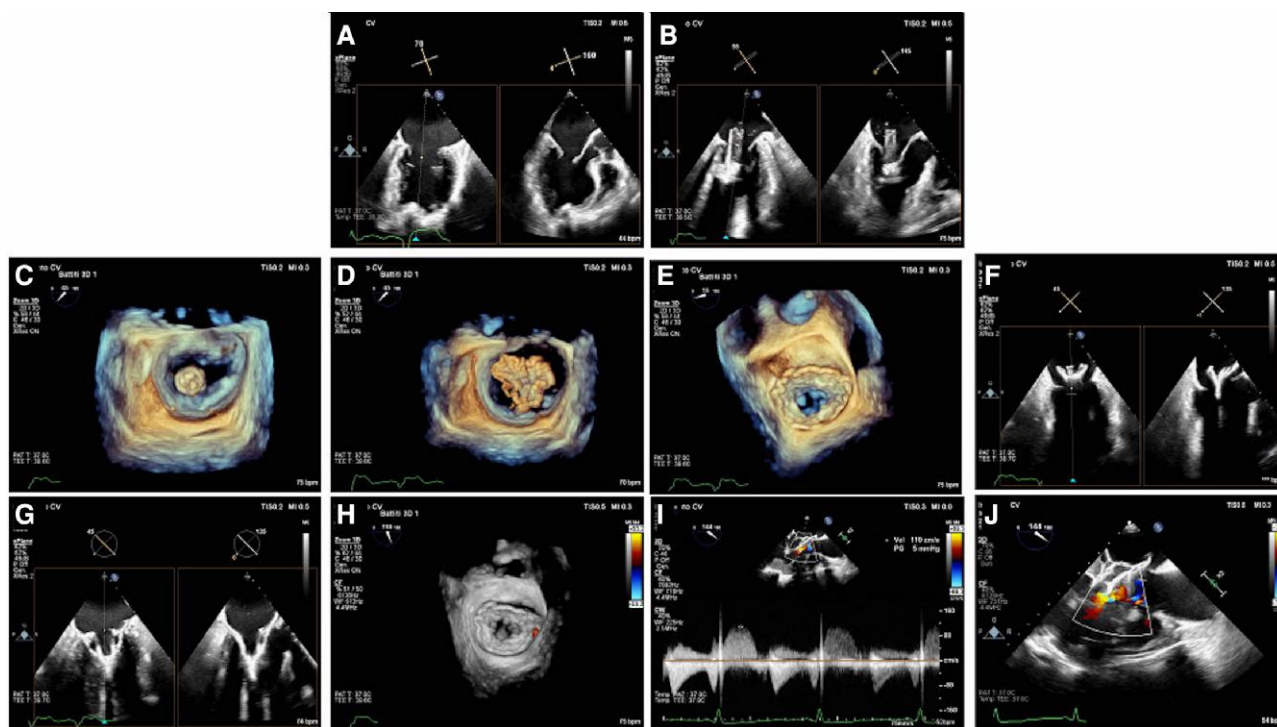
At baseline, the MR severity, the possible presence of LA thrombus, the pericardial effusion, and the wall motion abnormalities must be evaluated.

After baseline evaluation, the crucial steps of the procedure are as follows (Figure 54):

- (i) TA (see previous chapter): TOE is fundamental to localize/confirm the LV apical access site using simultaneous biplane view starting from commissural view during apical myocardial wall fingering.



**Figure 53** Pre-procedural planning at CT using a dedicated software (3-Mensio): prediction of neo-LVOT (blue arrow in the bottom left panel).



**Figure 54** TMVR. Example of Tendyne implantation. (A) Biplane imaging is used to localize the LV apex and to choose the site of incision, localizing the imprint of the interventionist's finger (arrow) according to the trajectory defined by pre-procedural CT. (B) Guide catheter insertion. (C–F) Valve deployment and orientation. (G) Sealing. (H) Assessment of presence of PVL. (I, J) Evaluation of LVOT obstruction.







16. Bourantas CV, van Mieghem NM, Soliman O, Campos CAM, Iqbal J, Serruys PW. Transcatheter aortic valve update 2013. *EuroIntervention* 2013;**9**:S84–90.
17. Yudi MB, Sharma SK, Tang GHL, Kini A. Coronary angiography and percutaneous coronary intervention after transcatheter aortic valve replacement. *J Am Coll Cardiol* 2018;**71**:1360–78.
18. Sharma SK, Rao RS, Chandra P, Goel PK, Bharadwaj P, Joseph G, et al. First-in-human evaluation of a novel balloon-expandable transcatheter heart valve in patients with severe symptomatic native aortic stenosis: the MyVal-1 study. *EuroIntervention* 2020;**16**:421–9.
19. Fontana GP, Bedogni F, Groh M, Smith D, Chehab BM, Garrett HE, et al. Safety profile of an intra-annular self-expanding transcatheter aortic valve and next-generation low-profile delivery system. *JACC Cardiovasc Interv* 2020;**13**:2467–78.
20. Seiffert M, Bader R, Kappert U, Rastan A, Krapp S, Bleiziffer S, et al. Initial German experience with transapical implantation of a second-generation transcatheter heart valve for the treatment of aortic regurgitation. *JACC Cardiovasc Interv* 2014;**7**:1168–74.
21. Abdel-Wahab M, Landt M, Neumann F-J, Massberg S, Frerker C, Kurz T, et al. 5-year outcomes after TAVR with balloon-expandable versus self-expanding valves. *JACC Cardiovasc Interv* 2020;**13**:1071–82.
22. Baumgartner H, Hung J, Bermejo J, Chambers JB, Edvardsen T, Goldstein S, et al. Recommendations on the echocardiographic assessment of aortic valve stenosis: a focused update from the European Association of Cardiovascular Imaging and the American Society of Echocardiography. *J Am Soc Echocardiogr* 2017;**30**:372–92.
23. Zamorano J, Gonçalves A, Lancellotti P, Andersen KA, González-Gómez A, Monaghan M, et al. The use of imaging in new transcatheter interventions: an EACVI review paper. *Eur Hear J Cardiovasc Imaging* 2016;**17**:835–835.
24. Witberg G, Codner P, Landes U, Schwartzberg S, Barbanti M, Valvo R, et al. Effect of transcatheter aortic valve replacement on concomitant mitral regurgitation and its impact on mortality. *JACC Cardiovasc Interv* 2021;**14**:1181–92.
25. Hahn RT, Saric M, Faletta FF, Garg R, Gillam LD, Horton K, et al. Recommended standards for the performance of transesophageal echocardiographic screening for structural heart intervention: from the American Society of Echocardiography. *J Am Soc Echocardiogr* 2022;**35**:1–76.
26. Shirazi S, Golmohammadi F, Tavosi A, Salehi M, Larti F, Sardari A, et al. Quantification of aortic valve area: comparison of different methods of echocardiography with 3-D scan of the excised valve. *Int J Cardiovasc Imaging* 2021;**37**:529–38.
27. Beneduce A, Capogrosso C, Moroni F, Ancona F, Falasconi G, Pannone L, et al. Aortic valve area calculation using 3D transesophageal echocardiography: implications for aortic stenosis severity grading. *Echocardiography* 2020;**37**(12):2071–81.
28. Cuffe C, Serfaty J-M, Cimadevilla C, Laissy J-P, Himbert D, Tubach F, et al. Measurement of aortic valve calcification using multislice computed tomography: correlation with haemodynamic severity of aortic stenosis and clinical implication for patients with low ejection fraction. *Heart* 2011;**97**:721–6.
29. Pawade T, Clavel M-A, Tribouilloy C, Dreyfus J, Mathieu T, Tastet L, et al. Computed tomography aortic valve calcium scoring in patients with aortic stenosis. *Circ Cardiovasc Imaging* 2018;**11**(3):e007146.
30. Bax JJ, Delgado V, Hahn RT, Leipsic J, Min JK, Grayburn P, et al. Transcatheter aortic valve replacement. *JACC Cardiovasc Imaging* 2020;**13**:124–39.
31. Nitsche C, Scully PR, Patel KP, Kammerlander AA, Koschutnik M, Dona C, et al. Prevalence and outcomes of concomitant aortic stenosis and cardiac amyloidosis. *J Am Coll Cardiol* 2021;**77**:128–39.
32. Bonelli A, Paris S, Nardi M, Henein MY, Agricola E, Troise G, et al. Aortic valve stenosis and cardiac amyloidosis: a misleading association. *J Clin Med* 2021;**10**:4234.
33. Anderson RH. Clinical anatomy of the aortic root. *Heart* 2000;**84**:670–3.
34. Maeno Y, Abramowitz Y, Kawamori H, Kazuno Y, Kubo S, Takahashi N, et al. A highly predictive risk model for pacemaker implantation after TAVR. *JACC Cardiovasc Imaging* 2017;**10**:1139–47.
35. Chieffo A, Giustino G, Spagnolo P, Panoulas VF, Montorfano M, Latib A, et al. Routine screening of coronary artery disease with computed tomographic coronary angiography in place of invasive coronary angiography in patients undergoing transcatheter aortic valve replacement. *Circ Cardiovasc Interv* 2015;**8**:e002025.
36. Suchá D, Tuncay V, Prakken NHJ, Leiner T, van Ooijen PMA, Oudkerk M, et al. Does the aortic annulus undergo conformational change throughout the cardiac cycle? A systematic review. *Eur Hear J Cardiovasc Imaging* 2015;**16**(12):1307–17.
37. Wang DD, Qian Z, Vukicevic M, Engelhardt S, Kheradvar A, Zhang C, et al. 3D printing, computational modeling, and artificial intelligence for structural heart disease. *JACC Cardiovasc Imaging* 2021;**14**:41–60.
38. Prihadi EA, van Rosendaal PJ, Vollema EM, Bax JJ, Delgado V, Ajmone Marsan N. Feasibility, accuracy, and reproducibility of aortic annular and root sizing for transcatheter aortic valve replacement using novel automated three-dimensional echocardiographic software: comparison with multi-detector row computed tomography. *J Am Soc Echocardiogr* 2018;**31**:505–514.e3.
39. Stella S, Italia L, Geremia G, Rosa I, Ancona F, Marini C, et al. Accuracy and reproducibility of aortic annular measurements obtained from echocardiographic 3D manual and semi-automated software analyses in patients referred for transcatheter aortic valve implantation: implication for prosthesis size selection. *Eur Hear J Cardiovasc Imaging* 2019;**20**:45–55.
40. Ruile P, Blanke P, Krauss T, Dorfs S, Jung B, Jander N, et al. Pre-procedural assessment of aortic annulus dimensions for transcatheter aortic valve replacement: comparison of a non-contrast 3D MRA protocol with contrast-enhanced cardiac dual-source CT angiography. *Eur Hear J Cardiovasc Imaging* 2016;**17**:458–66.
41. Bleiziffer S, Krane M, Deutsch MA, Elhmidy Y, Piazza N, Voss B, et al. Which way in? The necessity of multiple approaches to transcatheter valve therapy. *Curr Cardiol Rev* 2014;**9**:268–73.
42. Linke A, Wenaweser P, Gerckens U, Tamburino C, Bosmans J, Bleiziffer S, et al. Treatment of aortic stenosis with a self-expanding transcatheter valve: the International Multi-centre ADVANCE Study. *Eur Heart J* 2014;**35**:2672–84.
43. Blakeslee-Carter J, Dexter D, Mahoney P, Ahanchi S, Steerman S, Larion S, et al. A novel iliac morphology score predicts procedural mortality and Major vascular complications in transfemoral aortic valve replacement. *Ann Vasc Surg* 2018;**46**:208–17.
44. Ludman PF, Moat N, de Belder MA, Blackman DJ, Duncan A, Banya W, et al. Transcatheter aortic valve implantation in the United Kingdom. *Circulation* 2015;**131**:1181–90.
45. Pascual I, Carro A, Avanza P, Hernández-Vaquero D, Díaz R, Rozado J, et al. Vascular approaches for transcatheter aortic valve implantation. *J Thorac Dis* 2017;**9**:S478–87.
46. Petronio AS, de Carlo M, Bedogni F, Maisano F, Ettori F, Klugmann S, et al. 2-year results of CoreValve implantation through the subclavian access. *J Am Coll Cardiol* 2012;**60**:502–7.
47. De Palma R, Settergren M, Rück A, Svensson A, Feldt K, Saleh N. A path to avoid during transcatheter aortic valve implantation: case report. *Radiology* 2016;**280**:58–61.
48. Petronio AS, de Carlo M, Bedogni F, Marzocchi A, Klugmann S, Maisano F, et al. Safety and efficacy of the subclavian approach for transcatheter aortic valve implantation with the CoreValve revalving system. *Circ Cardiovasc Interv* 2010;**3**:359–66.
49. Fraccaro C, Napodano M, Tarantini G, Gasparetto V, Gerosa G, Bianco R, et al. Expanding the eligibility for transcatheter aortic valve implantation. *JACC Cardiovasc Interv* 2009;**2**:828–33.
50. Blanke P, Naoum C, Dvir D, Bapat V, Ong K, Muller D, et al. Predicting LVOT obstruction in transcatheter mitral valve implantation. *JACC Cardiovasc Imaging* 2017;**10**:482–5.
51. Bruschi G, de Marco F, Botta L, Cannata A, Oreglia J, Colombo P, et al. Direct aortic access for transcatheter self-expanding aortic bioprosthetic valves implantation. *Ann Thorac Surg* 2012;**94**:497–503.
52. Bapat VN, Attia RQ, Thomas M. Distribution of calcium in the ascending aorta in patients undergoing transcatheter aortic valve implantation and its relevance to the transaortic approach. *JACC Cardiovasc Interv* 2012;**5**:470–6.
53. Gammie JS, Bartus K, Gackowski A, D'Ambra MN, Szymanski P, Bilewska A, et al. Beating-heart mitral valve repair using a novel ePTFE cordal implantation device: a prospective trial. *J Am Coll Cardiol* 2018;**71**:25–36.
54. Halabi M, Ratnayaka K, Faranesh AZ, Chen MY, Schenke WH, Lederman RJ. Aortic access from the vena cava for large caliber transcatheter cardiovascular interventions. *J Am Coll Cardiol* 2013;**61**:1745–6.
55. Modine T, Sudre A, Delhaye C, Fayad G, Lemesle G, Collet F, et al. Transcatheter aortic valve implantation using the left carotid access: feasibility and early clinical outcomes. *Ann Thorac Surg* 2012;**93**:1489–94.
56. Wee IJY, Stonier T, Harrison M, Choong AMTL. Transcarotid transcatheter aortic valve implantation: a systematic review. *J Cardiol* 2018;**71**:525–33.
57. Mylotte D, Sudre A, Teiger E, Obadia JF, Lee M, Spence M, et al. Transcarotid transcatheter aortic valve replacement. *JACC Cardiovasc Interv* 2016;**9**:472–80.
58. Roberts WC, Ko JM. Frequency by decades of unicuspid, bicuspid, and tricuspid aortic valves in adults having isolated aortic valve replacement for aortic stenosis, with or without associated aortic regurgitation. *Circulation* 2005;**111**:920–5.
59. Jilali H, Chen M, Webb J, Himbert D, Ruiz CE, Rodés-Cabau J, et al. A bicuspid aortic valve imaging classification for the TAVR era. *JACC Cardiovasc Imaging* 2016;**9**:1145–58.
60. Jilali H, Makkar RR, Kashif M, Okuyama K, Chakravarty T, Shiota T, et al. A revised methodology for aortic-valvar complex calcium quantification for transcatheter aortic valve implantation. *Eur Hear J Cardiovasc Imaging* 2014;**15**:1324–32.
61. Tchetché D, Siddiqui S. Percutaneous management of bicuspid aortic valves: still remaining questions. *JACC Cardiovasc Interv* 2020;**13**:1760–2.
62. Iannopolo G, Romano V, Buzzatti N, de Backer O, Søndergaard L, Merkely B, et al. A novel supra-annular plane to predict TAVI prosthesis anchoring in raphe-type bicuspid aortic valve disease: the LIRA plane. *EuroIntervention* 2020;**16**:259–61.
63. Ueshima D, Nai Fovino L, Brenner SJ, Fabris T, Scotti A, Barioli A, et al. Transcatheter aortic valve replacement for bicuspid aortic valve stenosis with first- and new-generation bioprostheses: a systematic review and meta-analysis. *Int J Cardiol* 2020;**298**:76–82.
64. Costa G, Angelillis M, Petronio AS. Bicuspid valve sizing for transcatheter aortic valve implantation: the missing link. *Front Cardiovasc Med* 2022;**8**:770924.
65. Petronio AS, Angelillis M, De Backer O, Giannini C, Costa G, Fiorina C, et al. Bicuspid aortic valve sizing for transcatheter aortic valve implantation: development and

- validation of an algorithm based on multi-slice computed tomography. *J Cardiovasc Comput Tomogr* 2020;**14**:452–61.
66. Iannopolo G, Romano V, Esposito A, Guazzoni G, Ancona M, Ferri L, et al. Update on supra-annular sizing of transcatheter aortic valve prostheses in raphe-type bicuspid aortic valve disease according to the LIRA method. *Eur Heart J Suppl* 2022;**24**:C233–42.
  67. Maeno Y, Yoon S-H, Abramowitz Y, Watanabe Y, Jilalawi H, Lin M-S, et al. Effect of ascending aortic dimension on acute procedural success following self-expanding transcatheter aortic valve replacement: a multicenter retrospective analysis. *Int J Cardiol* 2017;**244**:100–5.
  68. Arias EA, Bhan A, Lim ZY, Mullen M. TAVI for pure native aortic regurgitation: are we there yet? *Interv Cardiol Rev* 2019;**14**:26–30.
  69. Alkhouli M, Sengupta P, Badhwar V. Toward precision in balloon-expandable TAVR: oversizing tight versus just right. *JACC Cardiovasc Interv* 2017;**10**:821–3.
  70. Gilard M, Eltchaninoff H, Iung B, Donzeau-Gouge P, Chevreul K, Fajadet J, et al. Registry of transcatheter aortic-valve implantation in high-risk patients. *N Engl J Med* 2012;**366**:1705–15.
  71. Holmes DR, Mack MJ, Kaul S, Agnihotri A, Alexander KP, Bailey SR, et al. 2012 ACCF/AATS/SCAI/STS expert consensus document on transcatheter aortic valve replacement. *J Thorac Cardiovasc Surg* 2012;**144**:e29–84.
  72. Otto CM, Kumbhani DJ, Alexander KP, Calhoun JH, Desai MY, Kaul S, et al. 2017 ACC expert consensus decision pathway for transcatheter aortic valve replacement in the management of adults with aortic stenosis. *J Am Coll Cardiol* 2017;**69**:1313–46.
  73. Dvir D, Jhaveri R, Pichard AD. The minimalist approach for transcatheter aortic valve replacement in high-risk patients. *JACC Cardiovasc Interv* 2012;**5**:468–9.
  74. Zamorano JL, Badano LP, Bruce C, Chan K-L, Gonçalves A, Hahn RT, et al. EAE/ASE recommendations for the use of echocardiography in new transcatheter interventions for valvular heart disease. *Eur Heart J* 2011;**32**:2189–214.
  75. Stella S, Melillo F, Capogrosso C, Fiscaro A, Ancona F, Latib A, et al. Intra-procedural monitoring protocol using routine transthoracic echocardiography with backup transoesophageal probe in transcatheter aortic valve replacement: a single centre experience. *Eur Heart J Cardiovasc Imaging* 2020;**21**:85–92.
  76. VASC-3 Writing Committee, G  n  reux P, Piazza N, Alu MC, Nazif T, Hahn RT, Pibarot P, et al. Valve Academic Research Consortium 3: updated endpoint definitions for aortic valve clinical research. *Eur Heart J* 2021;**42**:1825–57.
  77. Lancellotti P, Pibarot P, Chambers J, Edvardsen T, Delgado V, Dulgheru R, et al. Recommendations for the imaging assessment of prosthetic heart valves: a report from the European Association of Cardiovascular Imaging endorsed by the Chinese Society of Echocardiography, the Inter-American Society of Echocardiography, and the Brazilian. *Eur Heart J Cardiovasc Imaging* 2016;**17**:589–90.
  78. Hahn RT, Pibarot P, Weissman NJ, Rodriguez L, Jaber WA. Assessment of paravalvular aortic regurgitation after transcatheter aortic valve replacement: intra-core laboratory variability. *J Am Soc Echocardiogr* 2015;**28**:415–22.
  79. Kitamura M, Majunke N, Holzhey D, Desch S, Bani Hani A, Krieghoff C, et al. Systematic use of intentional leaflet laceration to prevent TAVI-induced coronary obstruction: feasibility and early clinical outcomes of the BASILICA technique. *EuroIntervention* 2020;**16**:682–90.
  80. Protosy V, Meineri M, Kitamura M, Flo Forner A, Holzhey D, Thiele H, et al. Echocardiographic guidance of intentional leaflet laceration prior to transcatheter aortic valve replacement: a structured approach to the bioprosthetic or native aortic scallop intentional laceration to prevent iatrogenic coronary artery obstruction proc. *J Am Soc Echocardiogr* 2021;**34**(6):676–89.
  81. Buzzatti N, Romano V, De Backer O, Soendergaard L, Rosseel L, Maurovich-Horvat P, et al. Coronary access after repeated transcatheter aortic valve implantation. *JACC Cardiovasc Imaging* 2020;**13**:508–15.
  82. Barbanti M, Costa G, Picci A, Criscione E, Reddavid C, Valvo R, et al. Coronary cannulation after transcatheter aortic valve replacement. *JACC Cardiovasc Interv* 2020;**13**:2542–55.
  83. S  ndergaard L. Transcatheter aortic valve implantation: don't forget the coronary arteries! *EuroIntervention* 2018;**14**:147–9.
  84. Tsuruta H, Hayashida K, Yashima F, Yanagisawa R, Tanaka M, Arai T, et al. Incidence, predictors, and midterm clinical outcomes of left ventricular obstruction after transcatheter aortic valve implantation. *Catheter Cardiovasc Interv* 2018;**92**:E288–98.
  85. J  rgensen TH, Thyregod HGH, Ihlemann N, Nissen H, Petursson P, Kjeldsen BJ, et al. Eight-year outcomes for patients with aortic valve stenosis at low surgical risk randomized to transcatheter vs. surgical aortic valve replacement. *Eur Heart J* 2021;**42**:2912–9.
  86. Blackman DJ, Saraf S, McCarthy PA, Myat A, Anderson SG, Malkin CJ, et al. Long-term durability of transcatheter aortic valve prostheses. *J Am Coll Cardiol* 2019;**73**:537–45.
  87. Lancellotti P, Martinez C, Radermecker M. The long quest for the holy grail in transcatheter aortic bioprosthesis. *J Am Coll Cardiol* 2019;**73**:554–8.
  88. Shames S, Koczo A, Hahn R, Jin Z, Picard MH, Gillam LD. Flow characteristics of the SAPIEN aortic valve: the importance of recognizing in-stent flow acceleration for the echocardiographic assessment of valve function. *J Am Soc Echocardiogr* 2012;**25**:603–9.
  89. De Backer O, Dangas GD, Jilalawi H, Leipsic JA, Terkelsen CJ, Makkar R, et al. Reduced leaflet motion after transcatheter aortic-valve replacement. *N Engl J Med* 2020;**382**:130–9.
  90. Chakravarty T, S  ndergaard L, Friedman J, De Backer O, Berman D, Kofoed KF, et al. Subclinical leaflet thrombosis in surgical and transcatheter bioprosthetic aortic valves: an observational study. *Lancet* 2017;**389**:2383–92.
  91. Latib A, Messika-Zeitoun D, Maisano F, Himbert D, Agricola E, Brochet E, et al. Reversible Edwards Sapien XT dysfunction due to prosthesis thrombosis presenting as early structural deterioration. *J Am Coll Cardiol* 2013;**61**:787–9.
  92. Spartera M, Ancona F, Barletta M, Rosa I, Stella S, Marini C, et al. Echocardiographic features of post-transcatheter aortic valve implantation thrombosis and endocarditis. *Echocardiography* 2018;**35**:337–45.
  93. Baumgartner H, Hung J, Bermejo J, Chambers JB, Edvardsen T, Goldstein S, et al. Recommendations on the echocardiographic assessment of aortic valve stenosis: a focused update from the European Association of Cardiovascular Imaging and the American Society of Echocardiography. *Eur Heart J Cardiovasc Imaging* 2017;**18**:254–75.
  94. Dayan V, Vignolo G, Soca G, Paganini JJ, Brusich D, Pibarot P. Predictors and outcomes of prosthesis-patient mismatch after aortic valve replacement. *JACC Cardiovasc Imaging* 2016;**9**:924–33.
  95. Makkar RR, Fontana G, Jilalawi H, Chakravarty T, Kofoed KF, De Backer O, et al. Possible subclinical leaflet thrombosis in bioprosthetic aortic valves. *N Engl J Med* 2015;**373**:2015–24.
  96. Leetmaa T, Hansson NC, Leipsic J, Jensen K, Poulsen SH, Andersen HR, et al. Early aortic transcatheter heart valve thrombosis. *Circ Cardiovasc Interv* 2015;**8**(4):e001596.
  97. Jabbour RJ, Tanaka A, Colombo A, Latib A. Delayed coronary occlusion after transcatheter aortic valve implantation: implications for new transcatheter heart valve design and patient management. *Interv Cardiol (London, England)* 2018;**13**:137–9.
  98. Vahanian A, Beyersdorf F, Praz F, Milojevic M, Baldus S, Bauersachs J, et al. 2021 ESC/EACTS guidelines for the management of valvular heart disease. *Eur Heart J* 2022;**43**:561–632.
  99. Lancellotti P, Zamorano JL, Habib G, Badano L, eds. *The EACVI Textbook of Echocardiography*. EACVI Textb. Echocardiogr. Oxford, UK: Oxford University Press; 2016.
  100. Sutaria N, Northridge DB, Shaw TR. Significance of commissural calcification on outcome of mitral balloon valvotomy. *Heart* 2000;**84**:398–402.
  101. Padial LR, Freitas N, Sagie A, Newell JB, Weyman AE, Levine RA, et al. Echocardiography can predict which patients will develop severe mitral regurgitation after percutaneous mitral valvulotomy. *J Am Coll Cardiol* 1996;**27**:1225–31.
  102. Min S-Y, Song J-M, Kim Y-J, Park H-K, Seo M-O, Lee M-S, et al. Discrepancy between mitral valve areas measured by two-dimensional planimetry and three-dimensional transoesophageal echocardiography in patients with mitral stenosis. *Heart* 2013;**99**:253–8.
  103. Anwar AM, Attia WM, Nosir YFM, Soliman OII, Mosad MA, Othman M, et al. Validation of a new score for the assessment of mitral stenosis using real-time three-dimensional echocardiography. *J Am Soc Echocardiogr* 2010;**23**:13–22.
  104. Lancellotti P, Pellikka PA, Budts W, Chaudhry FA, Donal E, Dulgheru R, et al. The clinical use of stress echocardiography in non-ischaemic heart disease: recommendations from the European Association of Cardiovascular Imaging and the American Society of Echocardiography. *Eur Heart J Cardiovasc Imaging* 2016;**17**:1191–229.
  105. Baumgartner H, Hung J, Bermejo J, Chambers JB, Evangelista A, Griffin BP, et al. EAE/ASE. Echocardiographic assessment of valve stenosis: EAE/ASE recommendations for clinical practice. *Eur J Echocardiogr* 2009;**10**:1–25.
  106. El Sabbagh A, Reddy YNV, Barros-Gomes S, Borlaug BA, Miranda VWR, Pislaru SV, et al. Low-gradient severe mitral stenosis: hemodynamic profiles, clinical characteristics, and outcomes. *J Am Heart Assoc* 2019;**8**(5):e010736.
  107. Spagnolo P, Giglio M, Di Marco D, Cannao PM, Agricola E, Bella PE, et al. Diagnosis of left atrial appendage thrombus in patients with atrial fibrillation: delayed contrast-enhanced cardiac CT. *Eur Radiol* 2021;**31**:1236–44.
  108. Writing Committee Members; Otto CM, Nishimura RA, Bonow RO, Carabello BA, Erwin JP, Gentile F, et al. 2020 ACC/AHA guideline for the management of patients with valvular heart disease: executive summary: a report of the American College of Cardiology/American Heart Association Joint Committee on Clinical Practice Guidelines. *J Am Coll Cardiol* 2021;**77**:450–500.
  109. Baumgartner H, Falk V, Bax JJ, De Bonis M, Hamm C, Holm PJ, et al. 2017 ESC/EACTS guidelines for the management of valvular heart disease. *Eur Heart J* 2017;**38**:2739–91.
  110. Wunderlich NC, Beigel R, Siegel RJ. Management of mitral stenosis using 2D and 3D echo-Doppler imaging. *JACC Cardiovasc Imaging* 2013;**6**:1191–205.
  111. Messika-Zeitoun D, Brochet E, Holmin C, Rosenbaum D, Cormier B, Serfaty J-M, et al. Three-dimensional evaluation of the mitral valve area and commissural opening before and after percutaneous mitral commissurotomy in patients with mitral stenosis. *Eur Heart J* 2007;**28**:72–9.
  112. Carpentier A, Adams DHFF. *Carpentier's Reconstructive Valve Surgery*. Philadelphia: Saunders; 2010.

113. Fatkin D, Roy P, Morgan JJ, Feneley MP. Percutaneous balloon mitral valvotomy with the Inoue single-balloon catheter: commissural morphology as a determinant of outcome. *J Am Coll Cardiol* 1993;**21**:390–7.
114. Wilkins GT, Weyman AE, Abascal VM, Block PC, Palacios IF. Percutaneous balloon dilatation of the mitral valve: an analysis of echocardiographic variables related to outcome and the mechanism of dilatation. *Br Heart J* 1988;**60**:299–308.
115. lung B, Cormier B, Ducimetière P, Porte JM, Nallet O, Michel PL, et al. Immediate results of percutaneous mitral commissurotomy. A predictive model on a series of 1514 patients. *Circulation* 1996;**94**:2124–30.
116. Faletta FF, Perk G, Pandian NG, Nesser H-J, Kronzon I. *Real-Time 3D Interventional Echocardiography*. London: Springer London; 2014.
117. Nunes MCP, Tan TC, Elmariah S, do Lago R, Margey R, Cruz-Gonzalez I, et al. The echo score revisited: impact of incorporating commissural morphology and leaflet displacement to the prediction of outcome for patients undergoing percutaneous mitral valvuloplasty. *Circulation* 2014;**129**:886–95.
118. Bouleti C, lung B, Laouénan C, Himbert D, Brochet E, Messika-Zeitoun D, et al. Late results of percutaneous mitral commissurotomy up to 20 years: development and validation of a risk score predicting late functional results from a series of 912 patients. *Circulation* 2012;**125**:2119–27.
119. Dreyfus J, Cimadevilla C, Nguyen V, Brochet E, Lepage L, Himbert D, et al. Feasibility of percutaneous mitral commissurotomy in patients with commissural mitral valve calcification. *Eur Heart J* 2014;**35**:1617–23.
120. Sharma A, Kelly R, Mbai M, Chandrasekhar Y, Bertog S. Transcatheter mitral valve lithotripsy as a pretreatment to percutaneous balloon mitral valvuloplasty for heavily calcified rheumatic mitral stenosis. *Circ Cardiovasc Interv* 2020;**13**(7):e009357.
121. Palacios IF, Sanchez PL, Harrell LC, Weyman AE, Block PC. Which patients benefit from percutaneous mitral balloon valvuloplasty? Prevaluloplasty and postvalvuloplasty variables that predict long-term outcome. *Circulation* 2002;**105**:1465–71.
122. Kronzon I, Glassman E, Cohen M, Winer H. Use of two-dimensional echocardiography during transseptal cardiac catheterization. *J Am Coll Cardiol* 1984;**4**:425–8.
123. Pandian NG, Isner JM, Hough TJ, Desnoyers MR, McInerney K, Salem DN. Percutaneous balloon valvuloplasty of mitral stenosis aided by cardiac ultrasound. *Am J Cardiol* 1987;**59**:380–1.
124. Agricola E. *Interventional echocardiography*. Edizioni Minerva Medica 2020.
125. Rao AS, Murthy RS, Naidu PB, Raghu K, Anjaneyulu AV, Raju PK, et al. Transesophageal echocardiography for the detection of left atrial thrombus. *Indian Heart J* 1994;**46**:37–40.
126. Alkhoul M, Rihal CS, Holmes DR. Transseptal techniques for emerging structural heart interventions. *JACC Cardiovasc Interv* 2016;**9**:2465–80.
127. Applebaum RM, Kasliwal RR, Kanojia A, Seth A, Bhandari S, Trehan N, et al. Utility of three-dimensional echocardiography during balloon mitral valvuloplasty. *J Am Coll Cardiol* 1998;**32**:1405–9.
128. Messika-Zeitoun D, Blanc J, lung B, Brochet E, Cormier B, Himbert D, et al. Impact of degree of commissural opening after percutaneous mitral commissurotomy on long-term outcome. *JACC Cardiovasc Imaging* 2009;**2**:1–7.
129. Thomas JD, Wilkins GT, Choong CY, Abascal VM, Palacios IF, Block PC, et al. Inaccuracy of mitral pressure half-time immediately after percutaneous mitral valvotomy. Dependence on transmitral gradient and left atrial and ventricular compliance. *Circulation* 1988;**78**:980–93.
130. Zamorano J, Perez de Isla L, Sugeng L, Cordeiro P, Rodrigo JL, Almeria C, et al. Non-invasive assessment of mitral valve area during percutaneous balloon mitral valvuloplasty: role of real-time 3D echocardiography. *Eur Heart J* 2004;**25**:2086–91.
131. Vilacosta I, Iturralde E, San Román JA, Gómez-Recio M, Romero C, Jiménez J, et al. Transesophageal echocardiographic monitoring of percutaneous mitral balloon valvulotomy. *Am J Cardiol* 1992;**70**:1040–4.
132. Salem MI, Makaryus AN, Kort S, Chung E, Marchant D, Ong L, et al. Intracardiac echocardiography using the AcuNav ultrasound catheter during percutaneous balloon mitral valvuloplasty. *J Am Soc Echocardiogr* 2002;**15**:1533–7.
133. Marmagkiolis K, Cilingiroglu M. Intracardiac echocardiography-guided percutaneous mitral balloon valvuloplasty. *Rev Port Cardiol* 2013;**32**:337–9.
134. Bartel T, Müller S, Biviano A, Hahn RT. Why is intracardiac echocardiography helpful? Benefits, costs, and how to learn. *Eur Heart J* 2014;**35**:69–76.
135. Bouleti C, lung B, Himbert D, Brochet E, Messika-Zeitoun D, Détaint D, et al. Long-term efficacy of percutaneous mitral commissurotomy for stenosis after previous mitral commissurotomy. *Heart* 2013;**99**:1336–41.
136. Kim J-B, Ha J-W, Kim J-S, Shim W-H, Kang S-M, Ko Y-G, et al. Comparison of long-term outcome after mitral valve replacement or repeated balloon mitral valvotomy in patients with stenosis after previous balloon valvotomy. *Am J Cardiol* 2007;**99**:1571–4.
137. lung B, Delgado V, Rosenhek R, Price S, Prendergast B, Wendler O, et al. Contemporary presentation and management of valvular heart disease. *Circulation* 2019;**140**:1156–69.
138. Cahill TJ, Prothero A, Wilson J, Kennedy A, Brubert J, Masters M, et al. Community prevalence, mechanisms and outcome of mitral or tricuspid regurgitation. *Heart* 2021;**107**:1003–9.
139. Lancellotti P, Pibarot P, Chambers J, La Canna G, Pepi M, Dulgheru R, et al. Multi-modality imaging assessment of native valvular regurgitation: an EACVI and ESC council of valvular heart disease position paper. *Eur Hear J Cardiovasc Imaging* 2022;**23**:e171–232.
140. Feldman T, Foster E, Glower DD, Kar S, Rinaldi MJ, Fail PS, et al. Percutaneous repair or surgery for mitral regurgitation. *N Engl J Med* 2011;**364**:1395–406.
141. Feldman T, Kar S, Elmariah S, Smart SC, Trento A, Siegel RJ, et al. Randomized comparison of percutaneous repair and surgery for mitral regurgitation. *J Am Coll Cardiol* 2015;**66**:2844–54.
142. Lim DS, Kar S, Spargias K, Kipperman RM, O'Neill WW, Ng MKC et al. Transcatheter valve repair for patients with mitral regurgitation: 30-day results of the CLASP study. *JACC Cardiovasc Interv* 2019;**12**(14):1369–78.
143. Obadia J-F, Messika-Zeitoun D, Leurent G, lung B, Bonnet G, Piriou N, et al. Percutaneous repair or medical treatment for secondary mitral regurgitation. *N Engl J Med* 2018;**379**:2297–306.
144. Stone GW, Lindenfeld J, Abraham WT, Kar S, Lim DS, Mishell JM, et al. Transcatheter mitral-valve repair in patients with heart failure. *N Engl J Med* 2018;**379**:2307–18.
145. Taramasso M, Latib A. Percutaneous mitral annuloplasty. *Interv Cardiol Clin* 2016;**5**:101–7.
146. Mangieri A, Colombo A, Demir OM, Agricola E, Ancona F, Regazzoli D, et al. Percutaneous direct annuloplasty with edge-to-edge technique for mitral regurgitation: replicating a complete surgical mitral repair in a one-step procedure. *Can J Cardiol* 2018;**34**(8):1088.e1–e2.
147. Latib A, Ancona MB, Ferri L, Montorfano M, Mangieri A, Regazzoli D, et al. Percutaneous direct annuloplasty with Cardioband to treat recurrent mitral regurgitation after MitraClip implantation. *JACC Cardiovasc Interv* 2016;**9**(18):e191–2.
148. Nickenig G, Hammerstingl C, Schueler R, Topilsky Y, Grayburn PA, Vahanian A, et al. Transcatheter mitral annuloplasty in chronic functional mitral regurgitation. *JACC Cardiovasc Interv* 2016;**9**:2039–47.
149. Messika-Zeitoun D, Nickenig G, Latib A, Kuck K-H, Baldus S, Schueler R, et al. Transcatheter mitral valve repair for functional mitral regurgitation using the Cardioband system: 1 year outcomes. *Eur Heart J* 2019;**40**:466–72.
150. Taramasso M, Hahn RT, Alessandrini H, Latib A, Attinger-Toller A, Braun D, et al. The international multicenter TriValve registry: which patients are undergoing transcatheter tricuspid repair? *JACC Cardiovasc Interv* 2017;**10**:1982–90.
151. Siminiak T, Wu JC, Haude M, Hoppe UC, Sadowski J, Lipiecki J, et al. Treatment of functional mitral regurgitation by percutaneous annuloplasty: results of the TITAN trial. *Eur J Heart Fail* 2012;**14**:931–8.
152. Sack S, Kahler P, Bilodeau L, Piérard LC, Lancellotti P, Legrand V, et al. Percutaneous transvenous mitral annuloplasty. *Circ Cardiovasc Interv* 2009;**2**:277–84.
153. Tops LF, van de Veire NR, Schuijff JD, de Roos A, van der Wall EE, Schalij MJ, et al. Noninvasive evaluation of coronary sinus anatomy and its relation to the mitral valve annulus. *Circulation* 2007;**115**:1426–32.
154. Mischke K, Knackstedt C, Mühlenbruch G, Schimpf T, Neef P, Zarse M, et al. Imaging of the coronary venous system: retrograde coronary sinus angiography versus venous phase coronary angiograms. *Int J Cardiol* 2007;**119**:339–43.
155. Choure AJ, Garcia MJ, Hesse B, Sevensma M, Maly G, Greenberg NL, et al. In vivo analysis of the anatomical relationship of coronary sinus to mitral annulus and left circumflex coronary artery using cardiac multidetector computed tomography. *J Am Coll Cardiol* 2006;**48**:1938–45.
156. Tops LF, Wood DA, Delgado V, Schuijff JD, Mayo JR, Pasupati S, et al. Noninvasive evaluation of the aortic root with multislice computed tomography. *JACC Cardiovasc Imaging* 2008;**1**:321–30.
157. Colli A, Besola L, Montagner M, Azzolina D, Soriani N, Manzan E, et al. Prognostic impact of leaflet-to-annulus index in patients treated with transapical off-pump echoguided mitral valve repair with NeoChord implantation. *Int J Cardiol* 2018;**257**:235–7.
158. Colli A, Zucchetta F, Torregrossa G, Manzan E, Bizzotto E, Besola L, et al. Transapical off-pump mitral valve repair with NeoChord Implantation (TOP-MINI): step-by-step guide. *Ann Cardiothorac Surg* 2015;**4**:295–7.
159. Colli A, Manzan E, Zucchetta F, Sarais C, Pittarello D, Gerosa G. Feasibility of anterior mitral leaflet flail repair with transapical beating-heart neochoord implantation. *JACC Cardiovasc Interv* 2014;**7**:1320–1.
160. Gerosa G, D'Onofrio A, Manzan E, Besola L, Bizzotto E, Zucchetta F, et al. One-stage off-pump transapical mitral valve repair and aortic valve replacement. *Circulation* 2015;**131**:e430–4.
161. Gammie JS, Bartus K, Gackowski A, D'Ambra MN, Szymanski P, Bilewska A, et al. Beating-heart mitral valve repair using a novel ePTFE cordal implantation device. *J Am Coll Cardiol* 2018;**71**:25–36.
162. De Bonis M, Lapenna E, La Canna G, Ficarra E, Pagliaro M, Torracca L, et al. Mitral valve repair for functional mitral regurgitation in end-stage dilated cardiomyopathy. *Circulation* 2005;**112**(9 Suppl):I402–8.
163. Maisano F, Franzen O, Baldus S, Schäfer U, Hausleiter J, Butter C, et al. Percutaneous mitral valve interventions in the real world: early and 1-year results from the ACCESS-EU, a prospective, multicenter, nonrandomized post-approval study of the MitraClip therapy in Europe. *J Am Coll Cardiol* 2013;**62**(12):1052–61.



164. Glower DD, Kar S, Trento A, Lim DS, Bajwa T, Quesada R, et al. Percutaneous mitral valve repair for mitral regurgitation in high-risk patients. *J Am Coll Cardiol* 2014;**64**: 172–81.
165. Praz F, Spargias K, Chrissoheris M, Büllsfeld L, Nickenig G, Deuschl F, et al. Compassionate use of the PASCAL transcatheter mitral valve repair system for patients with severe mitral regurgitation: a multicentre, prospective, observational, first-in-man study. *Lancet* 2017;**390**(10096):773–80.
166. Biner S, Perk G, Kar S, Rafique AM, Slater J, Shiota T, et al. Utility of combined two-dimensional and three-dimensional transesophageal imaging for catheter-based mitral valve clip repair of mitral regurgitation. *J Am Soc Echocardiogr* 2011;**24**:611–7.
167. Kahlert P, Plicht B, Schenk IM, Janosi R-A, Erbel R, Buck T. Direct assessment of size and shape of noncircular vena contracta area in functional versus organic mitral regurgitation using real-time three-dimensional echocardiography. *J Am Soc Echocardiogr* 2008;**21**:912–21.
168. Avenatti E, Mackensen GB, El-Tallawi KC, Reisman M, Gruye L, Barker CM, et al. Diagnostic value of 3-dimensional vena contracta area for the quantification of residual mitral regurgitation after MitraClip procedure. *JACC Cardiovasc Interv* 2019;**12**:582–91.
169. Zoghbi WA, Asch FM, Bruce C, Gillam LD, Grayburn PA, Hahn RT, et al. Guidelines for the evaluation of valvular regurgitation after percutaneous valve repair or replacement. *J Am Soc Echocardiogr* 2019;**32**(4):431–75.
170. Agricola E, Meucci F, Ancona F, Pardo Sanz A, Zamorano JL. Echocardiographic guidance in transcatheter structural cardiac interventions. *EuroIntervention* 2022;**17**: 1205–26.
171. Dietl A, Prieschnek C, Eckert F, Birner C, Luchner A, Maier LS, et al. 3D vena contracta area after MitraClip© procedure: precise quantification of residual mitral regurgitation and identification of prognostic information. *Cardiovasc Ultrasound* 2018;**16**:1.
172. Maisano F, Redaelli A, Pennati G, Fumero R, Torracca L, Alfieri O. The hemodynamic effects of double-orifice valve repair for mitral regurgitation: a 3D computational model. *Eur J Cardio-Thoracic Surg* 1999;**15**:419–25.
173. Sürder D, Pedrazzini G, Gaemperli O, Biaggi P, Felix C, Rufibach K, et al. Predictors for efficacy of percutaneous mitral valve repair using the MitraClip system: the results of the MitraSwiss registry. *Heart* 2013;**99**(14):1034–40.
174. Herrmann HC, Kar S, Siegel R, Fail P, Loghin C, Lim S, et al. EVEREST Investigators. Effect of percutaneous mitral repair with the MitraClip device on mitral valve area and gradient. *EuroIntervention* 2009;**4**:437–42.
175. Singh GD, Smith TW, Rogers JH. Multi-MitraClip therapy for severe degenerative mitral regurgitation: “anchor” technique for extremely flail segments. *Catheter Cardiovasc Interv* 2015;**86**:339–46.
176. Lim DS, Reynolds MR, Feldman T, Kar S, Herrmann HC, Wang A, et al. Improved functional status and quality of life in prohibitive surgical risk patients with degenerative mitral regurgitation after transcatheter mitral valve repair. *J Am Coll Cardiol* 2014;**64**: 182–92.
177. Feldman T, Kar S, Rinaldi M, Fail P, Hermiller J, Smalling R, et al. Percutaneous mitral repair with the MitraClip system. Safety and midterm durability in the initial EVEREST (Endovascular Valve Edge-to-Edge REpair Study) cohort. *J Am Coll Cardiol* 2009;**54**(8):686–94.
178. Kreidel F, Frerker C, Schlüter M, Alessandrini H, Thielsen T, Geidel S, et al. Repeat MitraClip therapy for significant recurrent mitral regurgitation in high surgical risk patients. *JACC Cardiovasc Interv* 2015;**8**:1480–9.
179. Neuss M, Schau T, Isotani A, Pilz M, Schöpp M, Butter C. Elevated mitral valve pressure gradient after MitraClip implantation deteriorates long-term outcome in patients with severe mitral regurgitation and severe heart failure. *JACC Cardiovasc Interv* 2017;**10**: 931–9.
180. Faletta FF, Pozzoli A, Agricola E, Guidotti A, Biasco L, Leo LA, et al. Echocardiographic-fluoroscopic fusion imaging for transcatheter mitral valve repair guidance. *Eur Heart J Cardiovasc Imaging* 2018;**19**:715–26.
181. Melillo F, Fisicaro A, Stella S, Ancona F, Capogrosso C, Ingallina G, et al. Systematic fluoroscopic-echocardiographic fusion imaging protocol for transcatheter edge-to-edge mitral valve repair intraprocedural monitoring. *J Am Soc Echocardiogr* 2021;**34**:604–13.
182. Foster E, Wasserman HS, Gray W, Homma S, Di Tullio MR, Rodriguez L, et al. Quantitative assessment of severity of mitral regurgitation by serial echocardiography in a multicenter clinical trial of percutaneous mitral valve repair. *Am J Cardiol* 2007;**100**: 1577–83.
183. Nickenig G, Estevez-Loureiro R, Franzen O, Tamburino C, Vanderheyden M, Lüscher TF, et al. Percutaneous mitral valve edge-to-edge repair. *J Am Coll Cardiol* 2014;**64**: 875–84.
184. Altiok E, Paetsch I, Jahnke C, Brehmer K, Reith S, Becker M, et al. Percutaneous edge-to-edge mitral valve repair. *J Am Coll Cardiol* 2011;**58**:e21.
185. Asch FM, Grayburn PA, Siegel RJ, Kar S, Lim DS, Zaroff JG, et al. Echocardiographic outcomes after transcatheter leaflet approximation in patients with secondary mitral regurgitation. *J Am Coll Cardiol* 2019;**74**:2969–79.
186. Zoghbi WA, Adams D, Bonow RO, Enriquez-Sarano M, Foster E, Grayburn PA, et al. Recommendations for noninvasive evaluation of native valvular regurgitation. *J Am Soc Echocardiogr* 2017;**30**:303–71.
187. Halaby R, Herrmann HC, Gertz ZM, Lim S, Kar S, Lindenfeld J, et al. Effect of mitral valve gradient after MitraClip on outcomes in secondary mitral regurgitation. *JACC Cardiovasc Interv* 2021;**14**:879–89.
188. Taramasso M, Kuwata S, Rodriguez H, Bieffer C, Nietlispach F, Maisano F. Percutaneous mitral valve repair and replacement: complementary or competitive techniques? *EuroIntervention* 2016;**12**:Y97–Y101.
189. Maisano F, Alfieri O, Banai S, Buchbinder M, Colombo A, Falk V, et al. The future of transcatheter mitral valve interventions: competitive or complementary role of repair vs. replacement? *Eur Heart J* 2015;**36**:1651–9.
190. Blanke P, Naoum C, Dvir D, Bapat V, Ong K, Muller D, et al. Predicting LVOT obstruction in transcatheter mitral valve implantation: concept of the neo-LVOT. *JACC Cardiovasc Imaging* 2017;**10**:482–5.
191. Gheorghi LL, Mobasseri S, Agricola E, Wang DD, Milla F, Swaans M, et al. Imaging for native mitral valve surgical and transcatheter interventions. *JACC Cardiovasc Imaging* 2021;**14**:112–27.
192. Kreidel F, Zaid S, Tamm AR, Ruf TF, Beiras-Fernandez A, Reinold J, et al. Impact of mitral annular dilation on edge-to-edge therapy with MitraClip-XTR. *Circ Cardiovasc Interv* 2021;**14**(8):e010447.